BLACK SLOUGH REACH SOUTH FORK NOOKSACK RIVER IN-STREAM RESTORATION PROJECT

EXISTING CONDITIONS ASSESSMENT REPORT

Lummi Natural Resources Department
2665 Kwina Rd
Bellingham, WA 98226
(360) 312-2319

Natural Systems Design | CGS COASTAL GEOLOGIC SERVICES

1900 N. Northlake Way, Suite 211
Seattle, WA 98103

THIS PAGE INTENTIONALLY LEFT BLANK

CONTENTS

1 Introduction 1

2 Project Goals 2

3 Watershed Setting 2

3.1 Reach Description 2

3.2 Watershed Characteristics 3

3.3 Species Use and Periodicity 5

4 Climate and Hydrology 7

4.1 Historic Climate 7

4.2 Watershed Hydrology 7

4.3 Peak Flows 11

4.4 Observed Changes in Climate and Hydrology 11

4.5 Projected Future Conditions 12

4.5.1 Data Sources and Previous Studies 12

4.5.2 Global Climate Models to Represent Future Climate 13

4.5.3 Future Air Temperature 14

4.6 Precipitation 17

4.6.1 Annual and Seasonal 17

4.6.2 Extreme Precipitation 19

4.7 Implications of Temperature and Precipitation Changes 19

4.8 Climate Change Impacts 21

4.8.1 Streamflows 21

4.8.2 Aquatic Habitat 24

5 Geomorphic Conditions 24

5.1 Valley Setting 24

5.2 Historical Channel and Floodplain Evolution 24

5.3 Field Reconnaissance and Topobathymetric Survey 33

5.4 Reach Characteristics 33

6 Hydraulic Analyses 40

6.1 Existing Conditions Model Development 40

6.1.1 Model Topography 41

6.1.2 Model Hydrology 42

6.1.3 Roughness 44

6.1.4 Computational Mesh 45
6.1.5 Model Validation 46
6.2 Existing Conditions Hydraulic Output 52
6.2.1 Low Flow Hydraulic Conditions....52
6.2.2 Two-Year Flow Hydraulic Conditions 54
6.2.3 Peak Flow (10-yr and 100-yr) Hydraulic Conditions 59
6.2.4 Climate Change Peak Flow (100-yr) Conditions....63
7 Instream Habitats and Limiting Factors 65
7.1 Limiting Factors and Habitat Metrics 65
7.1.1 Habitat Mapping Methods 65
7.1.2 Habitat Conditions....65
7.2 Instream Temperatures and Water Quality Conditions 68
8 Floodplain and Riparian Conditions 69
8.1 Groundwater Recharge and Storage Potential....70
8.1.1 Soils and Hydraulic Conductivity 70
8.1.2 Wetland Presence....73
8.2 Land Use, Riparian Shade, and Large Wood Potential 76
8.2.1 Implication for Instream Habitats....78
9 Summary of Impairments....80
10 Next Steps 81
11 Literature Cited 82

LIST OF TABLES

Table 1. Salmonid life stage periodicity in the South Fork Nooksack River. 6
Table 3. Modeled increase in future peak flow magnitudes in the SFNR (from Paul (2023), based on RCP 8.5. The range for each time period and return interval is based on modeling results for different peak flow duration (e.g., 1-hour versus 24-hour peak). 23
Table 4. Historical and projected future low flow metrics in the SFNR, downstream of the confluence with Black Slough (from Wenger et al., 2010) 23
Table 7. Comparison of peak flow estimates at the Wickersham gage and the upstream end of the project reach. 43
Table 8. Comparison of observed high water marks and modeled WSE for 2006 high flow event. 48
Table 10. Roughness values used in 2-D hydraulic model runs. 52
Table 11. Habitat goals, conditions, and trends in Black Slough....66
Table 13. Characteristics of dominant mapped soil series in Black Slough reach floodplain. 72

LIST OF FIGURES

Figure 1. Map of the South Fork Nooksack River Watershed 1
Figure 2. Lower South Fork Valley overview 3
Figure 3. Historical climate (1991-2020) at Black Slough, SF Nooksack River from the NW Climate Toolbox (Abatzoglou 2013). 7
Figure 4. Watershed hydrology map from Paul (2023). 9
Figure 5. Snow water equivalent at the Elbow Lake NRCS SNOTEL site (ELSW1) for period of record (1995-current). 9
Figure 6. Average daily streamflow (cfs) in the SF Nooksack River during the period of record of 2009-present at USGS Gage 12210000 (Saxon Road). The gray envelope extends from the 25th to the 75th percentile of observed discharge values for each day. 10
Figure 7. Average daily streamflow (cfs) in the SF Nooksack River during the period of record of 1935-2008 at USGS Gage 12090000 (Wickersham Road). The gray envelope extends from the 25th to the 75th percentile of observed discharge values for each day. 10
Figure 8. Exceedance probability for USGS Gage 12210000 at Saxon Road and USGS Gage 12090000 at Wickersham Road. 11
Figure 9. Historic average annual precipitation in Bellingham between 1858 and 2018, reproduced from Figure 7 of Whatcom County (2020). 12
Figure 10. The timing of the center of annual flow, given as Day of Water Year (i.e., October 1 = 1 and September 30 = 365) at the USGS Saxon Road Bridge gage. The data show a non-significant (p-value = 0.2) declining trend, suggesting a possible recent shift toward earlier streamflow. 12
Figure 11. Global change in air temperature relative to average for the historical period (black line) and for a projected future scenario based on RCP 4.5 (blue line) and RCP 8.5 (red line). Box plots to the right of the line plot illustrate the range of future warming projected with four different RCPs. Figure from: https://climate.nasa.gov/internal_resources/1974/ 13
Figure 12. Modeled historic and future summer (i.e., average of June, July, and August) maximum air temperature in the SF Nooksack River basin based on the RCP 4.5 emissions scenario and presenting the distribution of results for individual GCMs (dots) and the ensemble median (horizontal black line). Figure from Hegewisch and Abatzoglou (2024). 14
Figure 13. Modeled historic and future summer (i.e., average of June, July, and August) maximum air temperature in the SF Nooksack River basin based on the RCP 8.5 emissions scenario and presenting the distribution of results for individual GCMs (dots) and the ensemble median (horizontal black line). Figure from Hegewisch and Abatzoglou (2024). 15
Figure 14. Modeled historic and future summer (i.e., average of December, January, and February) mean air temperature in the SF Nooksack River basin based on the RCP 4.5 emissions scenario and presenting the distribution of results for individual GCMs (dots) and the ensemble median (horizontal black line). Figure from Hegewisch and Abatzoglou (2024). 16
Figure 15. Modeled historic and future summer (i.e., average of December, January, and February) air temperature in the SF Nooksack River basin based on the RCP 8.5 emissions scenario and presenting the distribution of results for individual GCMs (dots) and the ensemble median (horizontal black line). Figure from Hegewisch and Abatzoglou (2024). 16
Figure 16. Modeled historic and future mean annual total precipitation based on the RCP 8.5 emissions scenario and presenting the distribution of results for individual GCMs (dots) and the ensemble median (horizontal black line). Figure from Hegewisch and Abatzoglou (2024). 17
Figure 17. Modeled historic and future winter (i.e., average of December, January, and February) precipitation based on the RCP 8.5 emissions scenario and presenting the distribution of results for individual GCMs (dots) and

the ensemble median (horizontal black line). Figure from Hegewisch and Abatzoglou (2024). 18
Figure 18. Modeled historic and future mean summer (i.e., June, July, and August) total precipitation based on the RCP 8.5 emissions scenario and presenting the distribution of results for individual GCMs (dots) and the ensemble median (horizontal black line). Figure from Hegewisch and Abatzoglou (2024). 18
Figure 19. Modeled historic and future annual mean temperature versus annual total precipitation for the Nooksack HUC-8 based on RCP 8.5. 20
Figure 20. Modeled historic and future winter mean temperature versus total winter precipitation for the Nooksack HUC-8 based on RCP 8.5. 20
Figure 21. Modeled historic and future summer mean temperature versus summer precipitation for the Nooksack HUC-8 based on RCP 8.5. 21
Figure 22. Modeled historic and late century streamflow (y-axis, in cubic meters per second) at the USGS Wickersham gage (12209000) showing the ensemble medians for RCP 4.5 (red) and RCP 8.5 (blue) and the spread projected by individual GCMs (gray lines). Taken from Figure 17 of Murphy (2015). 22
Figure 23. Landform map of the Lower South Fork Nooksack River showing the alluvial valley and abandoned channel features with alluvial fans and landslide deposits along the valley margin. 26
Figure 24. Valley cross sections A-A’ and B’-B’ showing floodplain topography (2016 lidar) 27
Figure 25. Comparison of historical maps and imagery showing channel changes 1919-2023. 29
Figure 26. Historical channel traces in the project reach between 1885-2024. 30
Figure 27. Reference map of the Black Slough Reach study area (2023 NAIP imagery). 31
Figure 28. Relative Elevation Model (REM) of the Black Slough Reach study area. Topographic data source: 2016 Lidar and 2024 channel survey. 32
Figure 29. Oblique aerial photo (April 2024) showing the riprap revetment at RM 3. 34
Figure 30. Oblique aerial photo (April 2024) showing the unconfined channel segment between RM 2.6 and 2.9 and riprap revetment near RM 2.5. 35
Figure 31. Oblique aerial photo (April 2024) of the confluence with Black Slough and upstream channel segment. 36
Figure 32. Photo of the outlet from Black Slough at the confluence with the South Fork Nooksack River. 37
Figure 33. Oblique aerial photo of the South Fork Nooksack River 37
Figure 34. Logs and boulders placed along bank downstream of the Potter Road Bridge. 38
Figure 35. Oblique aerial view (April 2024) showing the left bank segment downstream of Potter Road. 38
Figure 36. Right bank segment upstream of RM 1.3 and disconnected floodplain wetland. 39

LIST OF APPENDICES

Appendix A Historical Imagery Map Book

THIS PAGE INTENTIONALLY LEFT BLANK

1 INTRODUCTION

The Lummi Nation Natural Resources Department (LNR) seeks to improve in-stream habitat conditions for the benefit of Endangered Species Act (ESA)-listed salmon species within the South Fork Nooksack River (SFNR) between river miles 1.3 and 3, known as the Black Slough reach (Figure 1). LNR has contracted with Natural Systems Design + Coastal Geologic Services, Inc. (NSD + CGS) to evaluate existing conditions within the black slough reach and develop engineering designs which respond to current degraded geomorphic, hydraulic, riparian, and instream habitat conditions. An important element of consideration for this reach, and the greater South Fork Nooksack River, are current and projected climate conditions, particularly the frequency and magnitude of precipitation events and their resulting impacts on instream temperatures, flows, and channel stability which influence the quantity and quality of available habitats for ESA-listed species.

Habitat degradation is the primary ecological concern for Nooksack River salmonid populations. The Nooksack River watershed supports nine species of Pacific salmonids: Chinook salmon (*Oncorhynchus tshawytscha*), coho salmon (O. kisutch), sockeye salmon (*O. nerka*), chum salmon (*O. keta*), pink salmon (*O. gorbuscha*), steelhead/ rainbow trout (O. mykiss), bull trout (*Salvelinus confluentus*), and Dolly Varden (*S. malma*). Puget Sound Chinook salmon, steelhead, and bull trout are listed as threatened under the Federal ESA. The project area comprises an important portion of spawning habitat for the SFNR population of Spring Chinook (WRIA 1 SRB 2005). This fact underscores the importance of this reach in maintaining salmonid populations in the region.

This report documents initial reach assessment work conducted by NSD + CGS and characterizes current conditions and functions of fluvial processes within the reach. Assessment work is organized by the following subjects: geographic conditions, climate and hydrology conditions, hydraulic conditions, instream habitat conditions, and floodplain and riparian conditions. Results and findings from this assessment will be used to identify areas within the reach that are low functioning, compared to historic or optimal conditions, and which may present opportunities for restoration. Restoration, or improvement opportunities for specific features or processes in the context of current land uses, climate conditions, and desired future conditions will inform engineering designs developed for the reach.

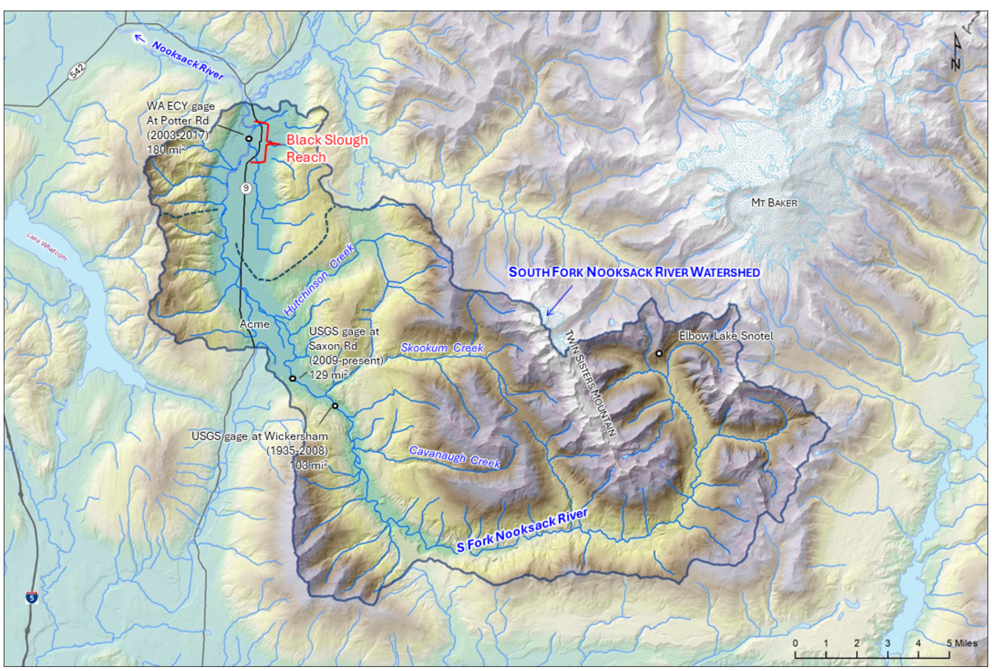

Figure 1. Map of the South Fork Nooksack River Watershed

2 PROJECT GOALS

The primary restoration goal for the Black Slough South Fork Nooksack River In-Stream Restoration Project (project) is to restore natural channel and floodplain processes for the improvement of salmonid spawning, rearing, and holding habitat, while improving late summer flow and thermal refugia for Chinook and steelhead. The timing of use within the SFNR for several species overlaps with peak water temperatures, underscoring the importance of addressing high water temperatures within the project reach. This assessment and subsequent design effort aim to implement both direct (identify, preserve, and enhance existing thermal refugia locations) and indirect (off-channel elements aimed at increasing shading and floodplain groundwater storage) actions to reduce or reverse warming within the project reach.

Existing habitat conditions and identified limiting factors are discussed further in Section 7.1 - Limiting Factors and Habitat Metrics. Specific restoration goals were developed in collaboration with LNR in response to the documented limiting factors within the project reach. The project goals are:

- Goal: Address limiting factors for early-run chinook (i.e., lack of deep pools with complex woody cover, low habitat diversity, and high instream temperatures).
- Goal: Address summer low flows and high instream temperatures through floodplain reconnection, wetland restoration, and promotion of groundwater storage.
- Goal: Reduce late summer stream temperature impacts by promoting stream/side channel shading and/or narrowing to reduce solar loading.
- Goal: Develop strategies that promote ecosystem resilience to climate change by improving floodplain connectivity to increase water storage, hyporheic cooling effects, and improve riparian health.

3 WATERSHED SETTING

3.1 Reach Description

The Black Slough project reach is located west of SR 9 near the town of Van Zandt, extending from RM 1.3 – 3.0 (Figure 2). The reach flows through a wide, low gradient alluvial valley and contains a single meandering gravel-bed channel. The Black Slough complex, which is the largest tributary to the project reach, crosses SR 9 on the right bank floodplain near the upstream end of the reach and flows through a well vegetated swale before joining the mainstem near RM 2.0. Potter road crosses the reach just upstream of RM 1.8, providing access to the west side of the river. Near the downstream end of the project reach, the mainstem abuts the BNSF railway along the right bank.

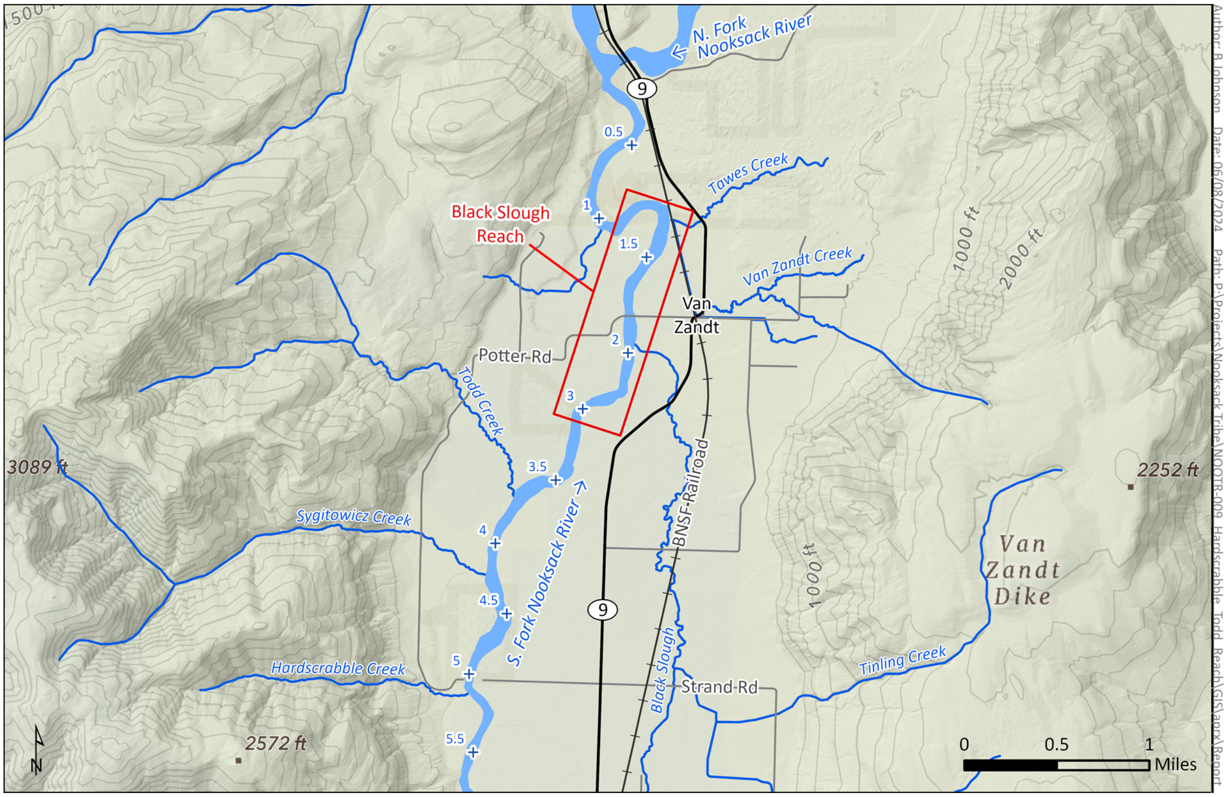

Figure 2. Lower South Fork Valley overview

3.2 Watershed Characteristics

The South Fork Nooksack River originates from headwaters in the Twin Sisters Mountain range and flows approximately 36 miles to the confluence with the Nooksack River near Deming, WA (Figure 1). Unlike the other forks of the Nooksack which drain glaciated terrain, the South Fork watershed drains mid-elevation forested foothills, with a maximum watershed elevation of 6,990 ft. The basin experiences a Mediterranean precipitation regime (wet winters, dry summers) typical of Western Washington (USFS 2006 as cited in Brown and Maudlin, 2007). Stream flow is driven primarily by rainfall with a spring-snow melt signature and infrequent rain-on-snow events, which produce the largest floods. The river is partially confined by hillslopes above RM 13 as it flows through a narrow valley containing active timberlands, while the downstream 13 miles of river flow through a broad alluvial valley with primarily rural residential and agricultural land use.

The South Fork watershed is underlain by three major groups of geologic units. The oldest units are composed of pre-Tertiary metamorphic and igneous bedrock that arrived on the North American continent during several accretionary events. This includes rocks from the Easton terrane, Bell Pass Melange, Chilliwack River terrane, and Nooksack terrane, which are present in the upper South Fork watershed (Gendaszek 2014). Uplift of the Cascade Range during the Eocene resulted in erosion of the underlying bedrock and deposition of sediment into the surrounding basins, forming the second major geologic unit within the South Fork basin. The deposited sediments were lithified into sandstone, mudstone, and coal of the Chuckanut formation, which is present in the lower reaches of the watershed along Stewart Mountain and Van Zandt Dike (Gendaszek 2014). The remainder of the watershed is underlain by Quaternary deposits. Pleistocene glacial terraces and glaciolacustrine deposits are widespread within the valley bottom of the upper watershed, while glacial deposits are overlain by a thick layer of alluvium in the lower watershed (Gendaszek, 2014).

Landslide activity is common within the valley, originating both from bedrock hillslopes and erodible glacial deposits. Shallow landslides and debris flows are frequent throughout the basin and help contribute to the high sediment supply of the river. Deep-seated earth flows and rock avalanches, while less common, also exert an influence on the valley. Notably, a series of rock avalanches deposits composed of Chuckanut Sandstone cover approximately 1200 acres of the valley bottom near the confluence of the North and South Fork Nooksack (Malick 2018). These deposits have confined the lower river downstream of the project reach.

The watershed is situated within the Tsuga heterophylla Zone (Franklin and Dryness 1988) of the Puget Trough ecosystem. The Tsuga heterophylla Zone is the most extensive vegetative zone in western Washington and has been heavily relied upon for timber production since the mid nineteenth century. There is a great deal of variation within this zone associated with latitude, elevation, and location relative to the Pacific Ocean and North Cascade mountain range. Large conifers typical of this zone are Douglas fir (Pseudotsuga menziesii), western hemlock (Tsuga heterophylla), grand fir (Abies grandis), Sitka spruce (Picea sitchensis), and western red cedar (Thuja plicata). Historically, large hardwoods such as bigleaf maple (Acer macrophyllum), black cottonwood (Populus balsamifera spp. trichocarpa), and red alder (Alnus rubra), were not common in the forests of the Tsuga heterophylla Zone, except in disturbed areas or riparian corridors. Today, all three of these hardwood species are common throughout this zone, as well as in disturbed areas, particularly adjacent to developed areas, riparian corridors, and areas which had previously been logged of coniferous trees for timber.

The lower valley below RM 13 is lightly developed with a mix of rural residential and agricultural land use. Christmas tree and dairy farms, and berry, hay, and corn fields are common throughout the area (Grah et al., 2018). The valley floor is generally cleared with scattered stands of young forest and a narrow riparian buffer along the river (Soicher et al., 2006). Several large wetland complexes are also present in the valley. Residential development is generally dispersed, with more concentrated development and businesses in the communities of Acme and Van Zandt (Figure 2). The valley is bisected by State Route (SR) 9 and the BNSF railroad grade which run roughly parallel through the valley bottom.

Three major tributaries, Black Slough, Van Zandt Creek, and Tawes Creek, enter the South Fork within the project reach.

Black Slough flows into the reach from the right bank approximately 300 feet downstream of RM 2.0. The watershed includes 9.0 square miles of hillslopes and valley bottom along the eastern side of the valley (USGS StreamStats). The largest tributary to Black Slough, Tinling Creek, itself has a drainage area of 2.8 square miles. Black Slough flows through abandoned channel features that parallel the South Fork for over 3 miles, intercepting runoff from the west facing slopes of Van Zandt Dike to the east. A large wetland complex occupies the series of abandoned meanders along the length of Black Slough. The basin has a total relief of 2,010 feet and a mean basin slope of 16 percent (USGS StreamStats).

Van Zandt Creek originates in the west facing hillslopes of Van Zandt Dike before entering a lower gradient and channelized reach as it flows through the community of Van Zandt. The stream has an overall watershed area of 1.3 square miles with a basin relief of 1,990 feet (USGS StreamStats). The stream then flows north and enters a wetland complex located north of Potter Road between SR 9 and the BNSF Railroad. Flow from Van Zandt Creek joins Tawes Creek within the wetland complex, which drains to the South Fork near RM 1.3 through a single channel beneath the BNSF railroad grade.

Tawes Creek also enters the reach from the right bank near RM 1.3, flowing from hillslopes along the east side of the valley before reaching the valley bottom near SR 9. The stream has a drainage area of 1.25 square miles and a maximum basin relief of 1,990 feet (USGS StreamStats). After crossing SR 9, the creek enters a wetland complex that is partially disconnected from the South Fork by the BNSF railroad grade. Tawes Creek passes under a railroad trestle before entering the South Fork.

3.3 Species Use and Periodicity

The South Fork Nooksack River is home to nine species and 11 populations of salmonids, including Spring Chinook, Bull Trout, and Summer Steelhead which are listed as threated under the Endangered Species Act (Table 1) (NIT 2018). The SFN supports year-round salmonid spawning and rearing with continuous rearing by various species and at least one species spawning at any given time. Heaviest spawning use occurs in late summer and early fall and rearing likely peaks in late winter through spring after juvenile emergence and before out-migration.

The Lower South Fork Nooksack (RM 0 to Skookum Creek) provides habitat for all Pacific Salmonid species. Pink Salmon, riverine Sockeye, Chum, Coho, and Coastal Cutthroat all spawn in the Lower SFN and associated tributaries. The Lower SFN is critical habitat for Spring Chinook as a core spawning area. The population of Spring Chinook in the SFN in particular faces a strong threat of extinction with returns in some years as below 100 spawners and as low as 10 fish (NIT 2018).

Table 1. Salmonid life stage periodicity in the South Fork Nooksack River.

South Fork Nooksack River Life Stage Periodicity

Species	Life Stage	Timing (E = early, M = mid, L = late)
Spring Chinook	Upstream Migration/holding	April E – Sept L
Spring Chinook	Spawning	Aug E – Sept L
Spring Chinook	Intragravel Development	Jan E – March L; Aug E – Dec L
Spring Chinook	Age-0 rearing	Jan E – Aug L
Spring Chinook	Age-0 outmigration	Jan E – Aug L
Spring Chinook	Age-1+ rearing	Jan E – Dec L
Spring Chinook	Age-1+ outmigration	Jan E – June L
Fall Chinook* (non-native)	Upstream Migration/holding	Aug L – Oct L
Fall Chinook* (non-native)	Spawning	Sept M – Nov E
Fall Chinook* (non-native)	Intragravel Development	Jan E – Feb L; Sept M – Dec L
Fall Chinook* (non-native)	Juvenile Rearing	Jan E – Dec L
Fall Chinook* (non-native)	Outmigration	April E – Aug L
Coho	Upstream Migration/holding	(Jan E – Feb L); Sept E – Dec L
Coho	Spawning	Jan E – March L; Oct E – Dec L
Coho	Intragravel Development	Jan E – May L; Oct E – Dec L
Coho	Juvenile Rearing	Jan E – Dec L
Coho	Outmigration	March E – July L
Pink	Upstream Migration/holding	July E – Oct L
Pink	Spawning	Aug E – Sept L
Pink	Intragravel Development	Jan E – May L; Aug E – Dec L
Pink	Fry	Jan E – June L; Dec E – Dec L
Pink	Outmigration	Jan E – June L
Chum	Upstream Migration/holding	Jan E – Feb L; Oct E – Dec L
Chum	Spawning	Jan E – Feb L; Oct E – Dec L
Chum	Intragravel Development	Jan E – April L; Oct E – Dec L
Chum	Fry	Feb E – July L
Chum	Outmigration	Feb E – July L
Sockeye	Upstream Migration/holding	May E – Nov L
Sockeye	Spawning	July E – Nov L
Sockeye	Intragravel Development	Jan E – April L; Aug E – Dec L
Sockeye	Fry and Juvenile Rearing	Jan E – Dec L
Sockeye	Outmigration	March E – July L
Winter Steelhead	Upstream Migration	Jan E – May L
Winter Steelhead	Holding	Jan E – June L; Oct E – Dec L
Winter Steelhead	Spawning	March E – July L
Winter Steelhead	Adult Outmigration	Jan E – July L
Winter Steelhead	Intragravel Development	Jan E – July L; ? Aug; Dec E – Dec L
Winter Steelhead	Juvenile Rearing	Jan E – Dec L
Winter Steelhead	Juvenile Outmigration	? Feb; March E – July L; ? Aug
Summer Steelhead	Upstream Migration	April E – Oct L
Summer Steelhead	Holding	Jan E – Dec L
Summer Steelhead	Spawning	Feb E – April L
Summer Steelhead	Adult Outmigration	Feb E – May L
Summer Steelhead	Intragravel Development	Feb E – June L
Summer Steelhead	Juvenile Rearing	Jan E – Dec L
Summer Steelhead	Juvenile Outmigration	? Feb; March E – July L; ? Aug
Bull Trout	Adult Upstream Migration	May E – Nov L
Bull Trout	Holding	Jan E – Dec L
Bull Trout	Spawning	Sept E – Nov L
Bull Trout	Adult Outmigration	Jan E – July L
Bull Trout	Intragravel Development	Jan E – May L; Sept E – Dec L
Bull Trout	Juvenile Rearing	Jan E – Dec L
Bull Trout	Smolt Outmigration	March E – Aug L

*Table originally developed in Upper South Fork Nooksack River Effectiveness Monitoring Report (NSD 2021). Table adapted from EPA 2016. Coastal Cutthroat and Dolly Varden not shown. *Fall Chinook periodicity were adapted from Anchor Environmental, LLC. 2003 and were updated for the South Fork based on spawning ground surveys and genetic analysis of smolt trap samples (D. Kruse 2020 - personal communication). Upstream migration refers to time when salmonid enters the South Fork. Question marks (?) are months in which there is a question whether the species life stage occurs.*

4 CLIMATE AND HYDROLOGY

4.1 Historic Climate

The Nooksack River watershed is subject to a maritime climate with air temperatures moderated by the ocean influence and therefore range from average minimum air temperatures that are just below the freezing point (~30 °F) during the winter to basin-average maximum temperatures up to about 72 °F in the summer (Figure 3). Mean total annual precipitation (based on 1981-2010) is approximately 110 inches, with the majority of precipitation falling during the late fall to early spring. The Black Slough reach on the SFNR is located at an elevation of 245 ft but receives streamflow from 179 mi^2 of the SFNR watershed, which reaches a maximum elevation of 6,990 ft (metrics from StreamStats, located just downstream of Black Slough's confluence with the main stem SF Nooksack). In the upper watershed, the average low temperatures are in the mid-20s during the winter months and much of the precipitation is stored as snow.

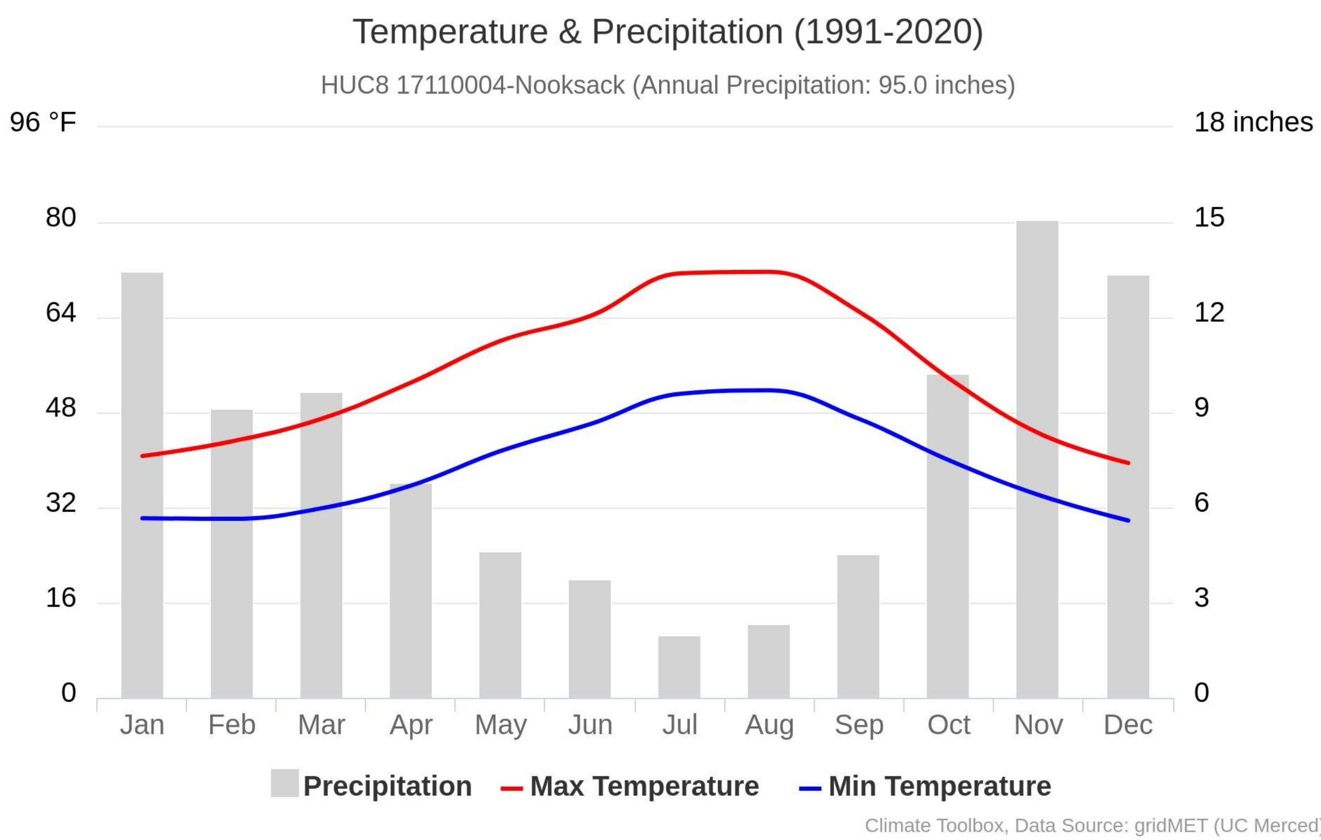

Figure 3. Historical climate (1991-2020) at Black Slough, SF Nooksack River from the NW Climate Toolbox (Abatzoglou 2013).

4.2 Watershed Hydrology

At the Black Slough Reach, the SF Nooksack watershed is 179 mi^2 and extends to a maximum elevation 6,990 ft at the Twin Sisters on the west slopes of the Cascade Range. The timing and magnitude of streamflow in the SFNR has been observed via stream gaging in three locations, including a Washington Department of Ecology gage (01F070) at the Potter Road Bridge (RM 1.8), a USGS gage (12210000) at the Saxon Road bridge (12.8), and a USGS gage (12090000) near Wickersham (RM 14.8). The Potter Road Bridge gage is located within the project reach, and the other two gages are located upstream (Figure 1). The timing and duration of gage operation varies between the three gages, and the Wickersham gage has the longest period of record whereas the Saxon Road gage has the most recent record (Table 2). In addition, a National Resource Conservation Service (NRCS) Snow Telemetry (SNOTEL) station provides snow depth observations in the upper watershed.

Table 2. Data sources for South Fork Nooksack hydrology observations.

DATA SOURCES	STATION ID	ELEVATION (FT)	DATE OF SERVICE	RIVER MILE	DRAINAGE AREA (SQ MI)
SFNR USGS gage at Wickersham	12090000	385.0	1934 - 2008	14.8	103
SFNR USGS gage at Saxon Rd.	12210000	349.8	2009 - present	12.8	129
SFNR WA ECY gage at Potter Rd.	01F070	229.4	2003 - 2017	1.8	179
Elbow Lake NRCS SNOTEL	ELSW1	3200.0	1995 - 2022	n/a	n/a

The SFNR watershed hydrology is influenced by a combination of rain and snow; approximately 10-40% of the winter precipitation falls as snow and a seasonal snowpack develops at its higher elevations (Figure 4, Figure 5). The streamflow in the project reach is influenced by this climate; for example, high intensity precipitation events that occur throughout the fall and winter result in high flows occurring in November through February (Figure 6, Figure 7). Additionally, the development and melt of the seasonal snowpack result in a second period of high flows in the late spring (Figure 6, Figure 7). Stream observations at both Wickersham and Saxon Rd. reflect this pattern of streamflow timing, with a more distinct two peak hydrograph at the Wickersham gage, likely due to its longer observational record. Low amounts of precipitation coupled with snowpack that is mostly melted out by June result in consistently low flows in the late summer months (Figure 6, Figure 7).

Flow duration curves at the Saxon and Wickersham stream gages show median annual flows (i.e., exceedance probabilities of 50%) of 671 and 562 cubic feet per second [cfs], respectively (Figure 8). The 10% exceedance probability flow reflects a relatively high annual flow (i.e., exceeded for only about 1 month each year) and is approximately 1,890 and 1,500 cfs at Wickersham and Saxon, respectively. The 90% exceedance probability flow reflects a relatively low annual flow (i.e., exceeded for about 11 months each year) and is approximately 142 and 137 cfs at Wickersham and Saxon, respectively. The higher streamflow at Saxon reflects its more downstream location which incorporates a larger drainage area, including inflow from Skookum Creek, a major tributary to the SFNR.

Streamflow in the SFNR at Potter Road, in the central portion of the project reach, is generally similar to or slightly higher than at the stream gages upstream due to the increased drainage area (Table 2). During summer low flows the flow magnitudes are similar, likely due to minimal inflow from the tributaries downstream of Saxon Road, many of which become dewatered during the summer months (e.g., Hardscrabble Creek). Seepage run data collected by the USGS, which consists of a longitudinal series of discharge measurements collected on the same day, indicate some gain in streamflow from groundwater contribution in the project reach (Gendaszek 2014)

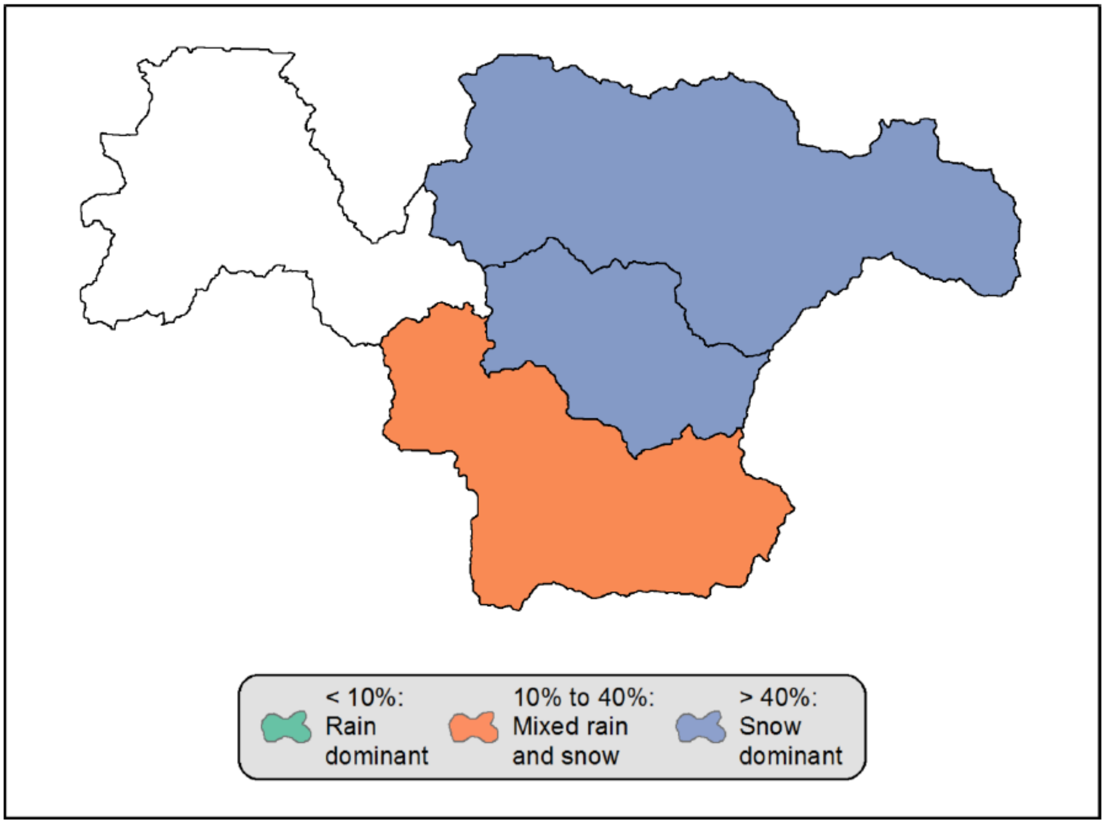

Figure 3: Watershed classifications for the North, Middle, and South Fork subbasins. The North and Middle Forks are classified as snow-dominant (> 40% of winter precipitation falling as snow) and the South Fork is classified as mixed snow and rain (between 10-40% of winter precipitation falling as snow), also referred to as transient or transitional (modified from Hamlet et al., 2013).

Figure 4. Watershed hydrology map from Paul (2023).

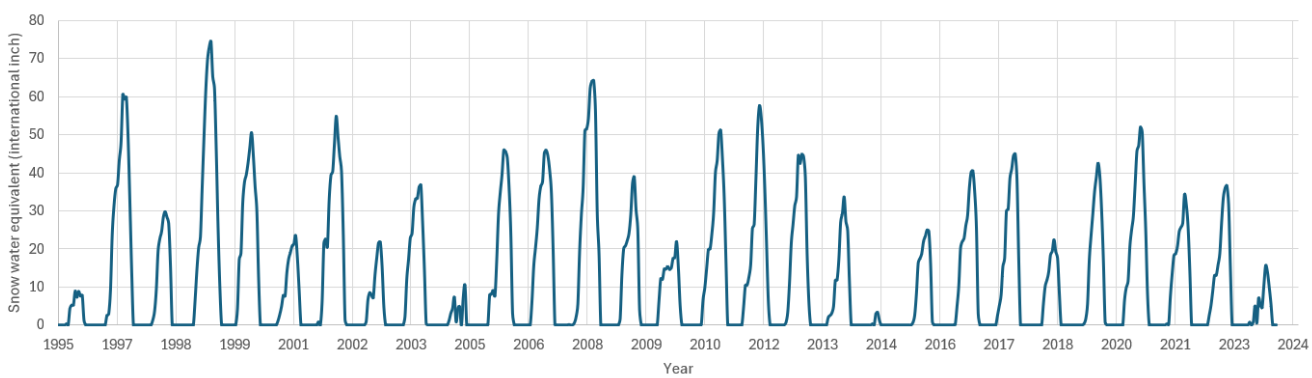

Figure 5. Snow water equivalent at the Elbow Lake NRCS SNOTEL site (ELSW1) for period of record (1995-current).

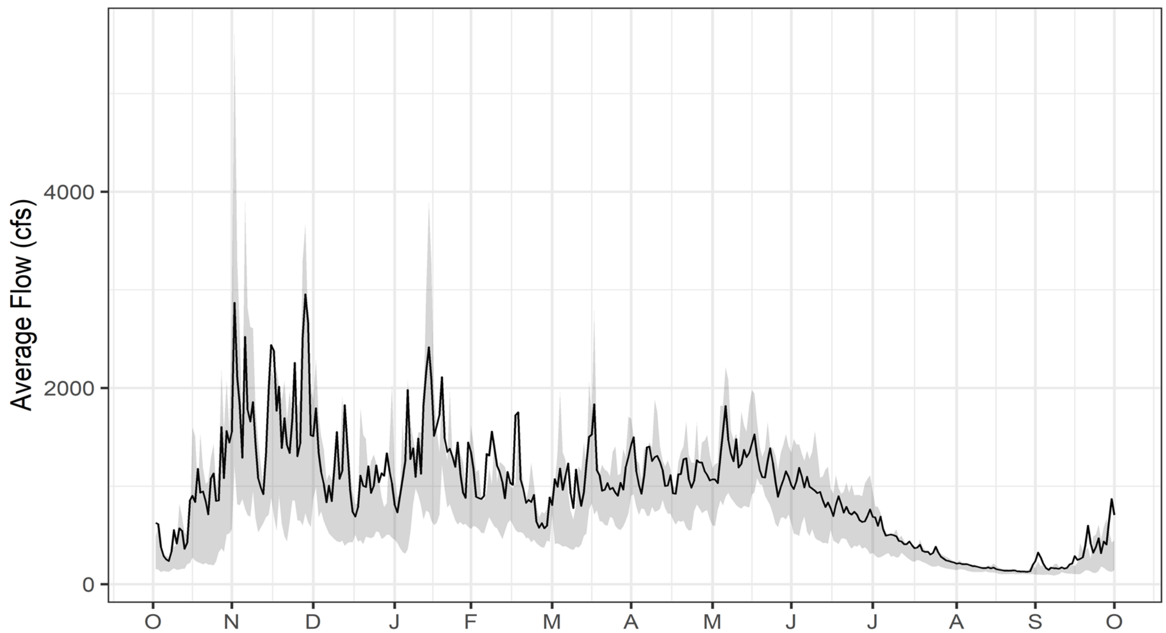

Figure 6. Average daily streamflow (cfs) in the SF Nooksack River during the period of record of 2009-present at USGS Gage 12210000 (Saxon Road). The gray envelope extends from the 25th to the 75th percentile of observed discharge values for each day.

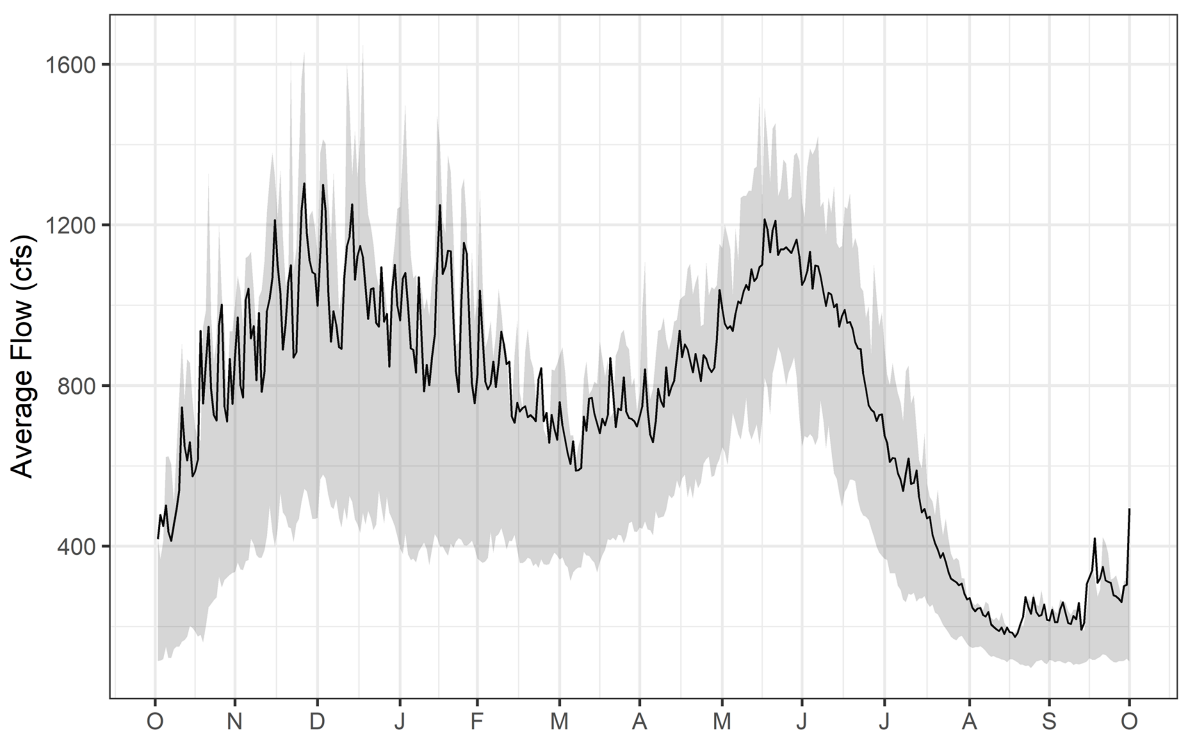

Figure 7. Average daily streamflow (cfs) in the SF Nooksack River during the period of record of 1935-2008 at USGS Gage 12090000 (Wickersham Road). The gray envelope extends from the 25th to the 75th percentile of observed discharge values for each day.

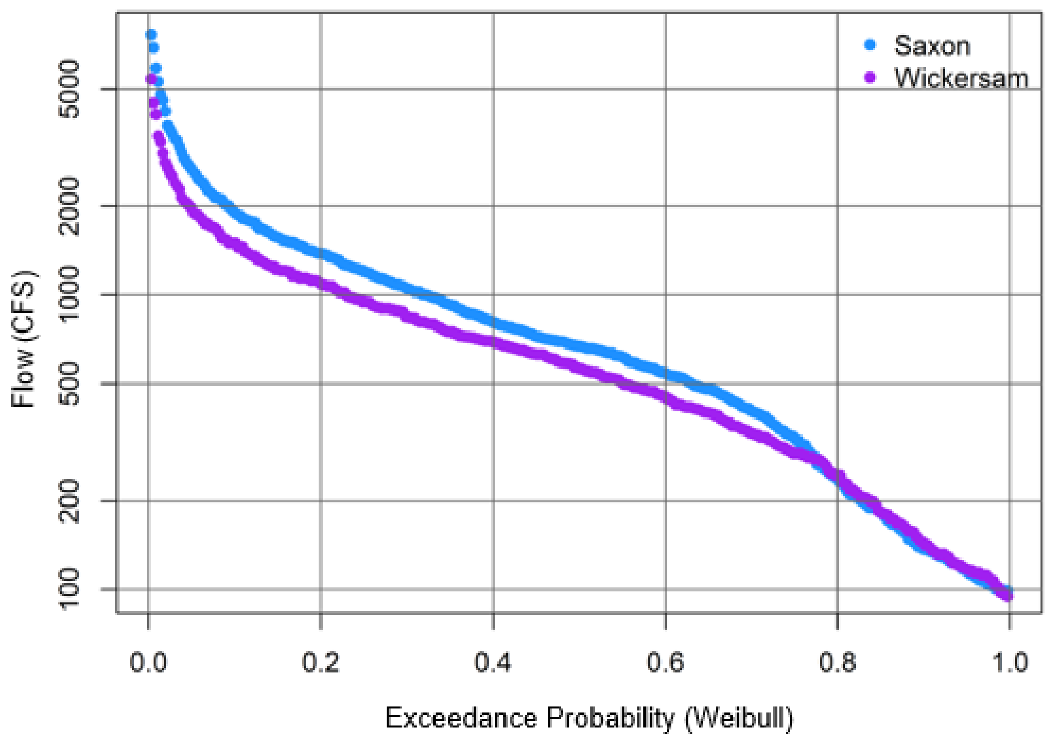

Figure 8. Exceedance probability for USGS Gage 12210000 at Saxon Road and USGS Gage 12090000 at Wickersham Road.

4.3 Peak Flows

Peaks flows for the project reach were quantified based on the 2-, 10-, and 100-yr events at the Wickersham Gage (USGS Gage 12090000). Thet are discussed further in in Section 6.1.2 and presented in Table 7.

4.4 Observed Changes in Climate and Hydrology

Average annual air temperature in Bellingham, WA has increased by 2.8 °F over the last century (Figure 9), and average annual precipitation has increased by approximately 1.9% per decade since the mid-1800s (Whatcom County 2020). Warming temperatures affect the amount of precipitation that is stored as snow and ice in the mountains along with the timing of snowmelt and therefore streamflow.

In the North Cascade mountains, glacier mass and seasonal snowpack have both declined, resulting in some observed shifts in snowmelt-driven streamflow to earlier in the year in western Washington (Whatcom County 2020). The SFNR watershed does not currently have glaciers but does accumulate and store a seasonal snowpack in the headwaters. Snowpack is highly variable between years at the one measurement location in the upper watershed (Figure 5.), with no clear trend but some suggestion that high snow years are somewhat diminished in the last decade as compared to the full record. An analysis of the timing of the center of annual streamflow (i.e., the day on which half the streamflow for the year has flowed past a certain point) suggests a possible (but uncertain) recent shift toward earlier streamflow (Figure 10). There is a non-significant declining trend in the timing, which may be reflective of reduced snow storage and earlier snowmelt.

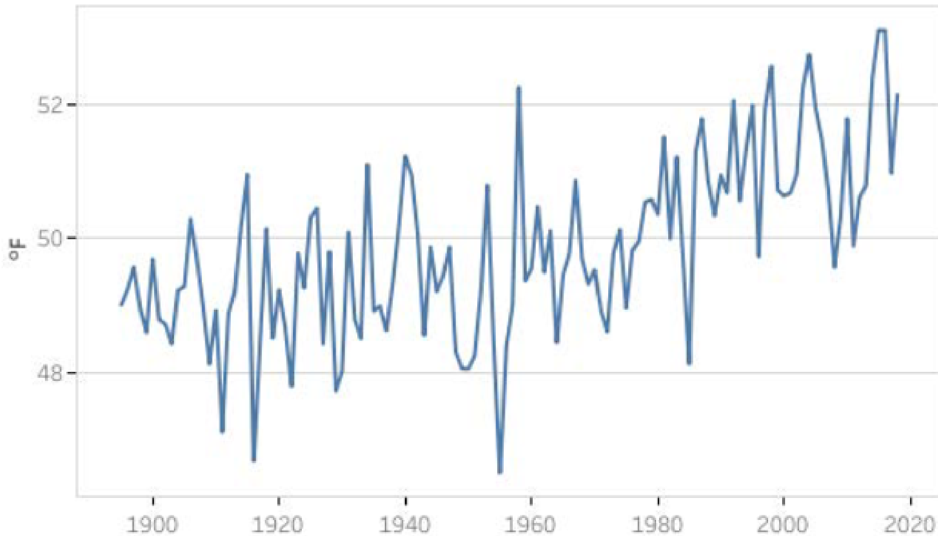

Figure 9. Historic average annual precipitation in Bellingham between 1858 and 2018, reproduced from Figure 7 of Whatcom County (2020).

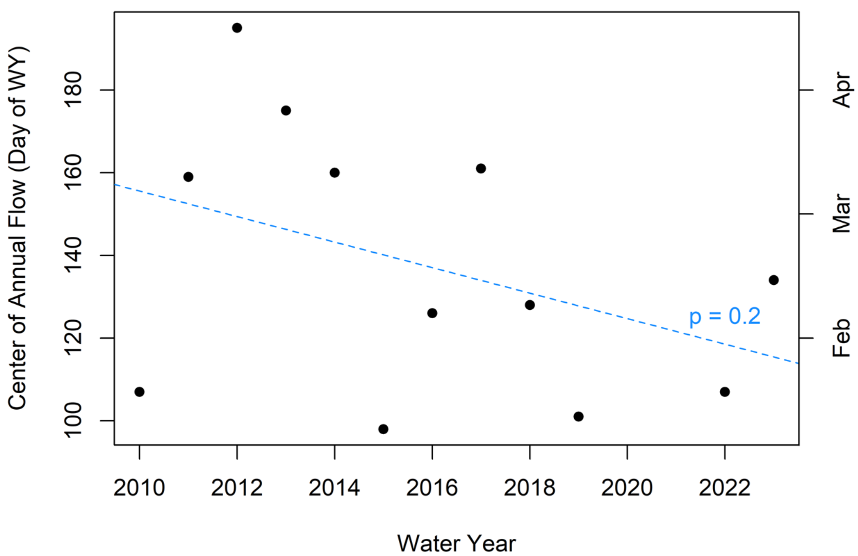

Figure 10. The timing of the center of annual flow, given as Day of Water Year (i.e., October 1 = 1 and September 30 = 365) at the USGS Saxon Road Bridge gage. The data show a non-significant (p-value = 0.2) declining trend, suggesting a possible recent shift toward earlier streamflow.

4.5 Projected Future Conditions

4.5.1 Data Sources and Previous Studies

Projected future climate conditions are derived from the climate toolbox (www.climatetoolbox.org), which provides a graphical user interface to access modeled climate (see section 4.5.2) and hydrology projections (Abatzoglou and Brown 2012). The effects on future climate conditions on future streamflows are quantified by several previous studies that have used projected future climate (e.g., temperature and precipitation) as inputs to hydrological models (Dickerson-Lange and Mitchell 2013; Murphy 2015; Paul 2023). In particular, low flow projec tions are taken from Wenger et al. (2010) who quantified extreme low flows at the stream segment scale, and Murphy (2015) who modeled future watershed hydrology along with glacier recession to quantify future low flows. Peak flow projections are taken from Paul (2023) who incorporated a regional weather forecast model to better resolve future extreme precipitation events and their effects on peak flow magnitudes. In addition, data and reporting from several relevant local efforts were reviewed and synthesized to characterize climate change impacts, including Butcher et al. (2016) and Whatcom County (2020 and 2021).

4.5.2 Global Climate Models to Represent Future Climate

Recent air temperatures have risen globally, and future air temperatures are projected to continue to rise due to increased greenhouse gas concentrations in the atmosphere. The magnitude of increase specific to the SFNR watershed is projected via gridded modeling that incorporates an ensemble of Global Climate Models (GCMs) from the Coupled Model Intercomparison Project Phase 5 (CMIP5), along with a “Representative Concentration Pathway” (RCP) scenario that approximates future greenhouse gas emissions. Although the GCMs all represent the physics of the atmosphere, there is spread in modeled future temperatures as a result of variability in how some atmospheric processes are represented mathematically. Therefore, it is common practice to use an ensemble of GCMs to better characterize the median and range of projected future conditions. In addition, the amount of future warming depends on the emissions scenario, with RCP 4.5 resulting in lower greenhouse gas concentrations and more moderate warming and RCP 8.5 resulting in higher greenhouse gas concentrations and greater warming. Thus, we present ensemble GCM projections for both RCP 4.5 and 8.5 for temperature and precipitation, below. Then, we switch to focusing on hydrologic projections for RCP 8.5 to conservatively characterize potential impacts. However, we note that the direction of the impacts (e.g., larger peak flows) is more certain than the magnitude (e.g., % increase), and we are presenting magnitudes that are associated with higher future greenhouse gas concentrations. All GCM projections have additionally been downscaled using higher resolution historical climate data (e.g., Livneh et al. (2013)) and statistical methods (e.g., Multivariate Adapted Constructed Analogs method (MACA; Abatzoglou & Brown, 2012).

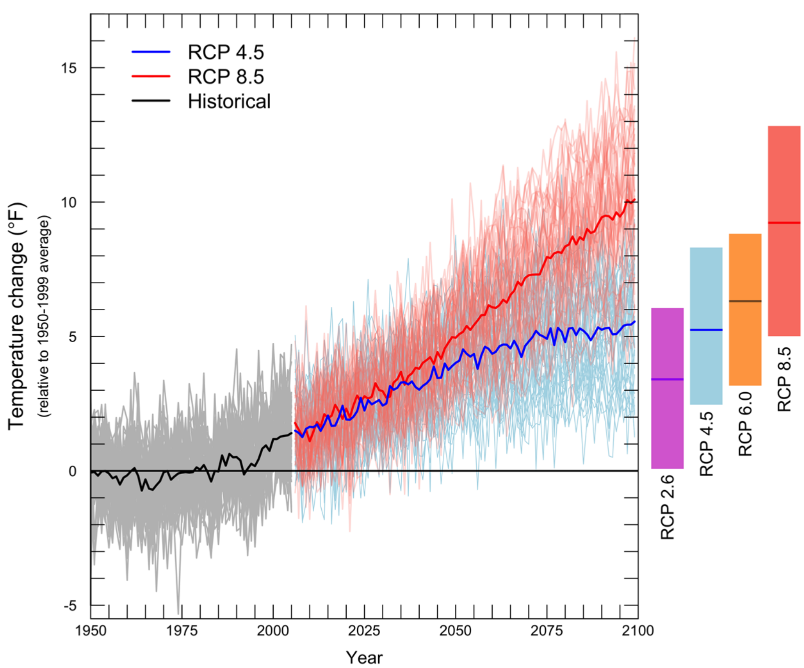

Figure 11. Global change in air temperature relative to average for the historical period (black line) and for a projected future scenario based on RCP 4.5 (blue line) and RCP 8.5 (red line). Box plots to the right of the line

plohttps://climate.nasa.gov/internal_resources/1974/

4.5.3 Future Air Temperature

Mean annual temperature in the SF Nooksack basin is projected to increase overall. Ensemble-median projections for end-of-century mean annual temperature range from 5.2 °F (+11%), based on RCP 4.5, to 9.0 °F (+19%), based on RCP 8.5. Projections for summer maximum temperatures in the SF Nooksack watershed indicate warming of 5.2 to 7.1 °F (+8% to +10%) by mid-century, based on GCM ensemble medians for RCP 4.5 (Figure 12) and 8.5 (Figure 13), respectively. By the end of the century, ensemble medians for modeled increases in summer maximum temperature range from 6.3 to 11.4 °F (+9% to +16%).

Summer maximum temperature is a major driver of water temperature during the hottest part of the year and is therefore a key metric for characterizing future aquatic habitat quality (discussed below), particularly as it relates to the suitability of stream temperatures for cold-water associated salmonids.

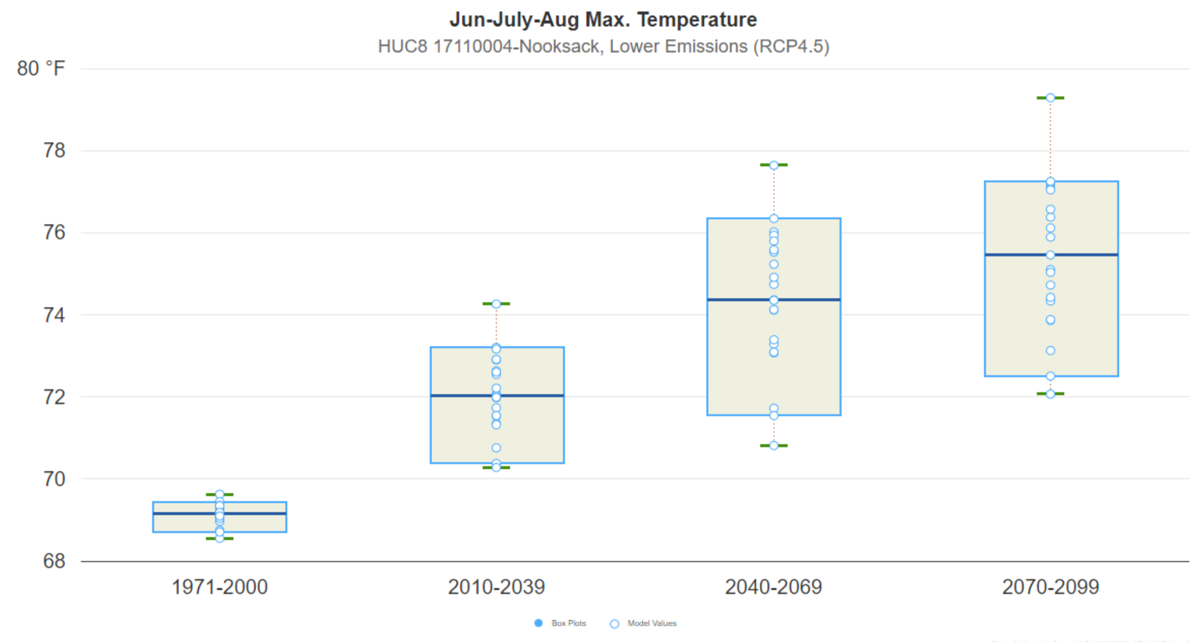

Figure 12. **Modeled historic and future summer (i.e., average of June, July, and August) maximum air temperature in the SF Nooksack River basin based on the RCP 4.5 emissions scenario and presenting the distribution of results for individual GCMs (dots) and the ensemble median (horizontal black line). Figure from Hegewisch and Abatzoglou (2024).**

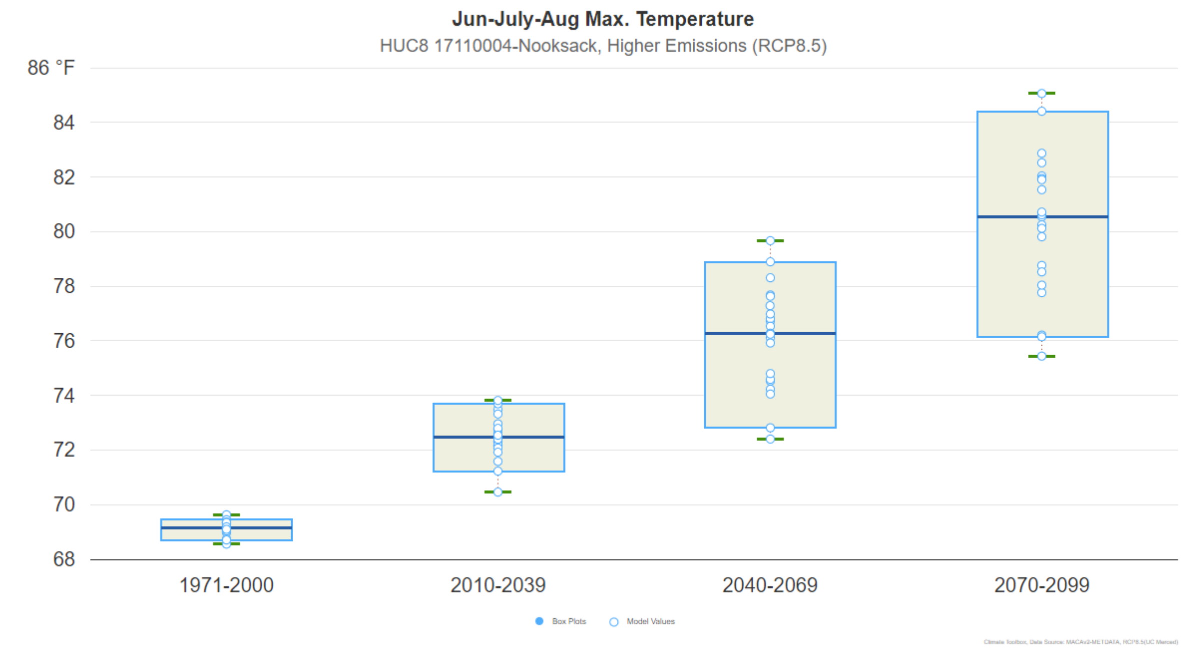

Figure 13. Modeled historic and future summer (i.e., average of June, July, and August) maximum air temperature in the SF Nooksack River basin based on the RCP 8.5 emissions scenario and presenting the distribution of results for individual GCMs (dots) and the ensemble median (horizontal black line). Figure from Hegewisch and Abatzoglou (2024).

Future winter mean temperature is projected to increase approximately 4.2 °F (+12%) to 5.3 °F (+15%) by mid-century, based on GCM ensemble medians for RCP 4.5 and 8.5, respectively. By late century, winter mean temperatures, ensemble medians for modeled increases in winter mean temperature range from 5.1 to 9.0 °F (+14.2 to +25.2%).

Winter temperature controls the amount of winter precipitation that falls as snow, and therefore influences the timing and magnitude of both winter flows that are driven by rainfall and spring flows that are influenced by snowmelt.

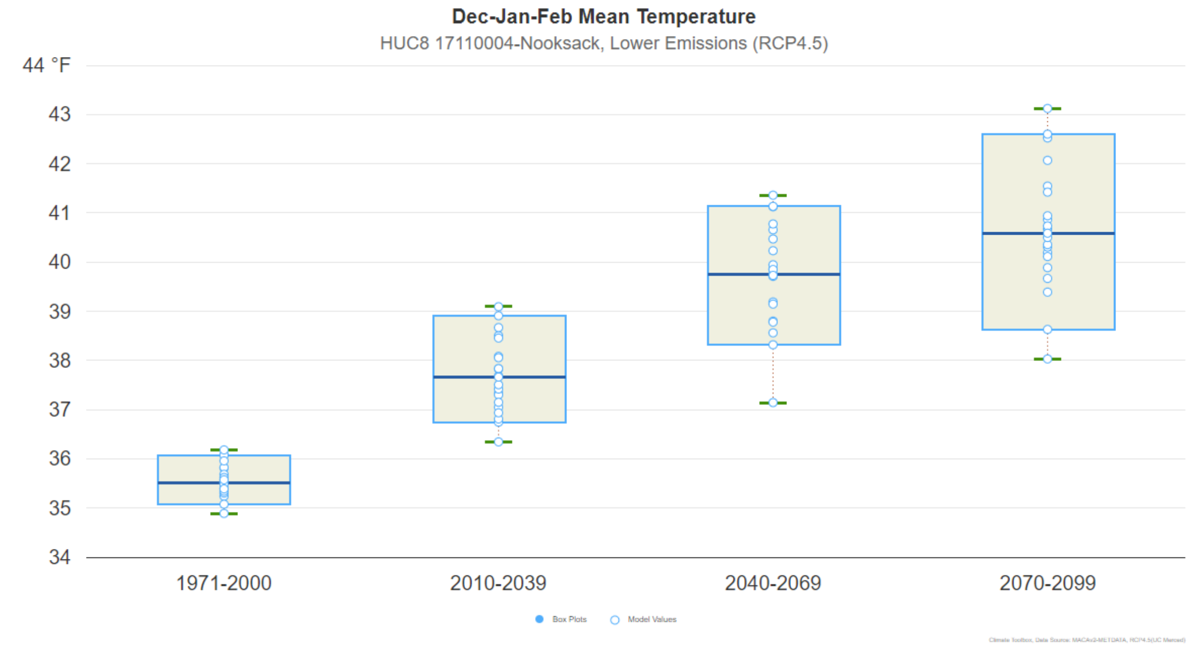

Figure 14. Modeled historic and future summer (i.e., average of December, January, and February) mean air temperature in the SF Nooksack River basin based on the RCP 4.5 emissions scenario and presenting the distribution of results for individual GCMs (dots) and the ensemble median (horizontal black line). Figure from Hegewisch and Abatzoglou (2024).

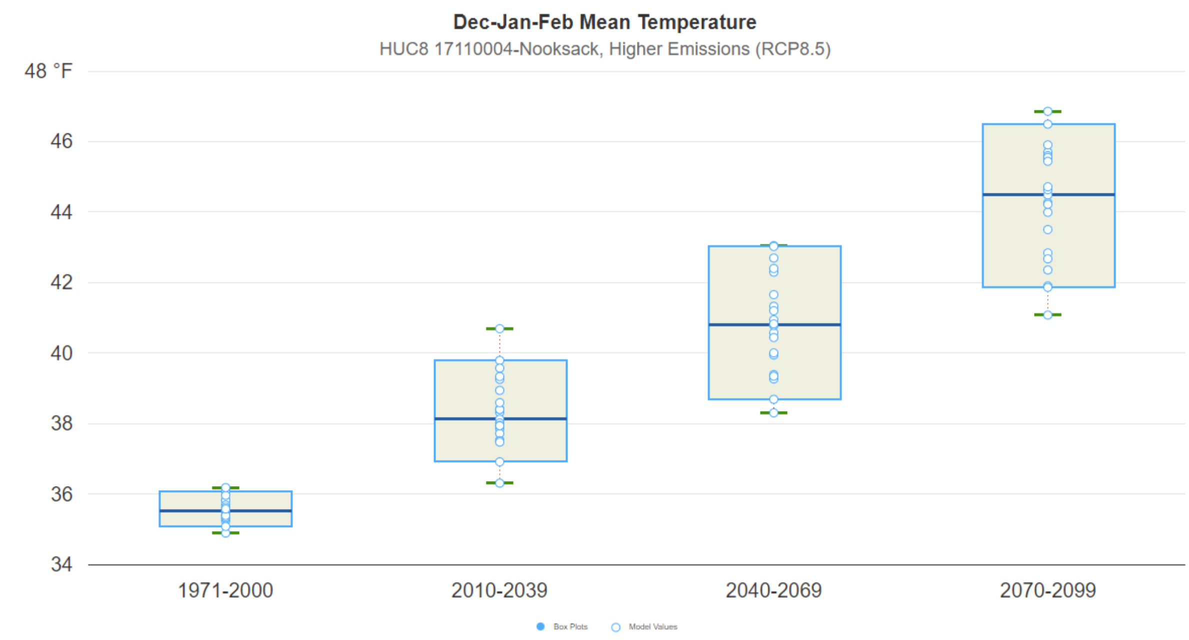

Figure 15. Modeled historic and future summer (i.e., average of December, January, and February) air temperature in the SF Nooksack River basin based on the RCP 8.5 emissions scenario and presenting the distribution of results for individual GCMs (dots) and the ensemble median (horizontal black line). Figure from Hegewisch and Abatzoglou (2024).

4.6 Precipitation

4.6.1 Annual and Seasonal

Total annual precipitation is projected to increase overall, but with increases in winter and fall, decreases in summer, and minimal change to spring precipitation. Ensemble-median projections for end-of-century increases in total annual precipitation range from 4.8 inches (+6 %), based on RCP 4.5, to 6.4 inches (+8%), based on RCP 8.5; Figure 17, note that only RCP 8.5 is shown below).

Total summer precipitation is projected to decline by end-of-century, with changes that range from -1 inch (-13%), based on RCP 4.5, to -1.8 inches (-23%, based on RCP 8.5; Figure 18). Increases in winter precipitation of 2.1 inches (+7%), based on RCP 4.5, to 3.9 inches (+13%), based on RCP 8.5 will combine with increased winter temperatures to result in more rain falling in the winter, which will contribute to increased runoff and streamflows (discussed below).

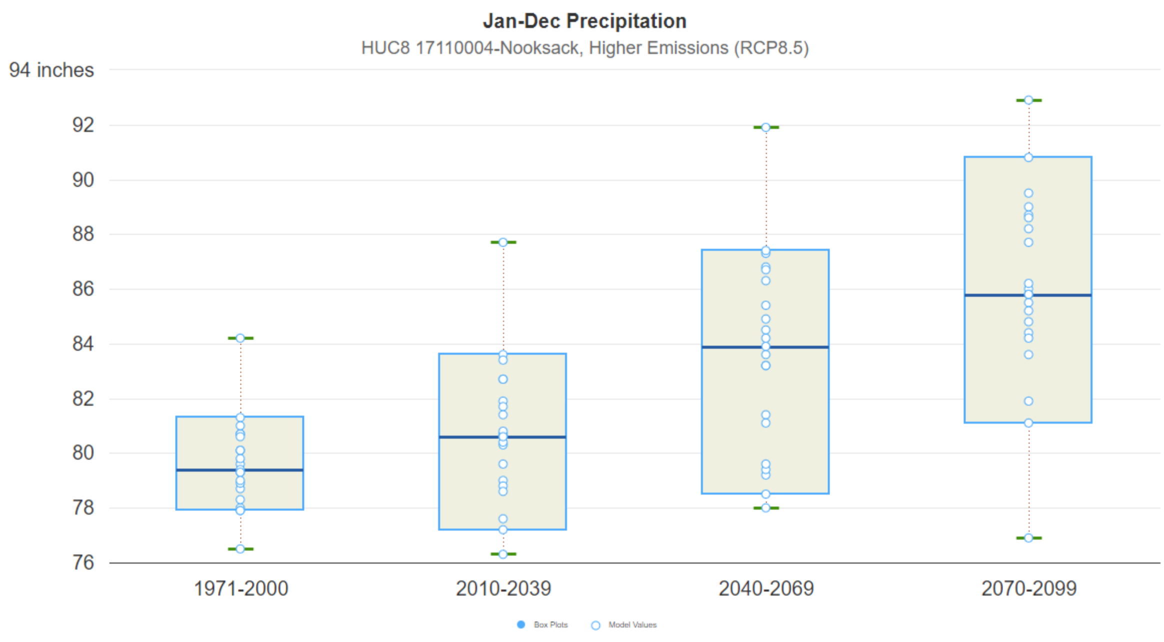

Figure 16. Modeled historic and future mean annual total precipitation based on the RCP 8.5 emissions scenario and presenting the distribution of results for individual GCMs (dots) and the ensemble median (horizontal black line). Figure from Hegewisch and Abatzoglou (2024).

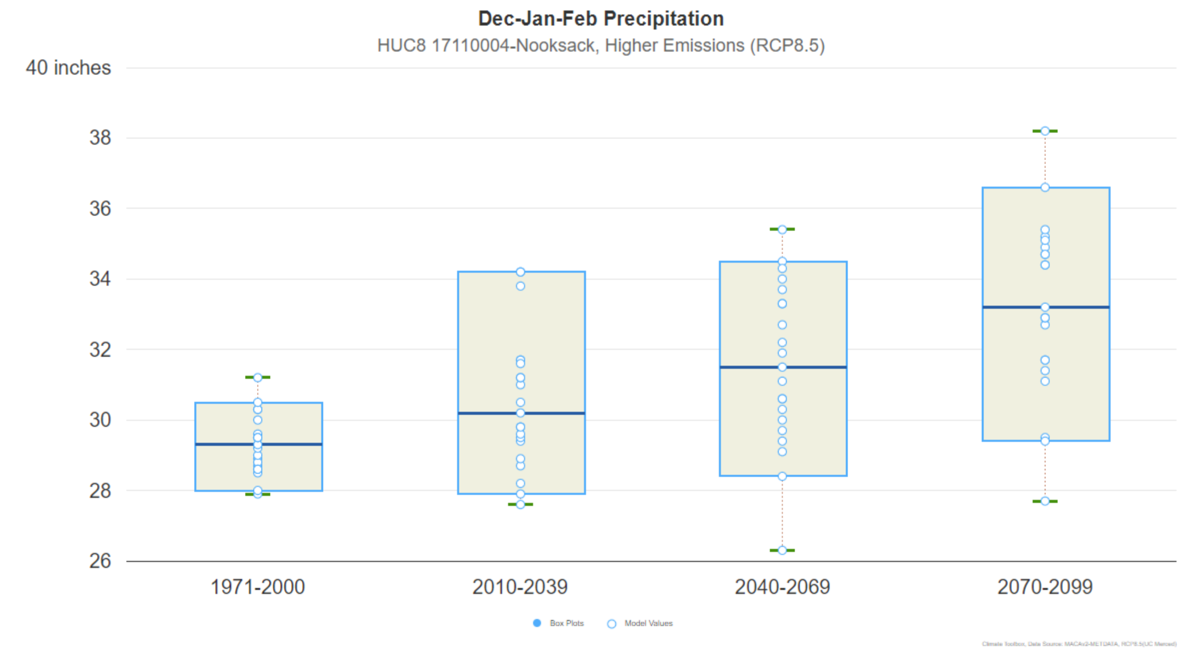

Figure 17. Modeled historic and future winter (i.e., average of December, January, and February) precipitation based on the RCP 8.5 emissions scenario and presenting the distribution of results for individual GCMs (dots) and the ensemble median (horizontal black line). Figure from Hegewisch and Abatzoglou (2024).

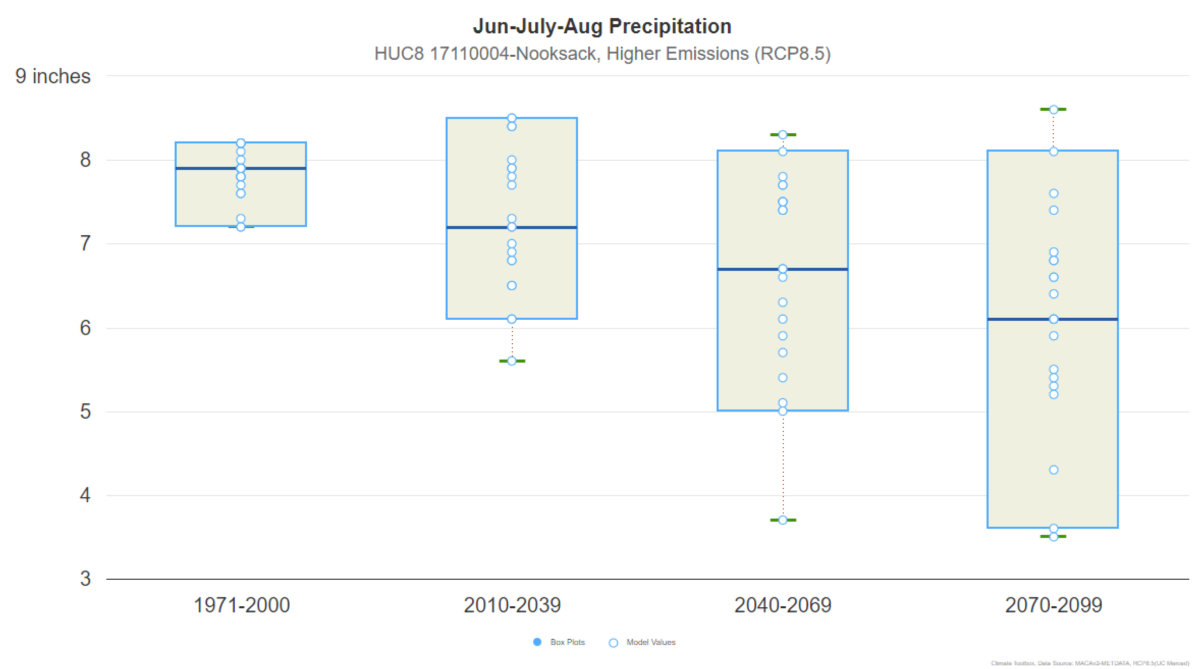

Figure 18. Modeled historic and future mean summer (i.e., June, July, and August) total precipitation based on the RCP 8.5 emissions scenario and presenting the distribution of results for individual GCMs (dots) and the ensemble median (horizontal black line). Figure from Hegewisch and Abatzoglou (2024).

4.6.2 Extreme Precipitation

In addition to projections for increasing winter precipitation averaged over monthly and seasonal time scales, the precipitation intensity (i.e., amount of precipitation per hour or day) associated with atmospheric river events is projected to increase (Warner and Mass 2017). Atmospheric river (AR) events occur when a narrow plume of water vapor extends from the tropical or subtropical Pacific Ocean to western North America, bringing warm air temperatures and intense precipitation (Ralph and Dettinger 2011), and are the main driver for peak flow events in Western Washington (Neiman et al. 2011). Increased precipitation intensity during these events due to increased temperature will contribute to increased peak flow events.

4.7 Implications of Temperature and Precipitation Changes

The projected increases in future temperatures across all seasons along with changing precipitation patterns combine in three major ways, which will influence hydrology, aquatic habitat, and terrestrial habitat:

1. On an annual basis, both temperature and precipitation are increasing, resulting in warmer air temperatures and more total precipitation (Figure 19).
2. During winter, both temperature and precipitation are increasing, resulting in warmer and wetter winters, along with change in the fraction of precipitation that falls as rain versus snow and consequent changes in timing and duration of spring freshet flows (Figure 20).
3. During summer, temperature is increasing and precipitation is decreasing, resulting in warmer and drier summers, which has implications for summer water availability to both aquatic and terrestrial ecosystems and for water temperature (Figure 21).

In all cases, the ensemble of GCMs project much less variability for the warming trend and more variability in the precipitation trend. This is illustrated in the figures below by the lack of overlap of groups of colored dots, which represent all of the GCM results for a given time period, relative to their position along the x-axis (future temperature) and by substantial overlap relative to their positions along the y-axis (future precipitation). Thus, in general, impacts related to warming have more certainty than impacts related to precipitation changes.

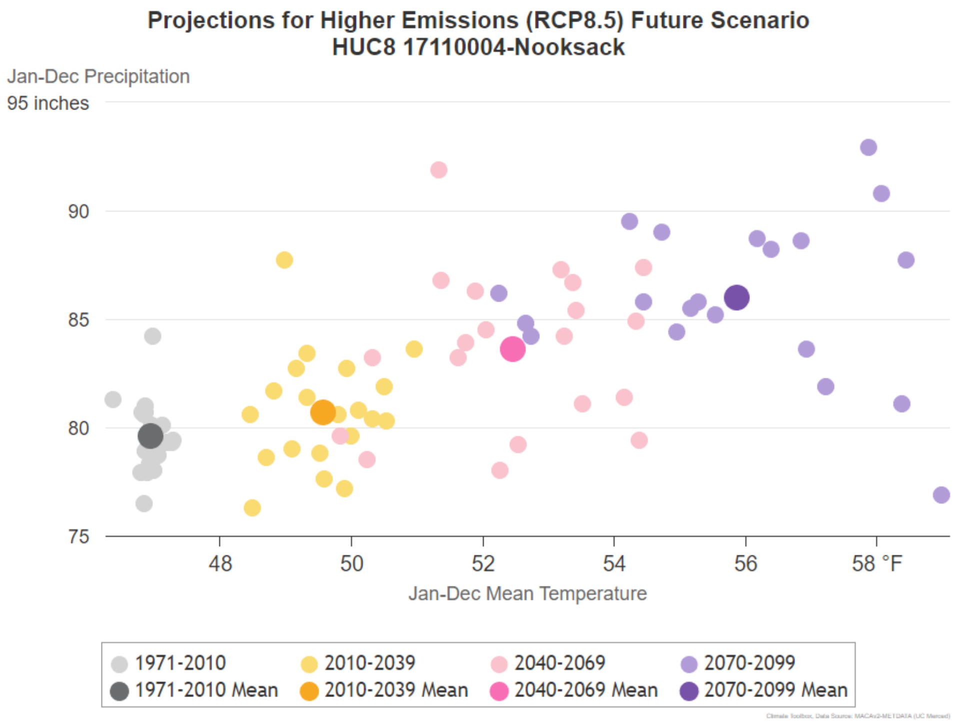

Figure 19. Modeled historic and future annual mean temperature versus annual total precipitation for the Nooksack HUC-8 based on RCP 8.5.

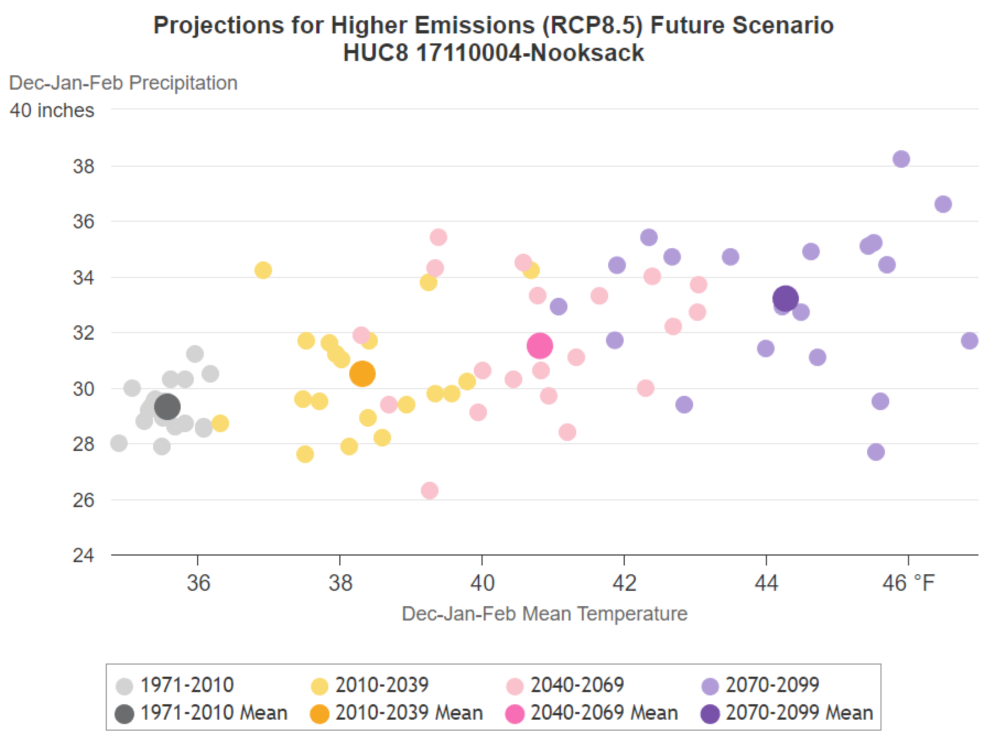

Figure 20. Modeled historic and future winter mean temperature versus total winter precipitation for the Nooksack HUC-8 based on RCP 8.5.

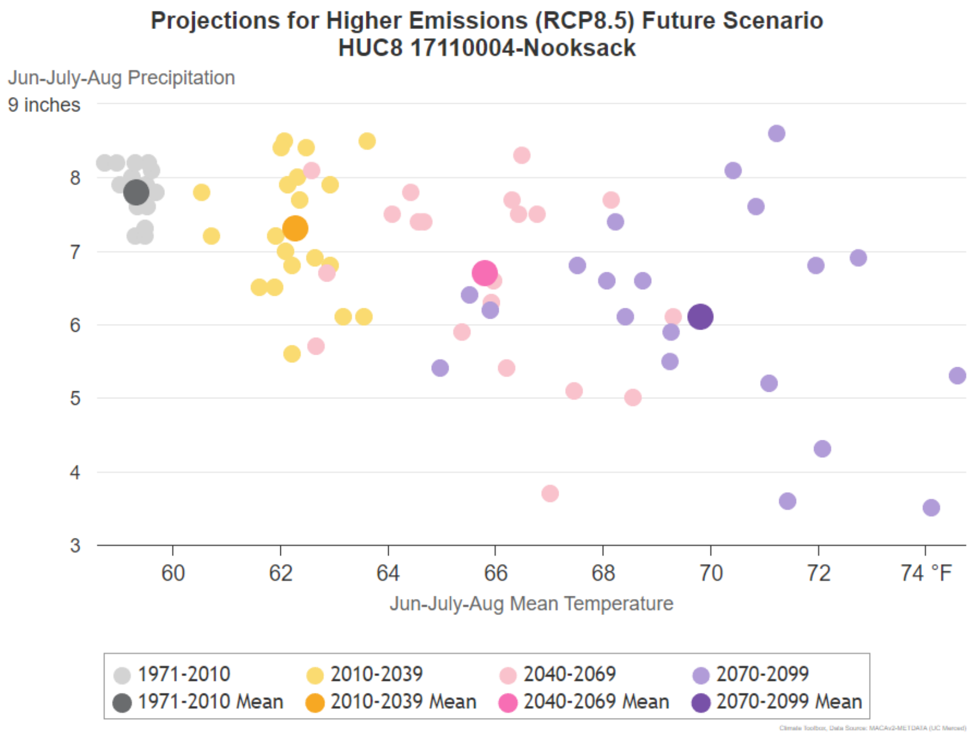

Figure 21. Modeled historic and future summer mean temperature versus summer precipitation for the Nooksack HUC-8 based on RCP 8.5.

4.8 Climate Change Impacts

4.8.1 Streamflows

Increases in temperature and changes in precipitation will have three direct impacts on the timing and magnitude of streamflows in the SFNR (Figure 22):

1. larger magnitude and more frequent peak flows during late fall through winter;
2. a decline in the snowmelt-driven freshet flows that historically occur in the late spring to early summer period, with a shift toward more streamflow earlier in the year, and;
3. lower and warmer summer streamflows.

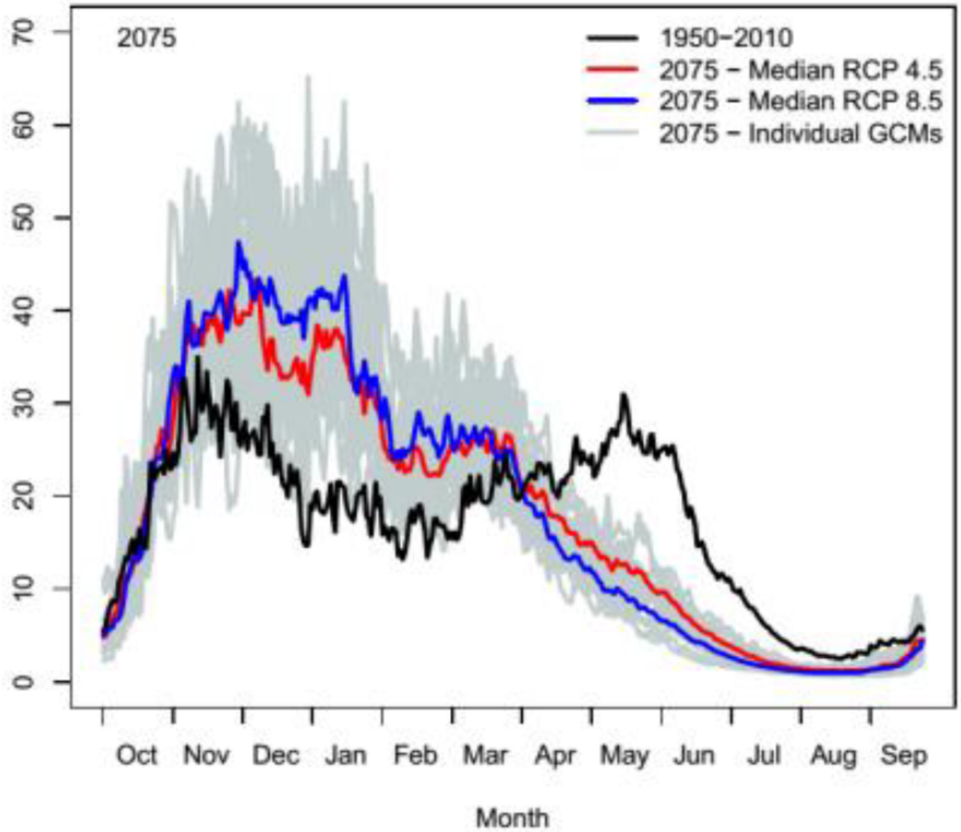

Figure 22. Modeled historic and late century streamflow (y-axis, in cubic meters per second) at the USGS Wickersham gage (12209000) showing the ensemble medians for RCP 4.5 (red) and RCP 8.5 (blue) and the spread projected by individual GCMs (gray lines). Taken from Figure 17 of Murphy (2015).

The magnitude of each of these hydrologic impacts can be projected by using modeled future temperature and precipitation data as the meteorological input data for hydrologic models that simulate streamflow based on climate and watershed characteristics (e.g., soils, landcover, topography).

Related to peak flows, increases in the frequency and intensity of winter precipitation events coupled with warmer winter temperatures will result in larger peak flow events (Table 3). These peak flow increases will be driven by increased precipitation during atmospheric river events combined with warmer temperatures that result in a larger area over which precipitation falls as rain rather than being stored as snow. Projections for future peak flows indicate increases of approximately 23% by mid-century and 34% by late-century based on RCP 8.5 (Paul 2023). RCP 8.5 is considered a high-end emissions scenario, and therefore the mid-century value based on RCP 8.5 is a reasonable proxy for late century conditions for a less extreme emissions scenario. The magnitude of increases varies a little between peak flows averaged over different durations (i.e., the 1-hour peak versus the 24-hour peak), but the difference is minimal. In addition to increases in magnitude the timing of peak flows, which historically occur most frequently in December, is projected to shift slightly earlier to November (Paul 2023). We note that other climate impacts modeling efforts have reported even higher increases in peak flows (e.g., a 51% increase in the Q10 in the SFNR; Wenger et al. 2010) but those projections are based on statistical downscaling whereas the more recent work is based on dynamically downscaled climate projections. The more recent approach is thought to be more robust for representing extreme precipitation events (Salathe et al. 2014).

Table 3. Modeled increase in future peak flow magnitudes in the SFNR (from Paul (2023), based on RCP 8.5. The range for each time period and return interval is based on modeling results for different peak flow duration (e.g., 1-hour versus 24-hour peak).

METRIC	DEFINITION	TIME PERIOD	PAUL (2023) MODELING: SFNR AT SAXON BRIDGE (DYNAMICAL DOWNSCALING, RCP 8.5)
			% change vs. historical
Q2	2-year peak flow	2040s	21-24
		2080s	31-38
Q5	5-year peak flow	2040s	22-24
		2080s	31-33
Q10	10-year peak flow	2040s	20-25
		2080s	31-33
Q100	100-year peak flow	2040s	18-29
		2080s	35-44

Related to snowpack and spring streamflows, less precipitation will be stored as snow during the winter months, which will result in a decline in late spring to early summer streamflow peaks that are driven by snowmelt. Basin-wide snow storage is projected to decline 54% (RCP 4.5) to 82% (RCP 8.5) by the 2080s. In the SFNR watershed, snowpack area on April 15 is projected to decline from a historical average of 44% to 26% by mid-century and 11% by late century (based on RCP 8.5 Paul 2023). The characteristic two-peak hydrograph, in which a first period of high flows occurs in winter due to heavy precipitation and a second period occurs in late spring or early summer due to snowmelt begin to coalesce into a single period of winter high flows by the end of the century (Figure 22).

Lastly, summer streamflow and extreme low flows are projected to decline due to the combination of reduced snow storage, reduced summer precipitation, and higher summer temperatures and evapotranspiration. (Table 4). Average summer streamflow in the Black Slough reach is projected to decline by 52% by mid-century and by 65% by late-century (based on RCP 8.5; Wenger et al. 2010). Streamflow magnitudes during extreme low flow events such as the 7-day minimum flow with a 1-year recurrence interval (7Q1) and with a 10-year recurrence interval (7Q10) are expected to decline by over 30% by late century.

Table 4. Historical and projected future low flow metrics in the SFNR, downstream of the confluence with Black Slough (from Wenger et al., 2010)

METRIC	DEFINITION	TIME PERIOD	STREAMFLOW	
			cfs	*% change vs. historical*
Mean Summer	Mean flow averaged over June, July, and August	historical	797	
		2040s	355	-52
		2080s	226	-65
7Q1	1-year minimum weekly flow	historical	157	
		2040s	122	-22
		2080s	102	-35
7Q10	10-year minimum weekly flow	historical	127	
		2040s	97	-24
		2080s	80	-37

4.8.2 Aquatic Habitat

Declining streamflows and increasing summer air temperatures are projected to result in increased summer stream temperatures and degraded aquatic habitat (Butcher et al., 2016; Truitt, 2018). August stream temperatures in the SFNR are projected to increase from a modeled historic average of 15.3 °C (59.5 °F) to a late century average of 19.2-21.1 °C (66.6-70.0 °F). Furthermore, late century stream temperatures are projected to exceed the 16 °C threshold (based on 7-DADMax) for core summer salmonid habitat for an average of 115 days per year as compared to 41 days during the historical period (based on RCP 8.5).

5 GEOMORPHIC CONDITIONS

5.1 Valley Setting

The Black Slough Reach of the South Fork Nooksack River flows through a broad, glacially formed valley flanked by hillslopes of Eocene sedimentary rock (Chuckanut formation). Channel migration processes have deposited alluvial sediments that have accumulated to a maximum thickness of about 90 feet (Dragovich et al. 1997). The alluvial valley is underlain by a combination of channel deposits composed primarily of cobble- and gravel-sized sediments and finer-grained overbank deposits composed of sand and silt. A large lobe of the Van Zandt Landslide Complex deposited a large volume of sediment approximately 1,300 years ago (Mallick 2018) that partially blocks the lower 1 mile of the South Fork Valley just downstream of the project reach to the confluence with the North Fork Nooksack River. The landslide deposits constrain the alluvial valley to approximately 1,100 feet in width. The alluvial valley then widens upstream of the slide deposits and ranges between 3,000 and 4,000 feet in width through the Black Slough reach (Figure 23 and Figure 24). Glacial outwash terraces flank the alluvial valley and are draped by alluvial fan deposits that have accumulated where tributary drainages emerge into the valley.

5.2 Historical Channel and Floodplain Evolution

Historical maps and aerial imagery, presented in Appendix A, show an evolution of floodplain topography in the Lower South Fork Valley that has resulted in a simplified, less sinuous planform resulting from land use and other hydromodifications. Numerous abandoned channel features are present in the floodplain topography indicating former channel alignments of the South Fork Nooksack River (Figure 25). Collins and Sheikh (2004) previously mapped historical channel changes for the period 1885-1998 and calculated an average annual migration rate of 4.8 m/yr (15.7 ft/yr) based on a series of transects between RM 0 and RM 13. NSD + CGS compiled additional imagery to map channel changes since the previous study and the combined data inventory is summarized below in Table 5. The time series of historical channel features is overlaid together in a map delineating the Historical Channel Migration Zone for the Black Slough Reach in Figure 25.

Surveys completed for the 1885 GLO plat map depict the South Fork Nooksack River as a highly sinuous, meandering channel with multiple secondary channel flow splits that form forested islands. The meander belt is approximately 2,000 feet wide, and meanders had a tight radius of curvature of approximately 500 feet. A prominent flow split upstream of RM 2, and the present-day location of Potter Road, created a secondary channel that connected with tributary inflow from the west side of the valley (Caron Creek). Changes between the 1885 and 1919 maps include a series of bend cutoffs between RM 1 and RM 1.5 that extended the length of the island downstream of Potter Road. The 1919 map depicts the two channels that split upstream of Potter Road as relatively equal in width. The earliest air photos from 1933 show a change toward a single, primary channel and abandoning the former channel that split to the west upstream of Potter Road. The 1933 imagery also shows a major bend cutoff that occurred upstream of Potter Road between RM 2 and RM 3. Black Slough formerly joined with the South Fork near the apex of this bend at the present-day location of the SR 9 bridge crossing Black Slough. Following the pre-1933 bend cutoff, Black Slough flows through the abandoned meander channel to the present-day confluence upstream of Potter Road at RM 2 (Figure 25 and Figure 26).

Previous assessment by Soicher et al. (2006) presents a detailed summary of historical changes in the South Fork Valley noting that influence of logging from the floodplain forest and systematic removal of wood and logjams. Initial clearing of the floodplain forest was largely completed prior to the 1930s. Ongoing efforts by U.S. Army Corps of Engineers cleared wood from the channel through the 1980s. Progressing through the aerial photo record depicts the increasing influence of riprap bank armoring in the project reach that limits opportunity for natural channel adjustments through bend migration.

The combined effects of wood removal and riprap armoring has altered the way that flow, sediment, and wood interact to form aquatic habitat features in the reach. The geomorphic response to early historical impacts is likely to have included an initial period of moderate channel incision coinciding with the bend cutoff at the outlet of Black Slough and abandonment of the split flow channel to the west of the Potter Road Bridge. Concentration of flow into a single, primary channel and loss of hydraulic resistance associated with removal of wood jams increases sediment transport capacity. There does not, however, appear to be a trend of ongoing, long-term incision in the reach. The presence of alluvial bars in the channel and absence of excessive bed coarsening are indicators that the balance between sediment supply and transport capacity is relatively stable. Comparison of ground surface elevations from floodplain features formed by deposition over different times in the historical record suggest the channel profile has been relatively stable since the mid-1900s.

The current channel configuration and extent of riprap bank armoring is shown on a recent aerial image in Figure 25 and Figure 26, and floodplain topography is shown in the Relative Elevation Map (REM) in Figure 27. The REM highlights several abandoned channel features forming swales on the floodplain surface. A prominent flow path to the east of the Potter Road bridge is obstructed by fill placed to raise the road elevation on the approach segment adjacent to the bridge. The REM also highlights an artificial levee constructed in the early 1980s that flanks the channel downstream of Potter Road between RM 1.5 and RM 1.8.

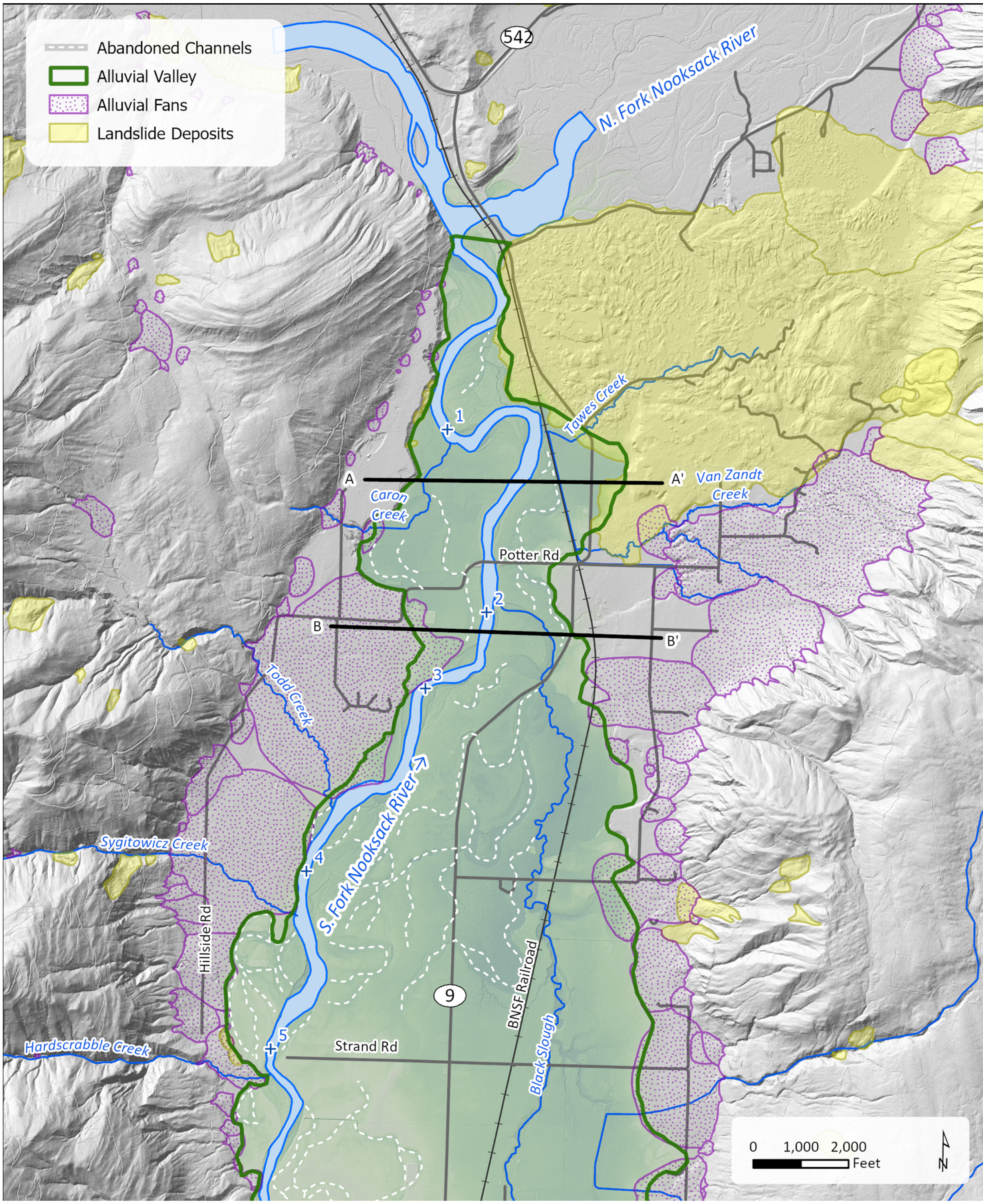

Figure 23. Landform map of the Lower South Fork Nooksack River showing the alluvial valley and abandoned channel features with alluvial fans and landslide deposits along the valley margin.

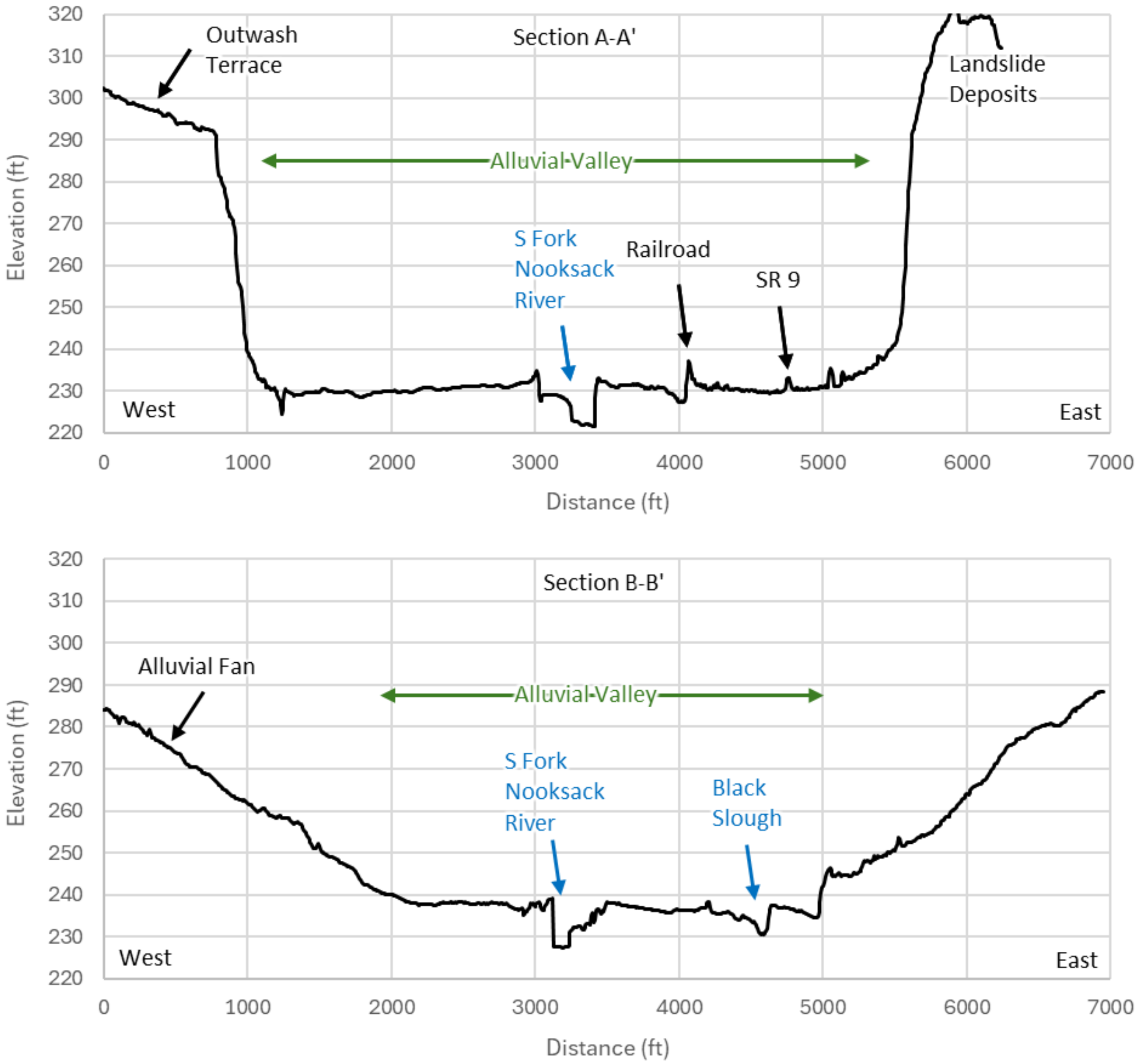

Figure 24. Valley cross sections A-A' and B'-B' showing floodplain topography (2016 lidar)

Table 5. Data inventory of historical maps and imagery.

YEAR	DATA SOURCE
1885	General Land Office plat map
1919	USGS topographic map of Van Zandt Quadrangle (1:62,500). Based on surveys 1917-1918
1933	BW Aerial photo mosaic. Source: Whatcom County Public Works. Georeferenced and digitized by Collins and Sheikh (2004)
1938	BW Aerial photo mosaic sourced from: US Army Corps of Engineers Seattle District. Georeferenced and digitized by Collins and Sheikh (2004).
1955	BW Aerial photo mosaic sourced from: Whatcom County Conservation District. Georeferenced and digitized by Collins and Sheikh (2004).
1967	BW Aerial photo mosaic sourced from: Whatcom County Conservation District. Georeferenced and digitized by Collins and Sheikh (2004).
1976	Color Aerial photo mosaic sourced from: Whatcom County Conservation District. Georeferenced and digitized by Collins and Sheikh (2004).
1986	BW Aerial photo mosaic. Source: Whatcom County Public Works. Georeferenced and digitized by Collins and Sheikh (2004)
1998	BW Aerial photo mosaic (USGS DOQQ)
2006	Color Aerial photo mosaic (USDA NAIP)
2016	Color Aerial photo mosaic (Whatcom County Pictometry)
2023	Color Aerial photo mosaic (USDA NAIP)
2024	Color Aerial photo mosaic derived from NSD drone imagery (April 2024)

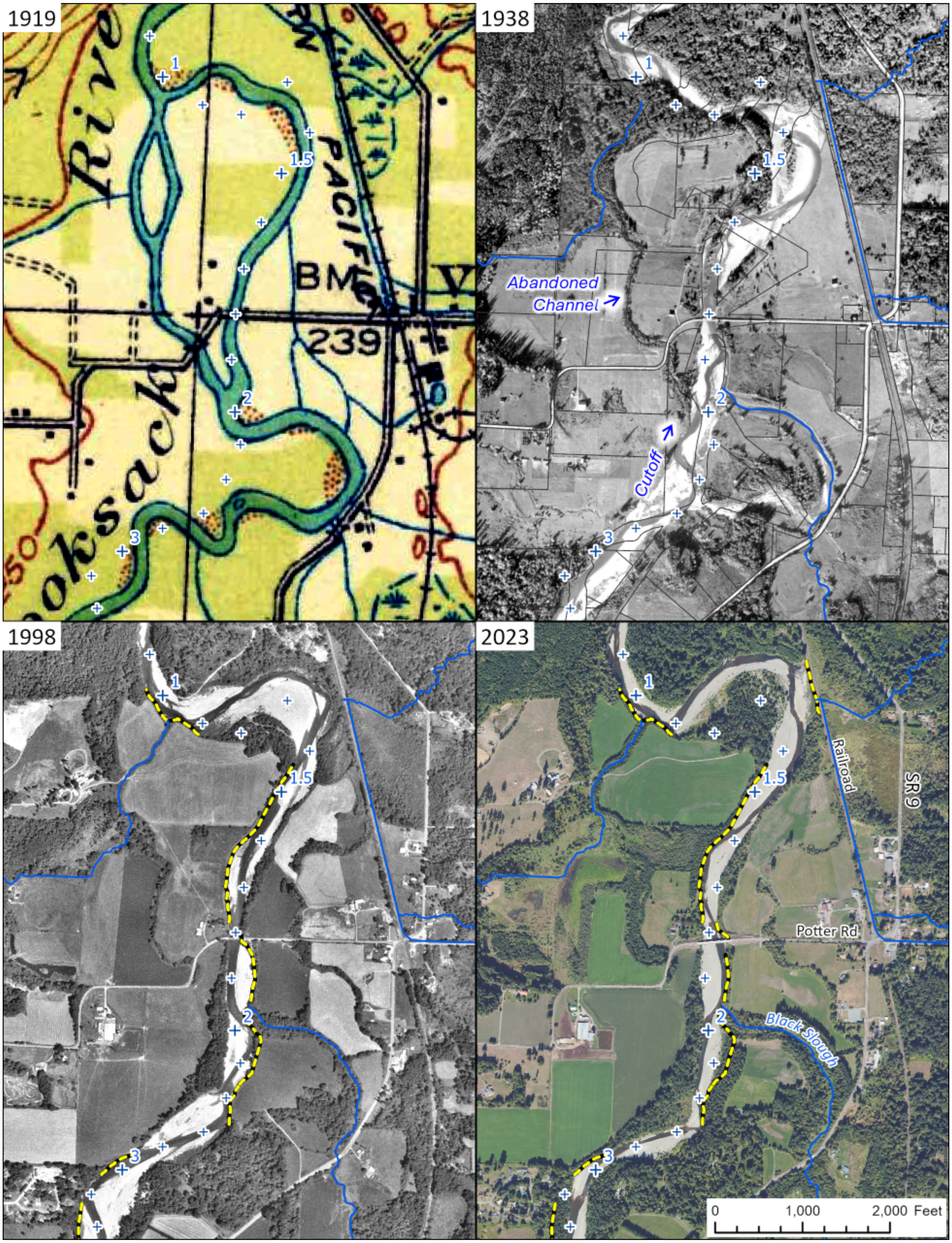

Figure 25. Comparison of historical maps and imagery showing channel changes 1919-2023.

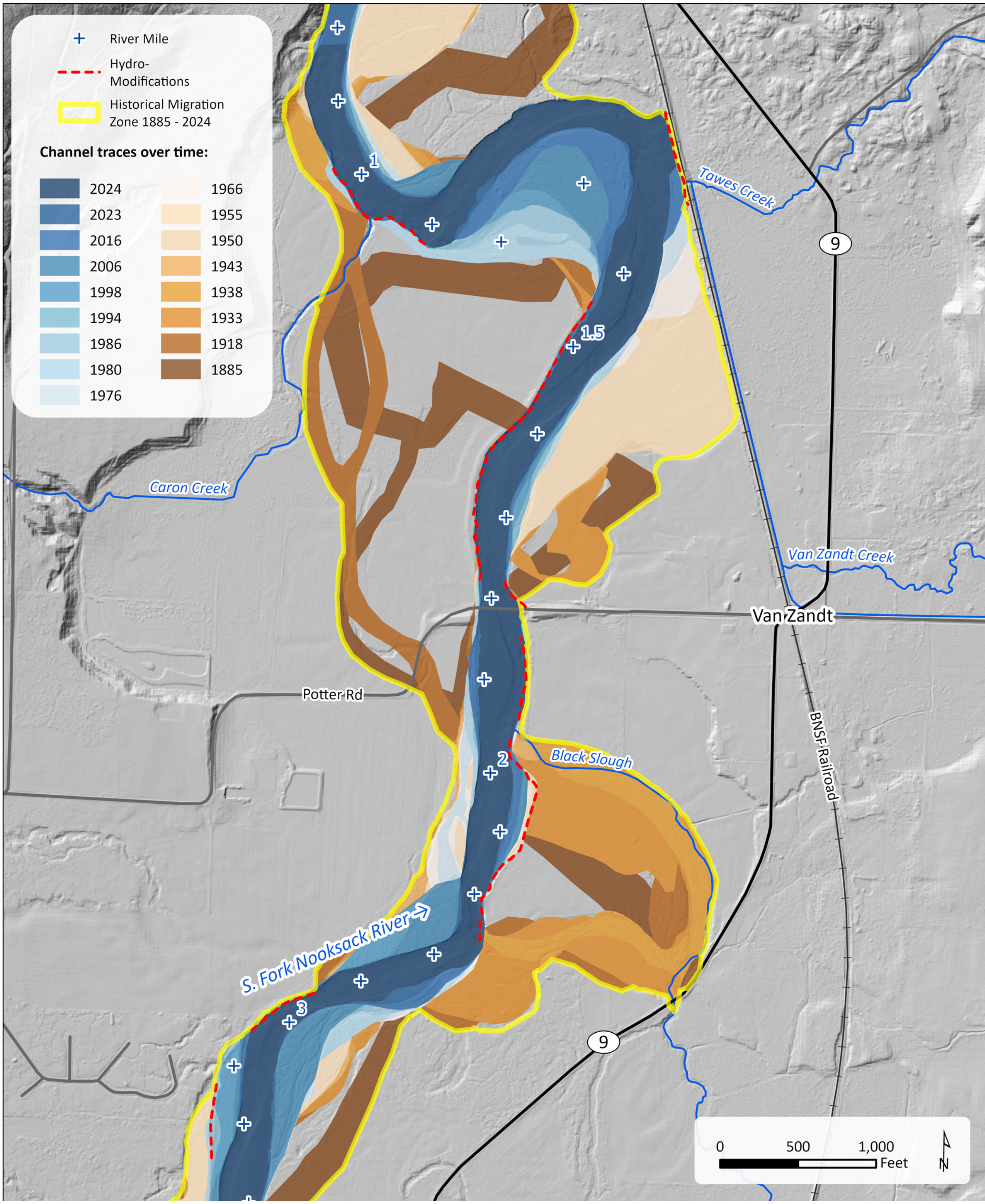

Figure 26. Historical channel traces in the project reach between 1885-2024.

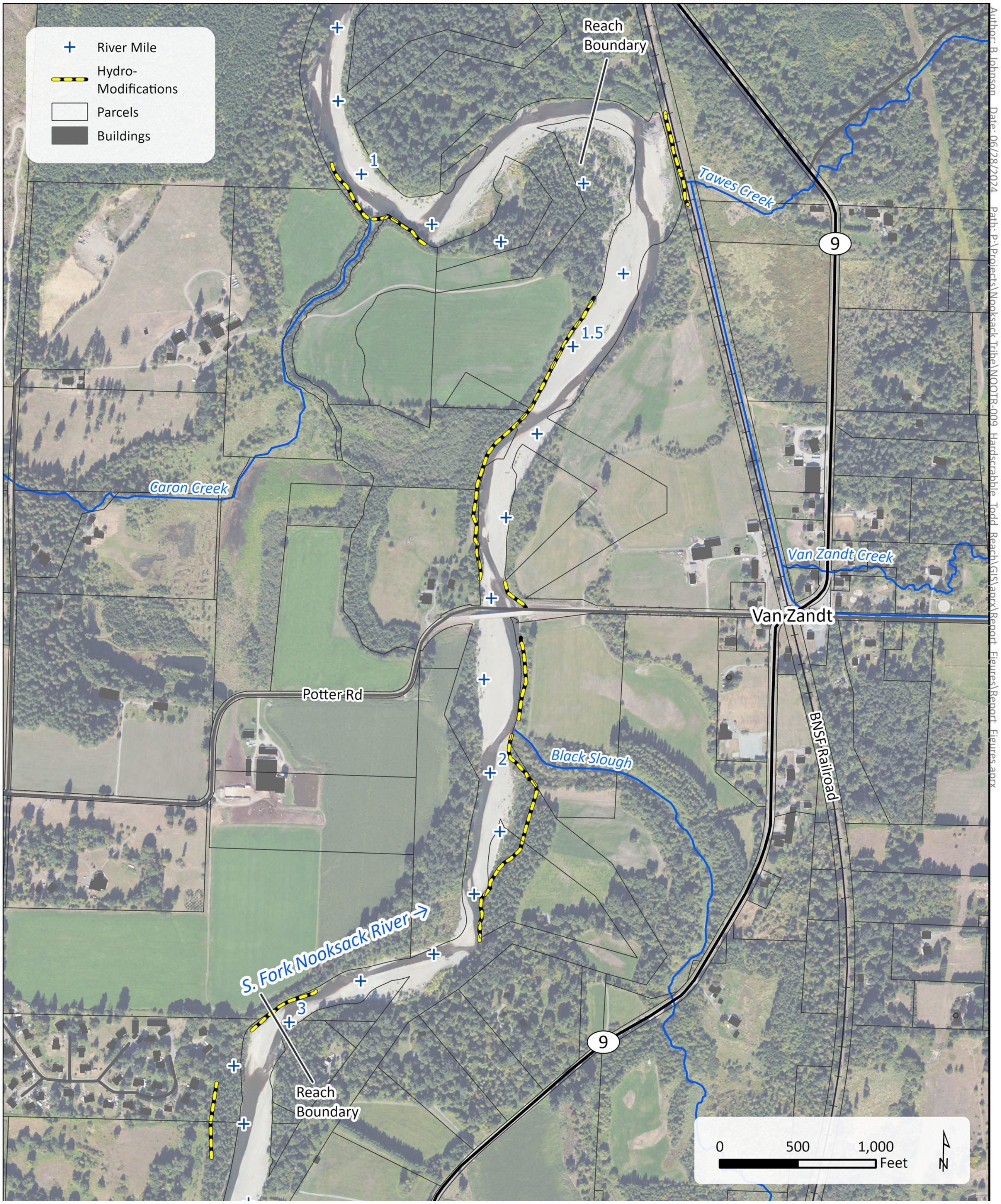

Figure 27. Reference map of the Black Slough Reach study area (2023 NAIP imagery).

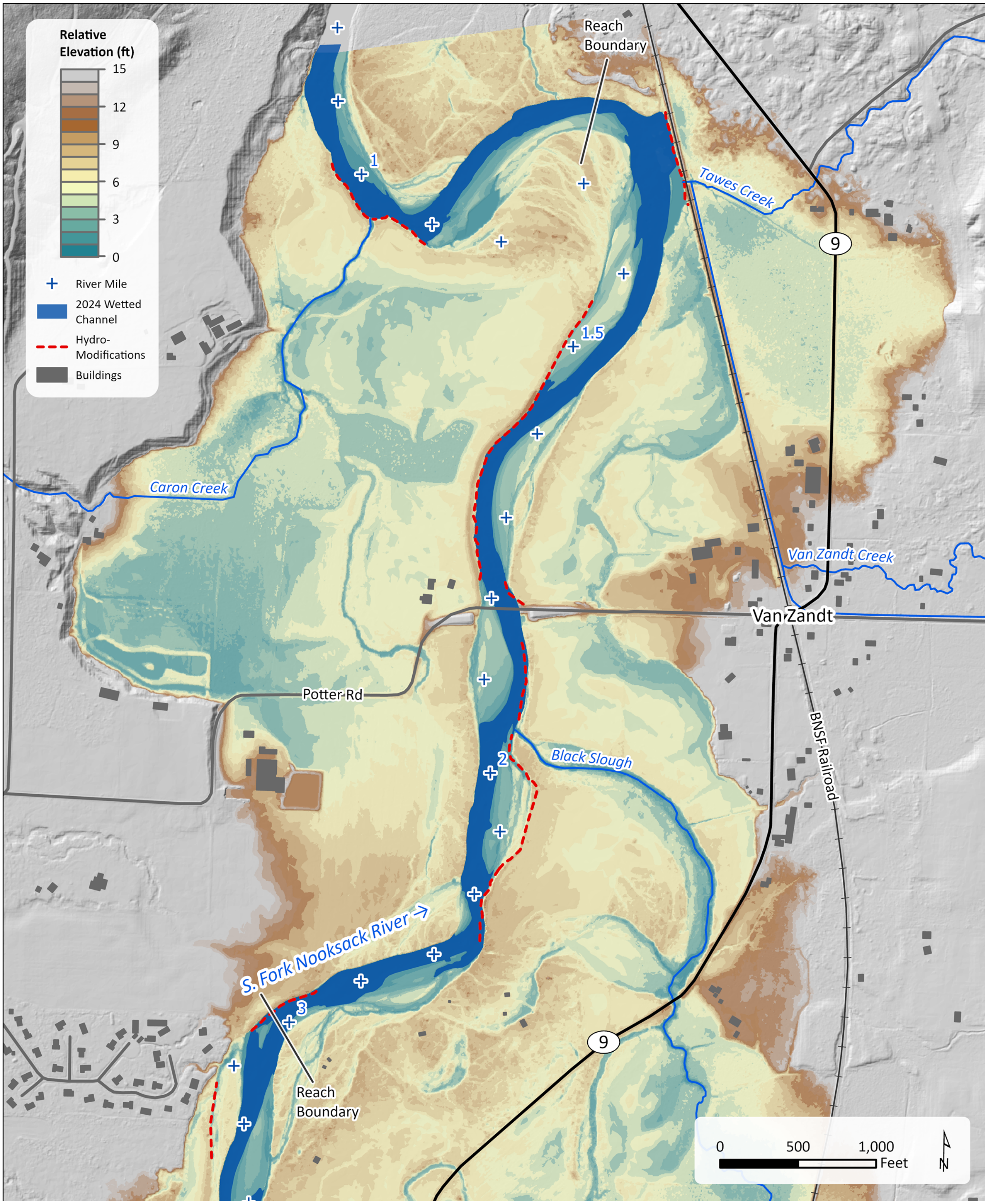

Figure 28. Relative Elevation Model (REM) of the Black Slough Reach study area. Topographic data source: 2016 Lidar and 2024 channel survey.

5.3 Field Reconnaissance and Topobathymetric Survey

NSD + CGS completed a field reconnaissance of the Black Slough Reach in coordination with LNRD to collect observations of current reach characteristics and to collect survey data of active channel in March and April of 2024. Flow was approximately 500 cfs at the USGS gage at Saxon Bridge during the field reconnaissance and survey. Geolocated photos were collected to record observations of the channel and floodplain characteristics. Survey points within the channel were collected from sonar depth measurements that were differenced from the water surface elevation to obtain the elevation of the channel bed. Drone operations were completed to collect aerial imagery that was processed using photogrammetry software to produce an orthomosaic image and Digital Surface Model (DSM). Accuracy was assessed for the orthomosaic and DSM with comparison to 34 ground control points surveyed in the field as well as comparison to 104 additional survey points on gravel bar surfaces yielding an estimated error of 0.2 feet for the DSM derived from drone imagery. A composite topobathymetric surface model was developed by combining sonar data in the wetted channel, drone DSM in gravel bars and areas of bare ground or light vegetation, and 2016 lidar data in floodplain areas outside of the active channel. The REM derived from the composite surface model is shown in Figure 28.

5.4 Reach Characteristics

The Black Slough reach has a low gradient, single thread channel with relatively low sinuosity (Table 6). The active channel (combined area of low flow, wetted channel and unvegetated gravel bars) has an average width of 250 feet. Channel width ranges between 150 feet in segments confined by riprap to 350 feet in areas with recent sediment deposition and bank erosion. There has been a series of riprap bank revetments (hydro-modifications) installed between the 1950s and 1980s to resist erosion along the channel (Figure 27). 53% of the channel length has riprap armor along one or both banks. Retention of large wood has been limited in the project reach. The large wood observed during the field reconnaissance was primarily loose wood that has drifted downstream and accumulated temporarily on bars or out of bank. There was one stable logjam observed at the downstream end of the reach adjacent to the railroad trestle near RM 1.3. The channel substrate is predominantly composed of gravel sized sediments with a median grain size diameter of 31 mm (1.2 in) and less than 10% of the sediment in the small cobble size class (64-90 mm / 2.5-3.5 in).

Table 6. Summary of reach characteristics

REACH CHARACTERISTIC	MEASUREMENT
Slope	0.0015%
Sinuosity (L channel / L valley)	1.16
Active Channel (Bankfull) Width	250 ft
Median Sediment Grain Size	31 mm (gravel)
% Armored Bank	53%

Segment 1 (RM 2.9 – RM 3.1)

The channel flows along a 500-foot-long riprap revetment that armors the left bank at the upstream end of the reach near RM 3 (Figure 29). The revetment was installed in the 1950s to protect the agricultural field from erosion. There has been scour along the toe of the riprap and portions of the bank have sloughed into the channel exposing the alluvial bank material. Overbank deposition has accumulated on the point bar that formed oppo site the left bank revetment and a small overflow channel crosses the floodplain on the inside of the bend reconnecting to the main channel from the right bank near RM 2.9.

Figure 29. Oblique aerial photo (April 2024) showing the riprap revetment at RM 3.

Segment 2 (RM 2.4 – RM 2.9)

The channel opens to an unconfined segment downstream of the left bank revetment. The channel has alternated between left bank and right bank erosion in recent decades; depositing a bar on the opposite bank as it migrates. The recent trend has shifted the thalweg toward the left bank and eroded approximately 25 ft between RM 2.6 and RM 2.8. The left bank erosion is reworking alluvial sediments deposited since the 1990s and wood recruitment is primarily young deciduous vegetation. Gravel deposition has formed a large bar surface that extends from the right bank upstream of RM 2.5 (Figure 30). An overflow channel was observed on the floodplain surface landward of the left bank and cutting off the inside of the bend between RM 2.4 and RM 2.8.

A riprap revetment armors the right bank where the channel makes a sharp bend to the north at RM 2.5. The riprap was installed in the 1950s to protect adjacent property from erosion and limits connectivity to the historic meander channel landward of the right bank. There has been scour at the toe of the riprap revetment at RM 2.5 and an approximately 60-foot-long segment of the riprap has failed allowing the channel to erode around the remaining riprap downstream.

Figure 30. Oblique aerial photo (April 2024) showing the unconfined channel segment between RM 2.6 and 2.9 and riprap revetment near RM 2.5.

Segment 3 (RM 2 – RM 2.5)

This segment follows the alignment of the bend cutoff channel that disconnected the historic meander prior to the 1930s. Black Slough currently flows through the lower half of this cutoff meander and joins the South Fork at its confluence near RM 2. Riprap armor was previously installed along the right bank but the thalweg has shifted toward the left bank since the 1990s and recent sediment deposition has filled in the channel that previously flowed along the riprap upstream of Black Slough (Figure 31). A large amount of mobile wood has accumulated on the upper bar and floodplain surface along the right bank, however, this wood is not well engaged with the flow and provides limited geomorphic function or habitat value. Riprap is exposed along the right bank for a segment of approximately 200 feet upstream of Black Slough. Black Slough drains through the relict meander channel to its confluence with the South Fork Nooksack near RM 2 (Figure 32). The lower segment of the slough has a fine-grained substrate and flanked by deposits with emergent vegetation.

Segment 4 (RM 1.6 – RM 2)

The South Fork continues in a relatively straight alignment downstream of Black Slough and crosses Potter Road near RM 1.8 (Figure 33). The Potter Road bridge was replaced with a longer span by Whatcom County in 2015. A second bridge crosses a slough channel to the west of the main bridge on Potter Road. There was a historic channel connection from the left bank to the slough channel that appears to have been connected through the 1950s. Imagery from 1967 shows the connection between the South Fork and the left bank slough channel was cleared and plowed for agricultural land use. There is a swale crossing the agricultural field that receives over flow during flood events which drain northwesterly through the old bridge and along the historic channel alignment. The slough channel connects to a constructed wetland in the left bank floodplain downstream of Potter Road.

The main channel thalweg has alternated between left and right bank through the Potter Road subreach forming a bar though deposition on the opposite bank. In recent years (since 2006) the thalweg has been oriented along the right bank upstream of the bridge and crosses over to the left bank just downstream of the bridge. There was a riprap revetment that previously armored the right bank upstream of the bridge since the 1960s, however, the right bank has eroded laterally approximately 40 feet since 2016 and none of the previously mapped riprap was observed in the 2024 field reconnaissance. The right bank erosion has initiated some localized wood recruitment creating some complexity upstream of the bridge, however, the recently recruited wood does not appear stable and is likely to be mobilized by future high flow events. There are some recently (2015) placed wood along both banks downstream of Potter that are anchored by large boulder and chain (Figure 34).

Downstream from Potter Road the channel flows along a left bank riprap revetment and an artificial levee follows the left bank between RM 1.6 and RM 1.8 (Figure 35). The levee and riprap revetment was likely installed in the early 1980s to limit erosion to an adjacent agricultural field. An approximately 100-foot-long segment of the riprap near RM 1.7 has washed out resulting in slumping of the bank material. Recent deposition has accumulated along the right bank forming a gravel bar downstream of Potter Road.

Figure 31. Oblique aerial photo (April 2024) of the confluence with Black Slough and upstream channel segment.

Figure 32. Photo of the outlet from Black Slough at the confluence with the South Fork Nooksack River.

Figure 33. Oblique aerial photo of the South Fork Nooksack River

Figure 34. Logs and boulders placed along bank downstream of the Potter Road Bridge.

Figure 35. Oblique aerial view (April 2024) showing the left bank segment downstream of Potter Road.

Segment 5 (RM 1.3 – RM 1.6)

The downstream segment of the project reach forms the upper half of a large amplitude meander between RM 1.1 and RM 1.5. The left bank riprap revetment extends downstream of RM 1.5. Recent channel migration trends have shifted the thalweg toward the right bank between RM 1.3 and RM 1.5 and intersects the railroad alignment near RM 1.3 where a recently placed (2015) riprap revetment protects the railroad embankment from erosion. The property to the landward side of the railroad (between the railroad and SR 9) is a large floodplain wetland mosaic that receives tributary inflows. The wetland mosaic is outside of the Historical Channel Migration Zone but would be connected to the mainstem in the absence of the fill placed for the railroad embankment.

The unprotected segment of the right bank upstream of RM 1.3 has eroded as much as 100 feet since 2016. Wood recruitment from the right bank erosion has contributed to formation of a logjam adjacent to the railroad trestle near RM 1.3. This jam appears to have developed from a large tree recruited to the channel in 2010 and wood has accumulated in front of the key piece. The size of the wood jam has varied since 2010 with additions and losses of racked wood but the core of the jam has remained stable. The amount of racked wood observed in the 2024 reconnaissance is the largest the jam has been in the photo record since 2010.

Downstream of RM 1.3 the meander continues westerly and connects to the outlet of Caron Creek which follows the flow path that was occupied by a split flow channel of the South Fork Nooksack River as recently as 1919 (Figure 25). A series of nine Engineered Logjams were previously constructed along the right bank in a 2010 project implemented by the Nooksack Indian Tribe.

Figure 36. Right bank segment upstream of RM 1.3 and disconnected floodplain wetland.

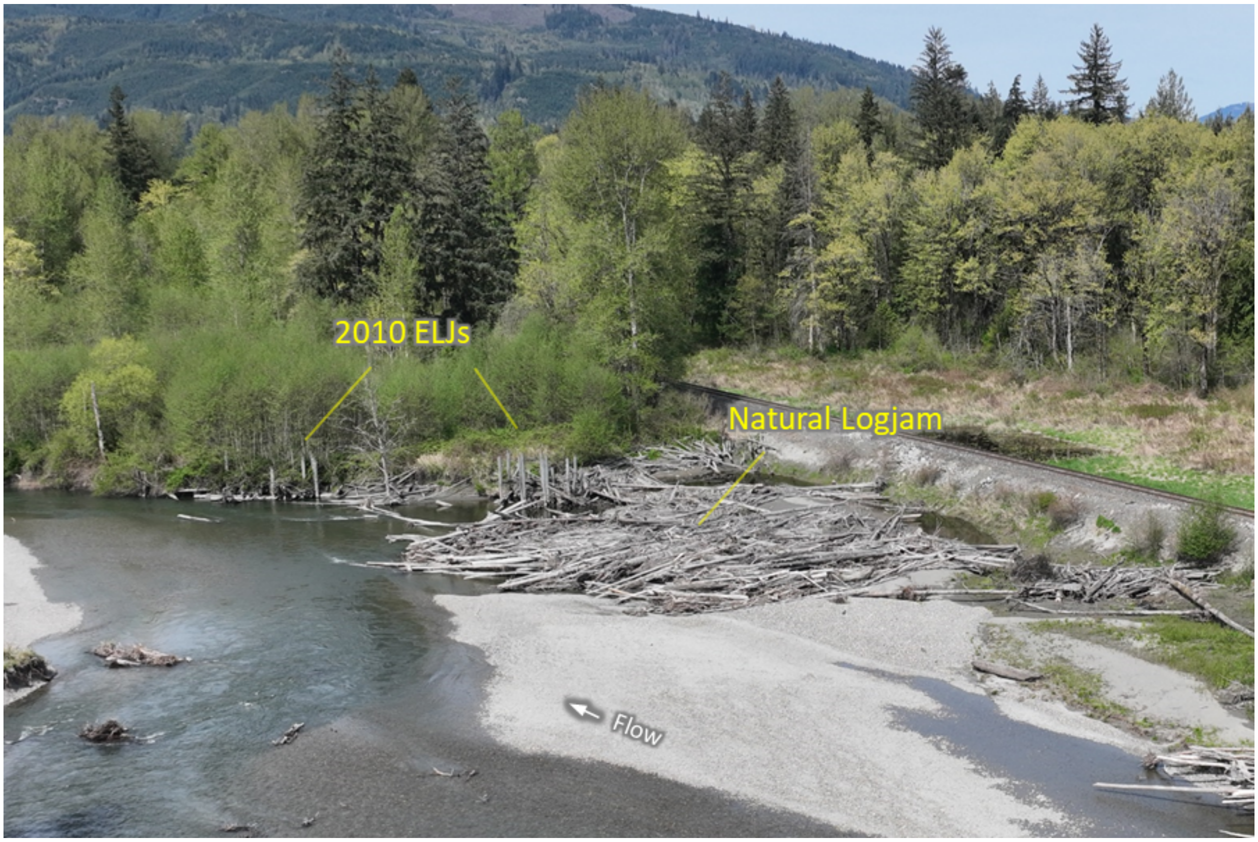

Figure 37. Oblique aerial view (April 2024) showing the 2010 ELJs placed downstream of RM 1.3 and natural wood recruitment near the railroad trestle.

6 HYDRAULIC ANALYSES

A hydraulic analysis of the project reach was conducted to better understand how hydraulic conditions relate to habitat conditions and geomorphic processes impacting the formation and evolution of channel and floodplain habitat features. The findings of the hydraulic analysis were used to inform our overall reach assessment and allow us to better understand conditions experienced at the specific flows modeled during this assessment.

6.1 Existing Conditions Model Development

The hydraulic analysis for this effort was performed using the two-dimensional capabilities within the Army Corps of Engineers HEC-RAS 6.4.1 computer program. Pre- and post-processing of model inputs and outputs was completed within the RASMapper user interface. RASMapper is a GIS-based module within HEC-RAS used to develop computational meshes, and model inputs. HEC-RAS then performs calculations to solve the two-dimensional form of the depth-integrated Navier-Stokes equations, also known as the ‘Shallow Water Equations’, to compute depth (within each cell in the mesh) and velocity (at each cell face in the mesh). Model inputs and parameters were developed as described in the following subsections.

A single hydraulic model was developed which includes both the Black Slough project reach and the Hardscrabble-Todd reach which abuts the project reach on the upstream side. The Nooksack Indian Tribe (NIT) is pursuing habitat restoration actions in the adjacent upstream reach on a similar timeline as the effort for this project (NSD + CGS) is supporting that effort as well) and there is at least a potential that proposed project actions in one reach or the other could influence hydraulic conditions in the other reach, particularly if project actions influence floodplain hydraulic conditions in Black Slough which flows back into the mainstem channel near the upstream end of the Black Slough reach. These considerations led us to develop a single, joint hydraulic model that encompasses both project reaches and the adjacent floodplain rather than independent models for each project reach (Figure 38).

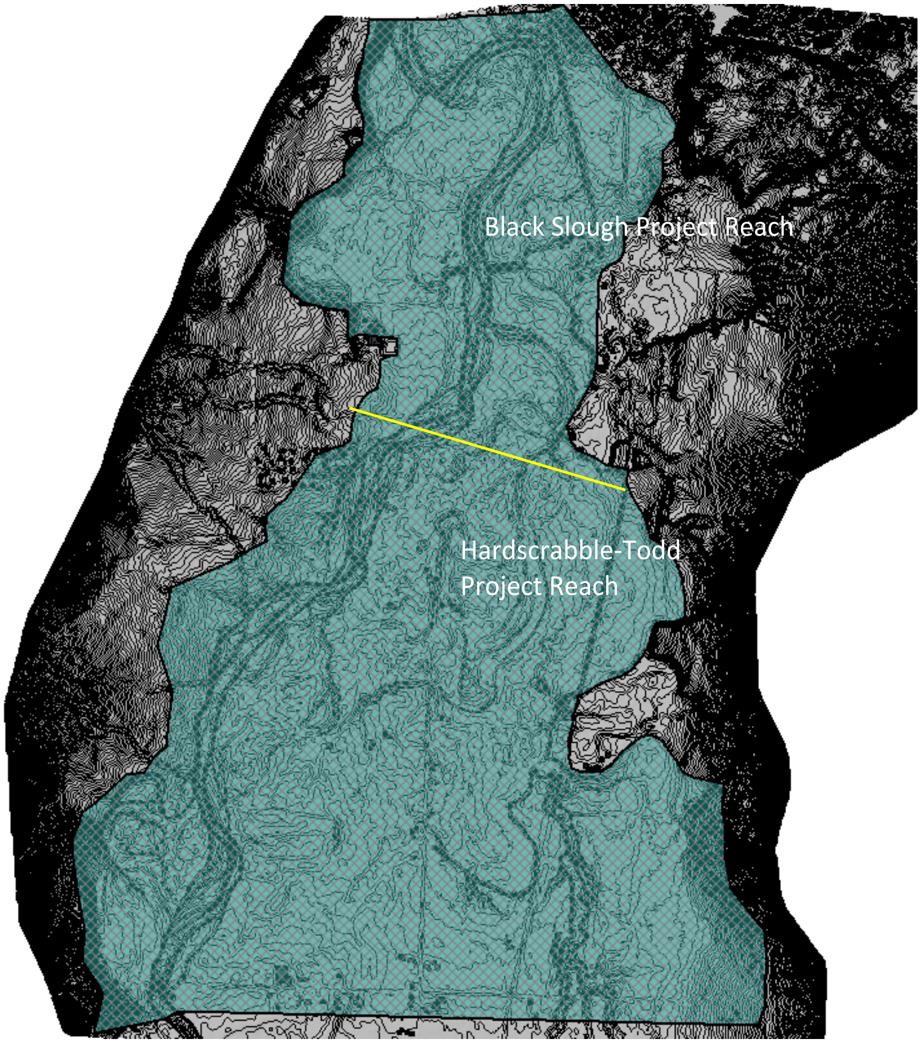

Figure 38. Hydraulic model domain extents.

6.1.1 Model Topography

The composite surface model developed during our site assessment was used as the underlying terrain when developing the hydraulic model. This terrain represents conditions as of the time of our data collection effort and notably relies on hydro flattened LiDAR to define topography within Black Slough proper on the right bank floodplain. An examination of the LiDAR dataset suggests that standing water was present in at least some locations within the slough and therefore likely does not represent actual topography in these locations.

For this assessment, the composite surface model was deemed to be a sufficient representation of real-world conditions. We have been in contact with the Washington State Department of Natural Resources (DNR) and expect that an updated topobathymetric LiDAR dataset will be published on the public LiDAR Portal available through the DNR website at some point later in 2024. When that becomes available we will develop a new composite surface to utilize with continued modeling efforts associated with future design and analysis phases.

6.1.2 Model Hydrology

Inflows to the hydraulic model were identified at the upstream end of the hydraulic model and at five of the largest tributary drainages that flow into the SFNR valley within the model domain (Figure 39). NSD + CGS and LNR previously agreed that 4 different flows would be modeled for this effort: two geomorphically relevant flows, the 100-year return interval flow, and the 100-year flow including climate change projections. Our team elected to model the following flows for this assessment:

- 2-yr flow (frequent, bed-mobilizing event)
- 10-yr flow (less frequent, low flood stage event)
- 100-yr flow (infrequent, extreme flood, design event)
- 100-yr + climate change (infrequent, future conditions extreme flood)

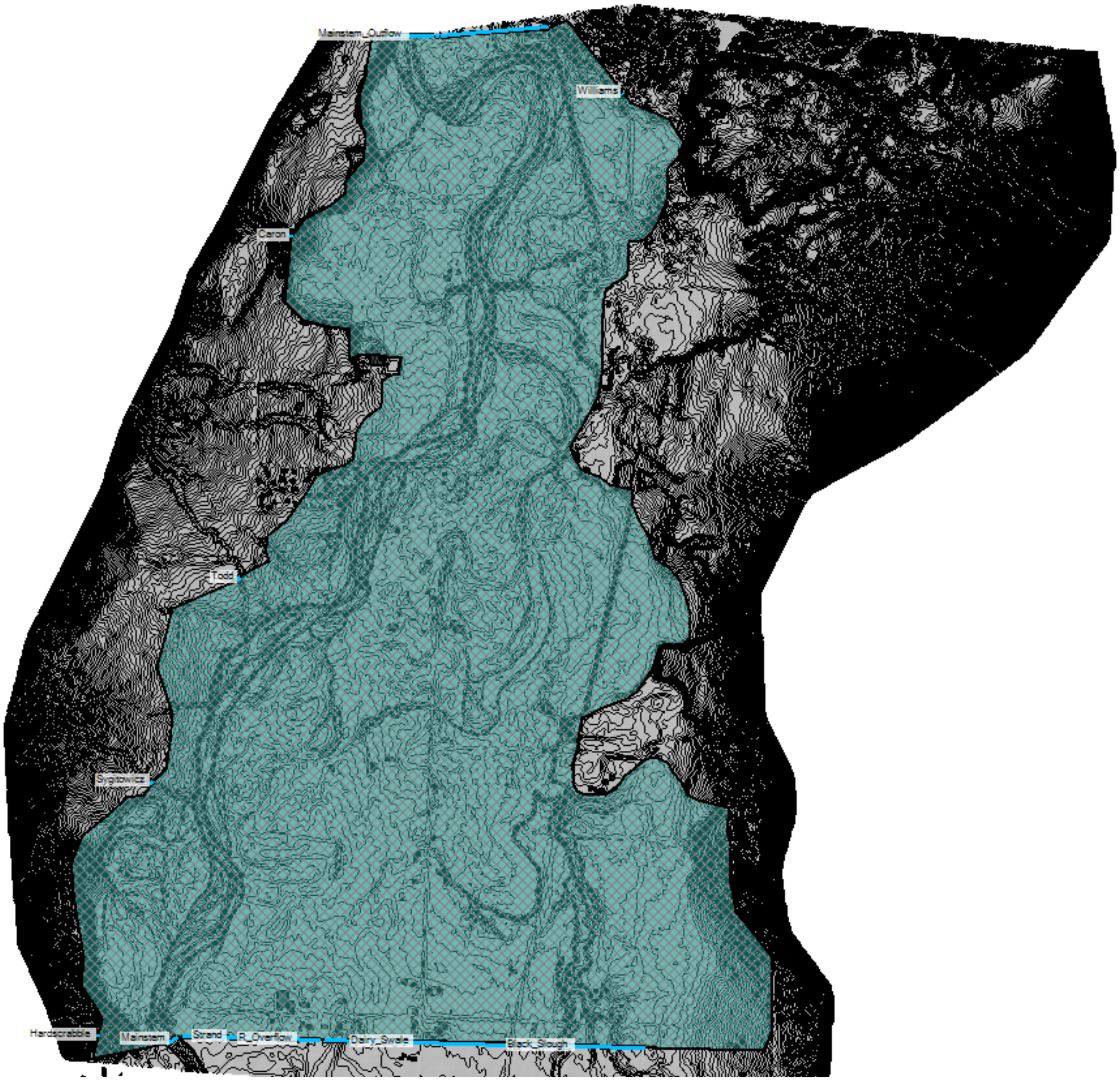

Figure 39. Inflow locations to hydraulic model domain.

Boundary conditions for the hydraulic model were based primarily on the effective model used by FEMA to delineate the Special Flood Hazard Area (SFHA) and floodway. The effective model is a 1-dimensional unsteady flow HEC-RAS model; floodplain topography and flow patterns are represented through multiple flow splits, junctions, and lateral connections. The effective model includes 10-yr and 100-yr model runs; for those flows the following approaches were taken to translate the inflows to the effective 1-D model to NSD's 2-D model:

- Mainstem channel and floodplain inflows at the upstream end of the model domain: time series discharge values from the effective model at each of the five cross-sections that span the SFNR valley were extracted from the effective model and used directly as inflows conditions.
- Lateral inflows: Lateral inflows at each of the five main tributaries were developed using estimates of peak flow magnitude generated from regional regression equations (accessed through the USGS StreamStats application) were fitted to the unit hydrograph used in the effective model to represent tributary inflows.
- Minor adjustments to the mainstem inflow peak value and hydrograph were made based on differences between tributary inflow in the NSD model and the effective model.

To generate boundary conditions for the 100-yr flow when considering climate change impacts, the unsteady flow hydrographs for the 100-yr event were scaled by a factor of 23% to represent the most probable 100-yr return interval flow in the year 2080.

The effective model did not include a 2-yr flow run so appropriate flow hydrographs had to be determined at all inflow locations. A peak flow analysis using the Wickersham gage (USGS gage number 12209000) was conducted in order to generate an estimate of the mainstem discharge magnitude at the 2-yr event. The Wickersham gage was replaced in 2008 by the Saxon gage (USGS gage number 12210000). The Wickersham gage was selected for this exercise due to its longer period of record compared to the Saxon gage (63 years and 16 years, respectively). Peak flow estimates for the 2-year flow were scaled to the ungaged flow location at the upstream end of the model domain using procedures outlined by Mastin et al. (2016). For tributary drainages, estimates of 2-yr peak flow magnitudes were developed using StreamStats. A quasi-steady state 2-yr flow hydrograph was developed for each inflow location; flow ramps up from a low, near baseflow value up to the 2-yr peak flow over a period of 12 hours and then the 2-yr peak flow is held steady for a total of 4 hours.

It's worth noting that the peak flow estimates for the 2-, 10-, and 100-yr events at the Wickersham Gage generated by NSD + CGS for this effort correlate well with other estimates (Table 7). However, the peak flow magnitude in the effective model (calculated by summing the inflows to the model domain) at the project location exceed the peak flow estimates from the Wickersham gage when scaled to the project location. This is likely due to the nested hydrograph form used in the effective model but it is important to note as flows for the 10-yr run in the effective model represents a flow between the 25- and 50-yr event at the Wickersham gage when scaled to the project area and the 100-yr run in the effective model represents closer to the 200-yr flow at the Wickersham gage scaled to the project reach.

Table 7. Comparison of peak flow estimates at the Wickersham gage and the upstream end of the project reach.

PEAK FLOW ESTIMATES AT UPSTREAM END OF MODEL DOMAIN						
Return Interval (years)	Wickersham Gage Peak Flow Estimates (cfs)			Scaled to Project Reach (cfs)		
	NSD	StreamStats	FEMA	NSD	StreamStats	Eff. Model
2	10,026	-	9,850	11,000	11,500	-
5	14,050	14,000	-	16,600	17,100	-

PEAK FLOW ESTIMATES AT UPSTREAM END OF MODEL DOMAIN						
10	16,600	16,700	16,200	20,300	20,900	27,240
25	19,700	20,000	19,000	25,000	25,600	-
50	21,920	22,300	21,700	28,400	29,100	36,470
100	24,070	24,600	24,500	32,200	32,800	39,660
200	26,170	26,900	-	35,800	36,400	-
500	28,900	30,000	31,100	40,800	41,300	47,400

6.1.3 Roughness

Hydraulic roughness was represented by variation in the assignment of Manning's n (Chow 1959) to the mesh. Hydraulic analyses require an assessment of the resistance (drag force) the ground surface and other physical features exert against movement of water. This drag force is commonly referred to as roughness. The most accepted method to assess roughness uses the Manning's n resistance factor (Chow 1959). Common factors that affect roughness values include: channel sediment size, gradation, and shape; channel shape, channel meandering, bank and floodplain vegetation, obstructions to flow, flow depth, and flow rate. The model domain was delineated into several roughness types using recent aerial photographs and in accordance with standard hydraulic reference manuals (Chow 1959; Barnes 1967; Hicks and Mason 1998); Figure 40 illustrates roughness polygons differentiated in this manner within the model domain. Initial model roughness values were selected based on general published values and engineering judgment. Roughness values for each roughness category were adjusted based on findings of the model validation effort (see section 6.1.5).

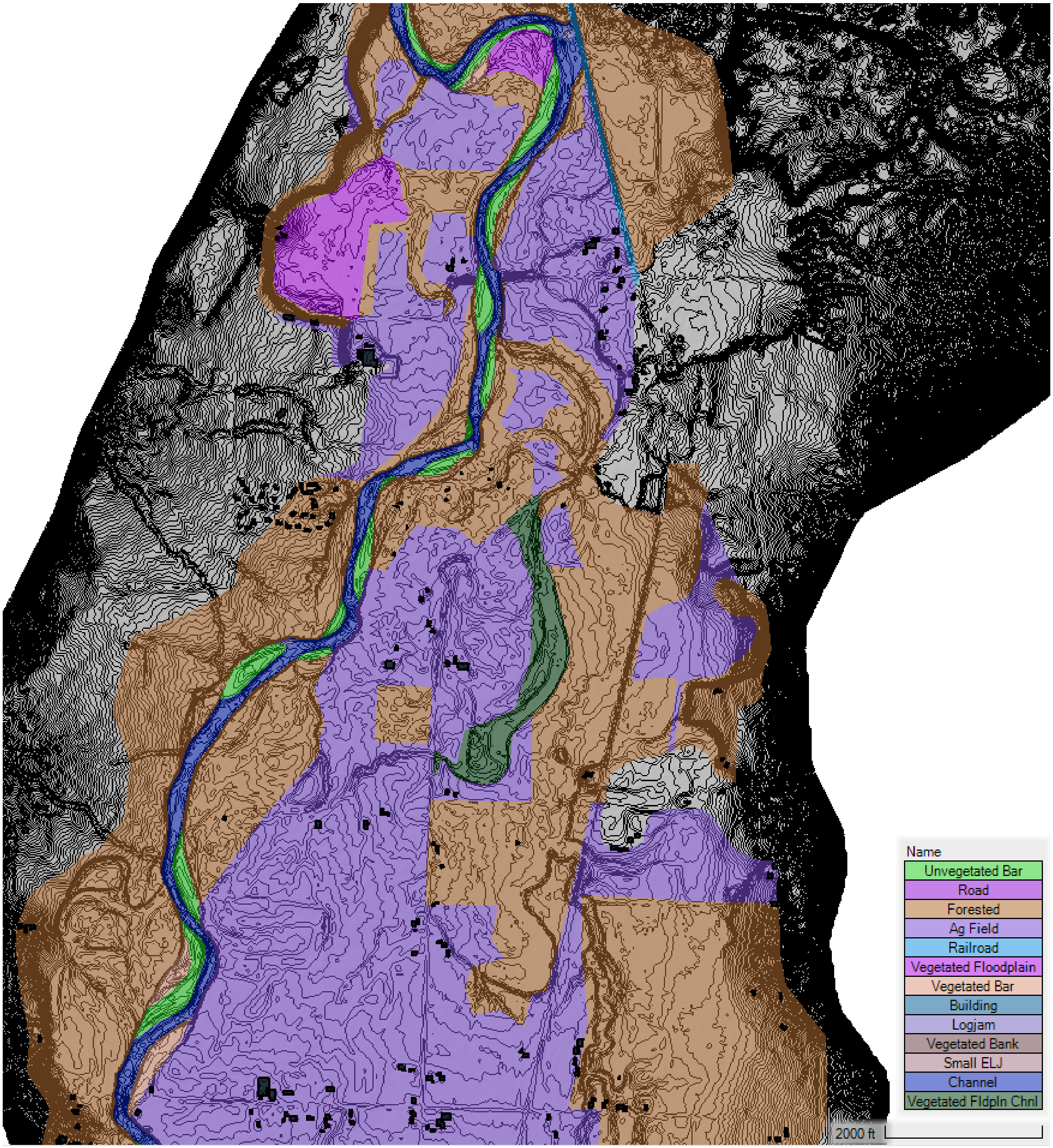

Figure 40. Roughness polygons within 2-D model developed by NSD.

6.1.4 Computational Mesh

The computational mesh required by the hydrodynamic model is a simplified representation of the TIN, a simplification necessary for the computational requirements of 2-D hydraulic models. However, the reduction in mesh density is not uniform; it is higher in areas of interest (such as the main channel) and less dense toward the model domain boundaries. Mesh density was built with 10-foot spacing in the main channel and adjacent areas of interest, and then reduced to 20, 30, 40, and 50-foot intervals toward the extent of the model boundaries. The boundaries of the mesh were extended from RM 0.85 to RM 5.15 and extended across the valley bottom model to ensure the 100-year inundation was within the model mesh. Breaklines were used to refine the model mesh and align cell faces with the prevailing flow direction along the main channel and other floodplain channels and side channels of interest.

Several culverts and bridges are present within the mainstem and floodplain along the project reach and within the hydraulic model domain. A majority of these hydraulic structures are represented in the effective model while in other locations the effective model does not appear to include real-world hydraulic structures. We conducted a detailed review of the hydraulic model domain, cross-referencing the LiDAR topography within the domain against the effective model. At locations where both the effective model and LiDAR topography suggest the presence of a hydraulic structure, the dimensions and elevations for the structure in the effective model were used in our model. In some instances, the LiDAR topography suggests the presence of a hydraulic structure, but no equivalent structure is included in the effective model; in these instances, estimates of appropriate dimensions were developed based on a review of local topography. The elevations and dimensions of the Potter Road Bridge were based on as-built drawings provided by Whatcom County Public Works. The representations of all hydraulic structures (with the exception of the Potter Road Bridge) have not been verified by field examinations or actual survey as this validation was not included in the agreed upon scope of work, however, as design and analysis progresses, field verification of the assumptions used in this modeling effort may be worthwhile.

6.1.5 Model Validation

We attempted to validate our hydraulic model results using several flows covering a wide range of hydraulic conditions based on available data: low flow, moderate flood, and extreme flood.

NSD + CGS conducted bathymetric survey of the mainstem channel covering both the Black Slough and Hardscrabble-Todd project reaches in February of 2024; new orthoimages of both reaches and model domain were also collected around the same time frame. In total NSD + CGS spent 4 days in the field collecting these data; we elected to model a flow representative of median conditions during data collection (approximately 500 cfs at the Saxon gage, scaled to 635 cfs at the project reach). NSD developed an inundation polygon based on the new orthoimage and also utilized field data to generate a water surface elevation representing median conditions during data collection. Modeled water surface elevations and inundation extents were compared to the available data and revisions to the mainstem roughness value were made in iterative fashion until we felt that agreement with available data had been optimized (Figure 41 and Figure 42).

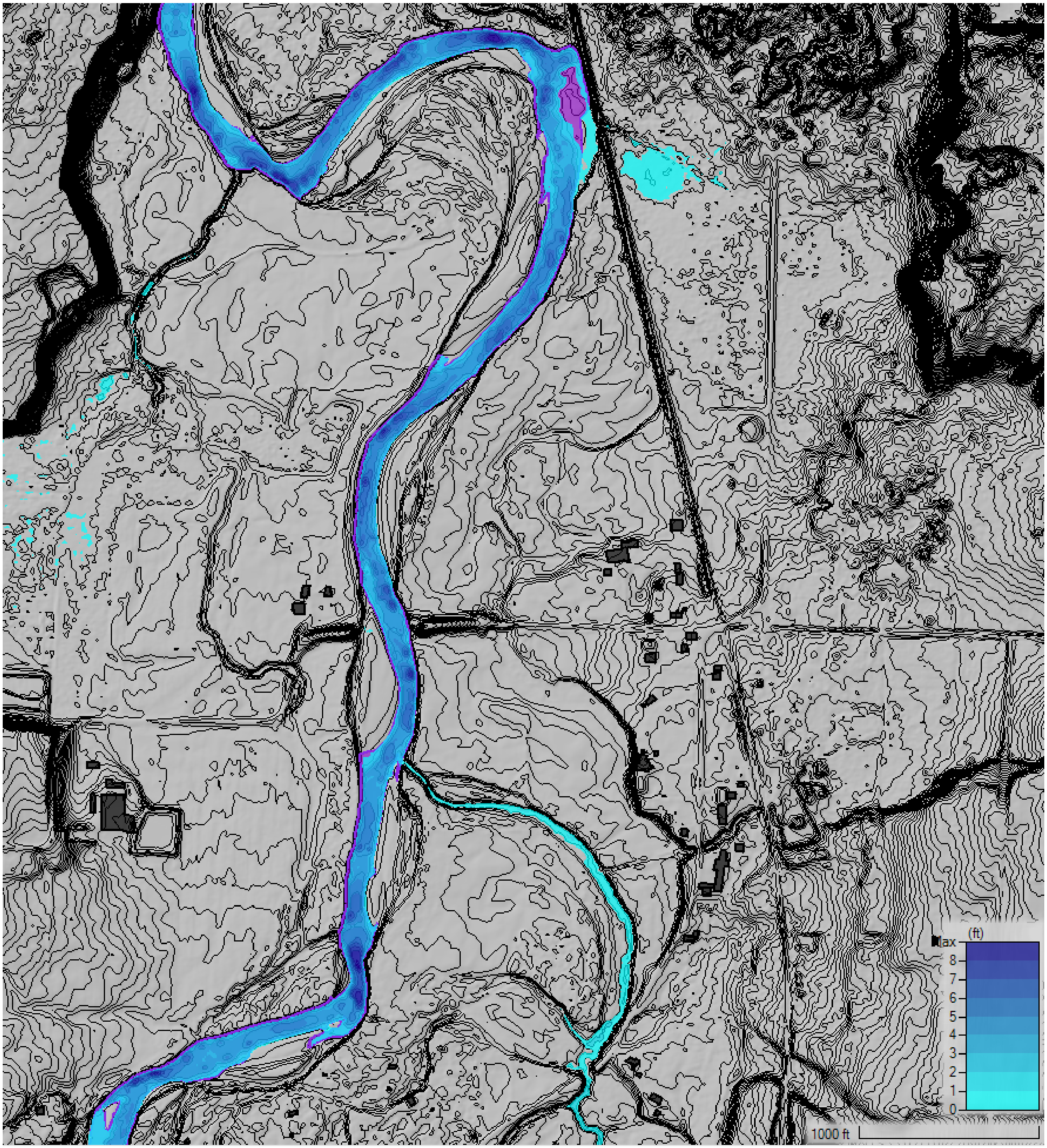

Figure 41. Plan view comparison of low flow model validation extents (blue depth legend) compared to digitized wetted extents (purple polygon).

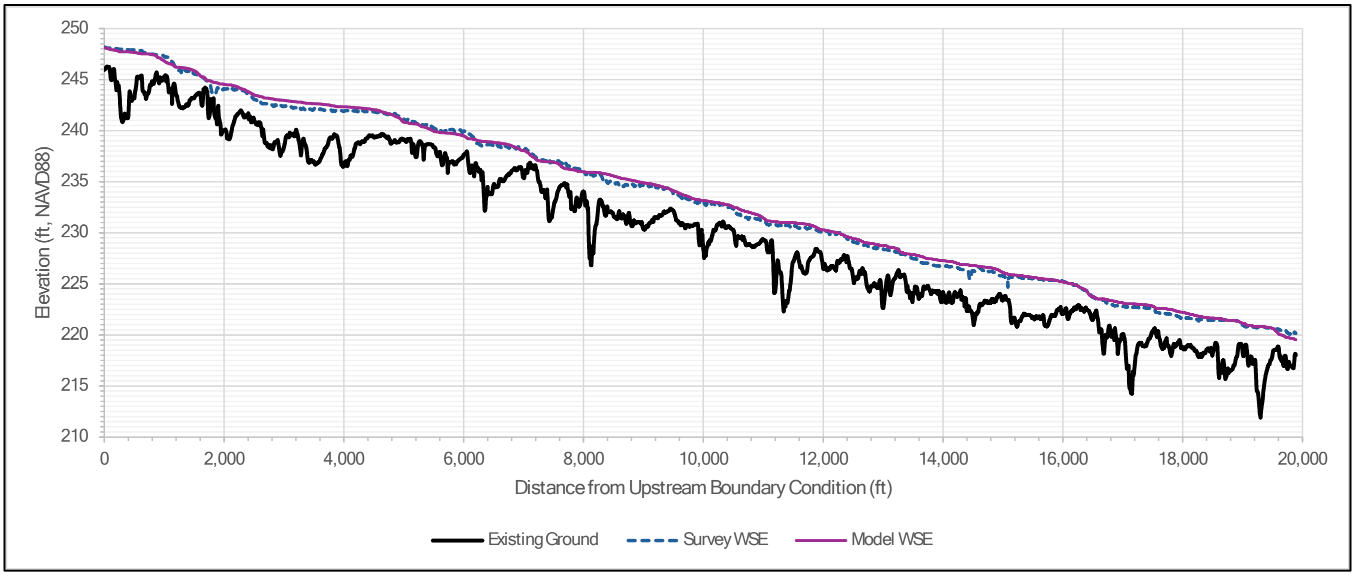

Figure 42. Profile comparison of low flow model validation extents compared to digitized water surface elevation.

For validating the hydraulic model at moderate flood levels we utilized historic high water marks (HWMs) collected in 2006 as part of the model calibration effort for the effective model. While developing the effective model, Northwest Hydraulic Consultants (NHC) surveyed several HWMs following a November 2006 high flow event (NHC 2010) and used the time series of discharge values at the Wickersham gage to develop inflow conditions to the 1-D model. We extracted discharge values from cross-sections at the upstream end of our 2-D model to use as inflow boundary conditions with slight adjustments made to accommodate tributary inflows which were represented as lateral inflows in the effective model. In essence we used the same 2006 event to validate our 2-D hydraulic model in a similar fashion to what NHC performed with the 1-D effective model. Roughness values were modified based on a review of simulated maximum water surface elevations of the November 2006 high flow:

- Initially we lowered roughness values from those used for the low flow validation effort based on previous experience and recent literature (Kopecki et al. 2017).
- Further refinement of roughness values was performed iteratively based on results until water surface elevations were in good agreement with the HWMs documented by NHC (Figure 43 and Table 8).

Table 8. Comparison of observed high water marks and modeled WSE for 2006 high flow event.

POINT	OBSERVED ELEV.	MODELED WSE	DIFFERENCE	COMMENTS
#78a-11-06-06	231.70	231.25	-0.45	
#81-11-06-06	233.25	232.97	-0.28	
#74-11-06-06	238.18	238.84	0.66	
#81a-11-06-06	233.13	237.61	4.48	Seems inconsistent with nearby points
#82-11-06-06	235.78	235.39	-0.39	
#75-11-06-06	238.23	240.15	1.92	At Hwy 9/Black Slough Crossing
#76-11-06-06	240.41	240.28	-0.13	
#100-11-06-06	241.98	241.72	-0.26	
#99-11-06-06	244.02	243.58	-0.44	
#79-11-06-06	241.29	242.19	0.90	At Nelson Road

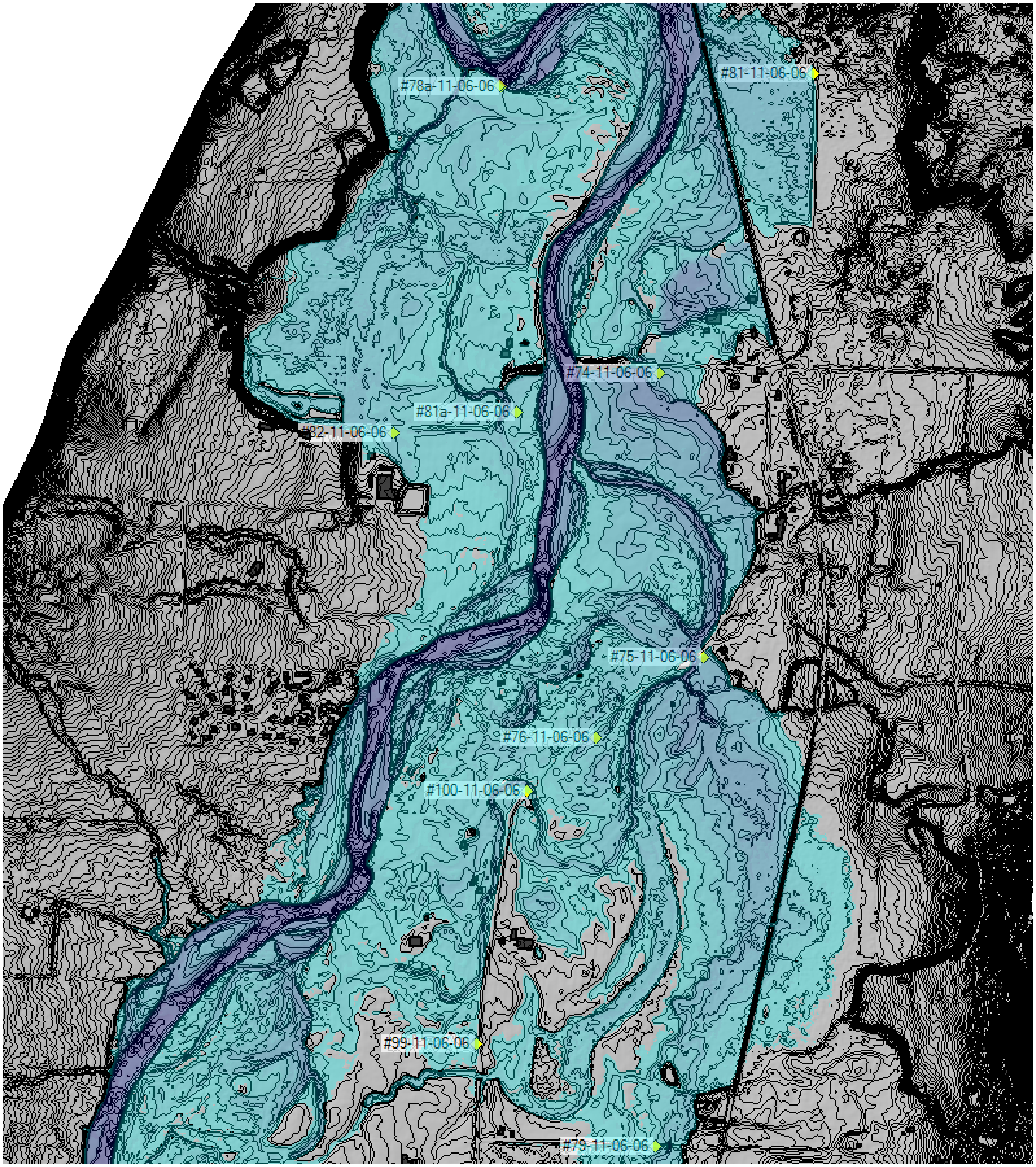

Figure 43. Location of high water marks documented by NHC following 2006 high flow event.

Of the 11 HWMs within the 2-D model domain, six had modeled surface WSEs within ±0.5 ft of the surveyed elevation, an additional two were within ±1.0 ft of the surveyed elevation, and the remaining three were either located in close vicinity to hydraulic structures (which could perform differently in 1-D and 2-D models) or seem inconsistent with nearby HWMs; point #81a in particular seems inconsistent with others (it is located between points #82 and #74 but is the lowest elevation so the WSE would have to dip at this point to be logical). Overall, our model calibrated well with these HWMs giving us confidence that the model is performing well for flows in the range of the 2006 event (peak flow of 16,000 cfs at the Wickersham gage or similar, to a 10-yr event).

An additional model validation effort we utilized was a comparison of discharge-weighted water surface elevation (WSE) from our 2-D model to the base flood elevation (BFE, Q100 water surface elevation) for the mainstem in the effective model. We performed this comparison at five total cross-sections ranging from the far upstream end of the model domain to the far downstream end. Additional adjustments to the model were necessary to get the simulated WSEs to better agree with BFEs in the effective model; these consisted of both further adjustments to roughness values for the Q100 and decreasing the friction slope at the outflow boundaries to address an artificial decrease in WSE at the outflow boundary (Figure 44). The discharge-weighted WSEs generally agree well with the effective BFEs (Table 9) with the notable exception that the far upstream cross-section at the model inflow boundary is significantly higher than the effective BFE and is likely due to boundary condition effects; however, at the next downstream cross-section considered in this comparison (~1,700 ft downstream) boundary effects appear to be resolved and the NSD + CGS model agrees closely with the effective model (Figure 45).

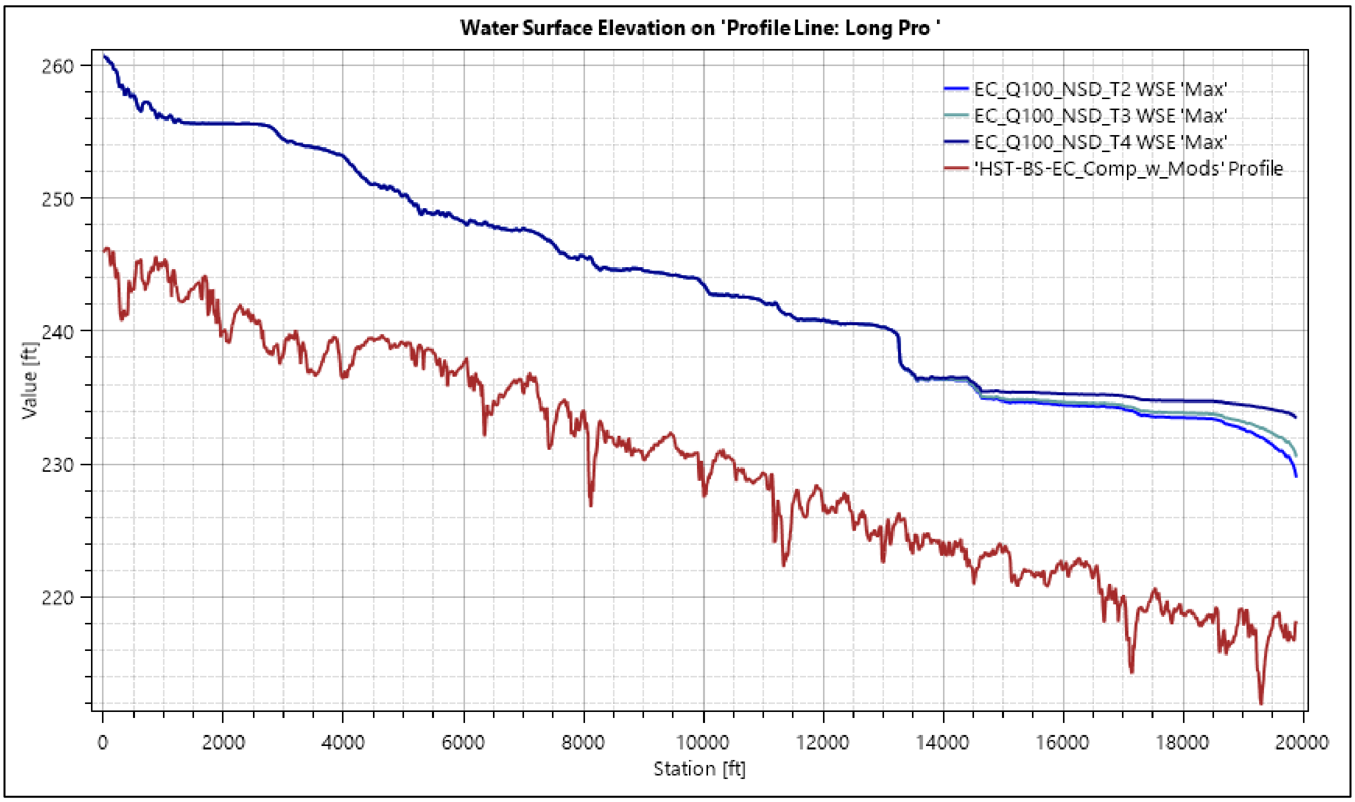

Figure 44. Profile comparison of modeled WSEs during the 100-yr event.

Table 9. Comparison of Effective BFEs and Modeled Q100 Discharge-Weighted WSE in the mainstem.

CROSS-SECTION	EFFECTIVE BFE	MODELED WSE	DIFFERENCE	COMMENTS
23600	259.64	262.03	2.39	At inflow boundary
21924	255.86	256.08	0.22	~1700 ft D/S of inflow boundary

CROSS-SECTION	EFFECTIVE BFE	MODELED WSE	DIFFERENCE	COMMENTS
12949	241.76	242.66	0.90	~0.5 miles U/S of Potter Rd Bridge
4524	234.12	234.13	0.01	~300 ft U/S of outflow boundary
4216	233.85	233.87	0.02	At outflow boundary

Figure 45. WSE and BFE comparison at two cross-sections near upstream end of model domain.

As a last model validation effort, we compared inundated extents from the 2-year model run to field indicators observed in the field. The peak flow from the December 2023 storm was 12,700 cfs at the Saxon gage which corresponds relatively well to the 11,000 cfs mainstem inflow used in the 2-year run for our model. The location of debris lines at several locations were compared to inundated extents predicted from the model which indicated a good agreement between simulated and actual inundated extents for an approximate 2-year flow. While this last validation effort wasn't as quantitative as others, it is further evidence that our model is reasonably simulating actual hydraulic conditions at the full range of flows being utilized for this analysis. Roughness values used in the model are summarized in Table 10.

Table 10. Roughness values used in 2-D hydraulic model runs.

ROUGHNESS CATEGORY	LOW FLOW (0-2,500 CFS)	2-YEAR (8,000-14,000 CFS)	10-YEAR (14,000-20,000 CFS)	100-YEAR (20,000 CFS+)
Unvegetated Bar	0.045	0.040	0.030	0.020
Road	0.015	0.015	0.015	0.015
Forested	0.120	0.120	0.080	0.065
Ag Field	0.035	0.035	0.035	0.030
Railroad	0.080	0.080	0.070	0.070
Vegetated Floodplain	0.100	0.100	0.070	0.050
Vegetated Bar	0.060	0.060	0.050	0.040
Building	0.500	0.500	0.500	0.500
Logjam	0.150	0.150	0.150	0.150
Vegetated Bank	0.050	0.050	0.045	0.038
Small ELJ	0.080	0.080	0.080	0.080
Channel	0.045	0.040	0.030	0.020
Vegetated Floodplain Channel	0.050	0.050	0.040	0.030

6.2 Existing Conditions Hydraulic Output

6.2.1 Low Flow Hydraulic Conditions

Hydraulic conditions within the Black Slough reach are relatively uniform under existing conditions at the approximate median flow modeled for this analysis. Wetted width remains relatively uniform on the order of 100 – 115 ft within the larger active channel. Throughout a majority of the reach, the low flow channel meanders back and forth within the active channel with alternating (largely unvegetated) gravel bars on the left and right banks from the upstream end of the reach, through the Potter Road Bridge and down to the large meander near RM 1.3. Depths and velocities are also largely consistent; depths range from approximately 2-3 ft and velocities are on the order of 1.5-3 ft/sec in a majority of the channel, consistent with large sections of the reach being classified as run from a habitat perspective. Figure 46 illustrates simulated depths and velocities within the project reach.

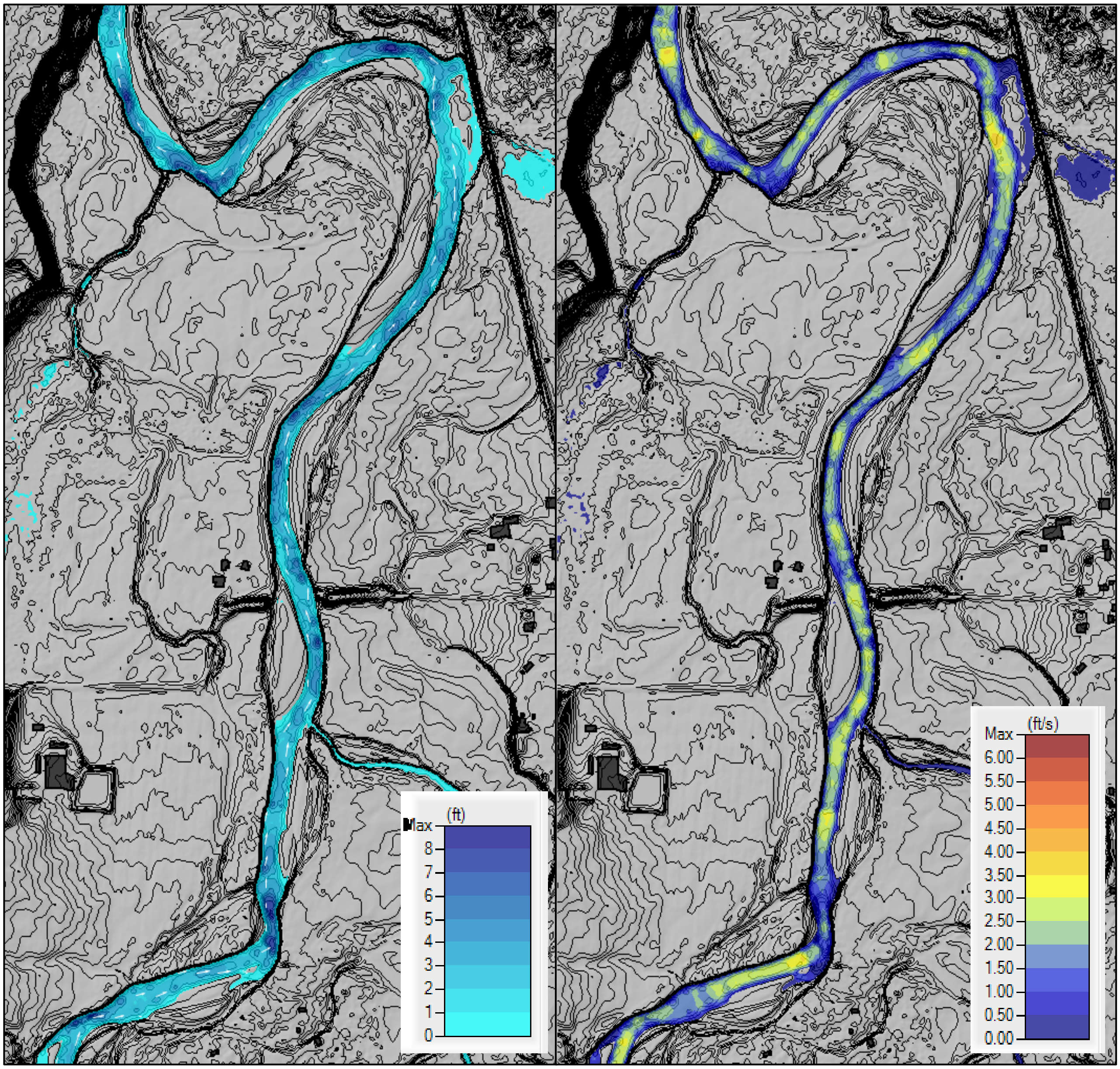

Figure 46. Simulated depths and velocities within the Black Slough reach at approximate median flow.

Very few instances of split flow or side channels exist in the reach at the approximate median flow and overall hydraulic diversity in the reach is low. The upstream and downstream ends of gravel bars and tributary inflow locations are associated with wider inundated areas and at least a portion of the channel experiences near-zero velocities in these areas. ELJs installed near the RM 1.3 meander provide the most diverse hydraulic conditions with off-channel inundated areas, diverse edge habitat, and pool formation occurring associated with previously installed ELJs (Figure 47).

The outside of meander bends are slightly deeper and more likely to contain localized pools; pool depth at this flow ranges from approximately 5-8 ft depending on the pool-forming mechanism and local channel form (pools in more confined sections with wood tend to be the deepest pools in the reach). The highest velocities present in the reach at the approximate median flow tend to be at riffle locations where local hydraulic gradient steepens. In these locations, velocity increases to approximately 3-4 ft/sec on average through riffles.

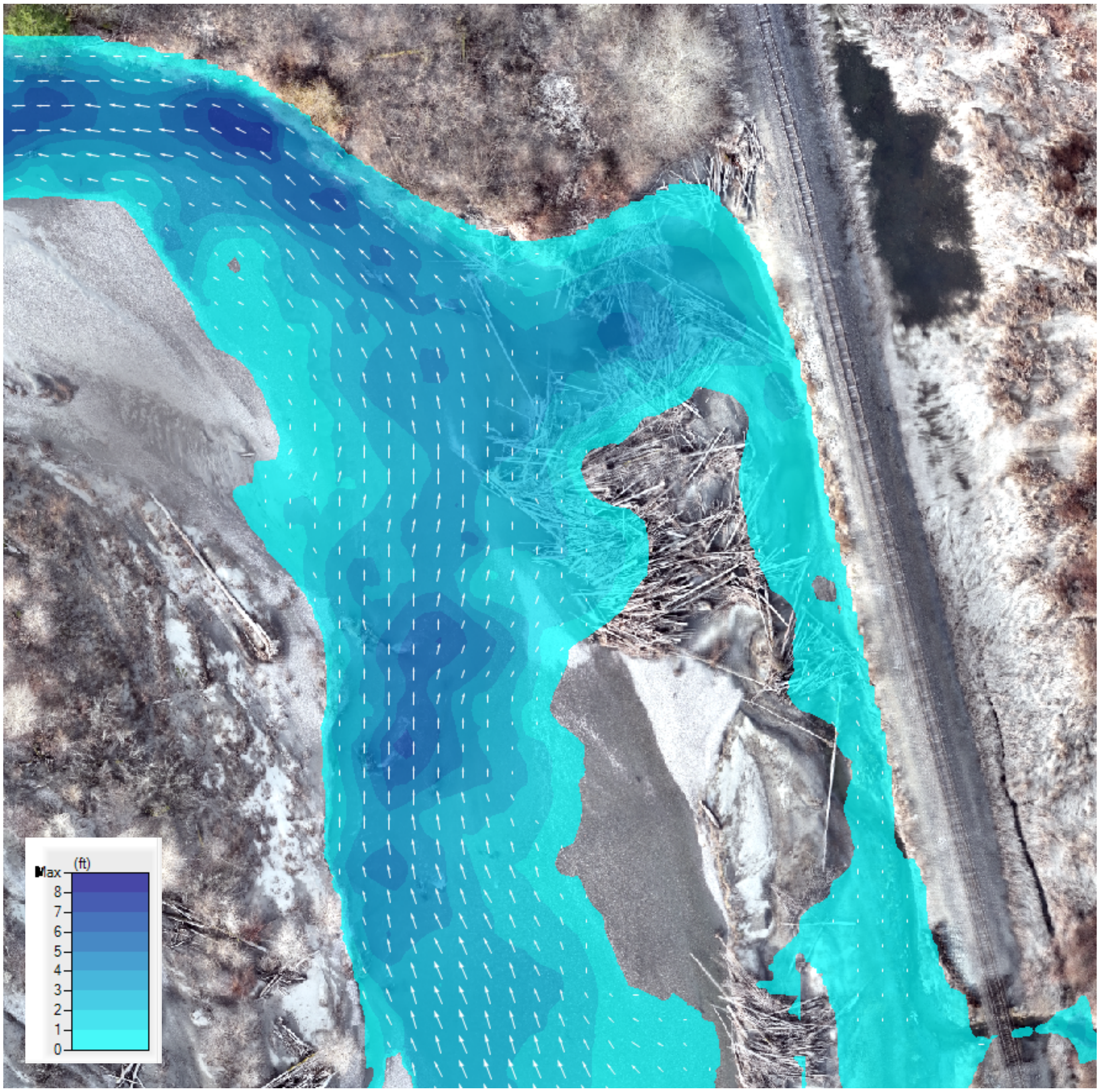

Figure 47. Overlay of simulated depths near RM 1.3 in Black Slough reach at approximate median flow.

6.2.2 Two-Year Flow Hydraulic Conditions

Hydraulic conditions during the 2-year event are a good indicator of frequently experienced conditions which have the potential to mobilize channel bed sediment and contribute heavily to channel forming processes; the 2-yr event is slightly higher than the bankfull event of 1.4 years as predicted by Casto and Jackson (2001). Understanding hydraulic conditions of the 2-yr event under existing conditions is therefore helpful in understanding the forces that drive and maintain habitat within the project reach.

The bankfull discharge is commonly understood to indicate the initiation of bank overtopping and floodplain activation; given that the 2-yr event we modeled exceeds the 1.4 year return interval of the estimated bankfull flow it is reasonable to expect to see floodplain activation during the 2-yr event which is indeed the case for much of the Black Slough reach (Figure 48). All gravel bars are fully inundated at the 2-yr flow and in several locations flow overtops the banks and activates adjacent floodplain.

Depths and velocities at the 2-yr flow vary considerably throughout the project reach (Figure 48). Depths in the mainstem are typically on the order of 8-12 ft in the mainstem with most gravel bars experiencing depths on the order of 1-5 ft; floodplain depths also vary from shallow sheet flow to concentrated flow in floodplain swales several feet deep. Velocities also vary considerably, and notably exhibit a noticeable pattern of velocity increases in more confined sections lacking floodplain activation. Floodplain velocities are almost exclusively 1 ft/sec or lower, with very few inundated portions of the floodplain experiencing higher velocities, even in floodplain swales. Peak velocities in the mainstem tend to occur at meander bends where the channel is confined and are on the order of 10 ft/sec while in less confined sections velocity in the main conveyance portion of the channel ranges from approximately 6-7 ft/sec. This increase in velocity at confined sections correlates with an increase in shear stress and sediment transport capacity. Shear stresses in locations of peak velocity approaches or narrowly exceeds 1 lb/sq ft whereas in less confined portions of the channel with wider gravel bars or inset floodplain shear stress is on the order of 0.5-0.7 lb/sq ft, correlating well with the median grain size and the shear stress required for incipient motion.

Near the upstream end of the project reach, both the right and left bank floodplain surfaces are activated. The right bank is overtopped at this flow and concentrates into a sinuous floodplain channel which joins Black Slough proper near Highway 9. The left bank at the upstream end of the reach inundates an inset floodplain and also activates a floodplain channel which flows through a private agricultural field and flows toward the west side of Potter Road. This floodplain channel appears to have been modified and exhibits a muted topography which spreads flow further west along Potter Road; our model suggests that the 2-yr flow barely overtops Potter Road just east of the location where Potter Road turns south and becomes Hillside Road. Confirmation of this inundated area through anecdotal evidence from local residents would be helpful in the future from local residents would be helpful and may potentially provide an opportunity for further model refinement. Additionally, several privately constructed structures (houses, barns, sheds, etc.) are located immediately adjacent to simulated 2-yr wetted extents which could provide an additional opportunity for verification of model performance; presently, no such anecdotal evidence related specifically to the 2-yr flow has been acquired.

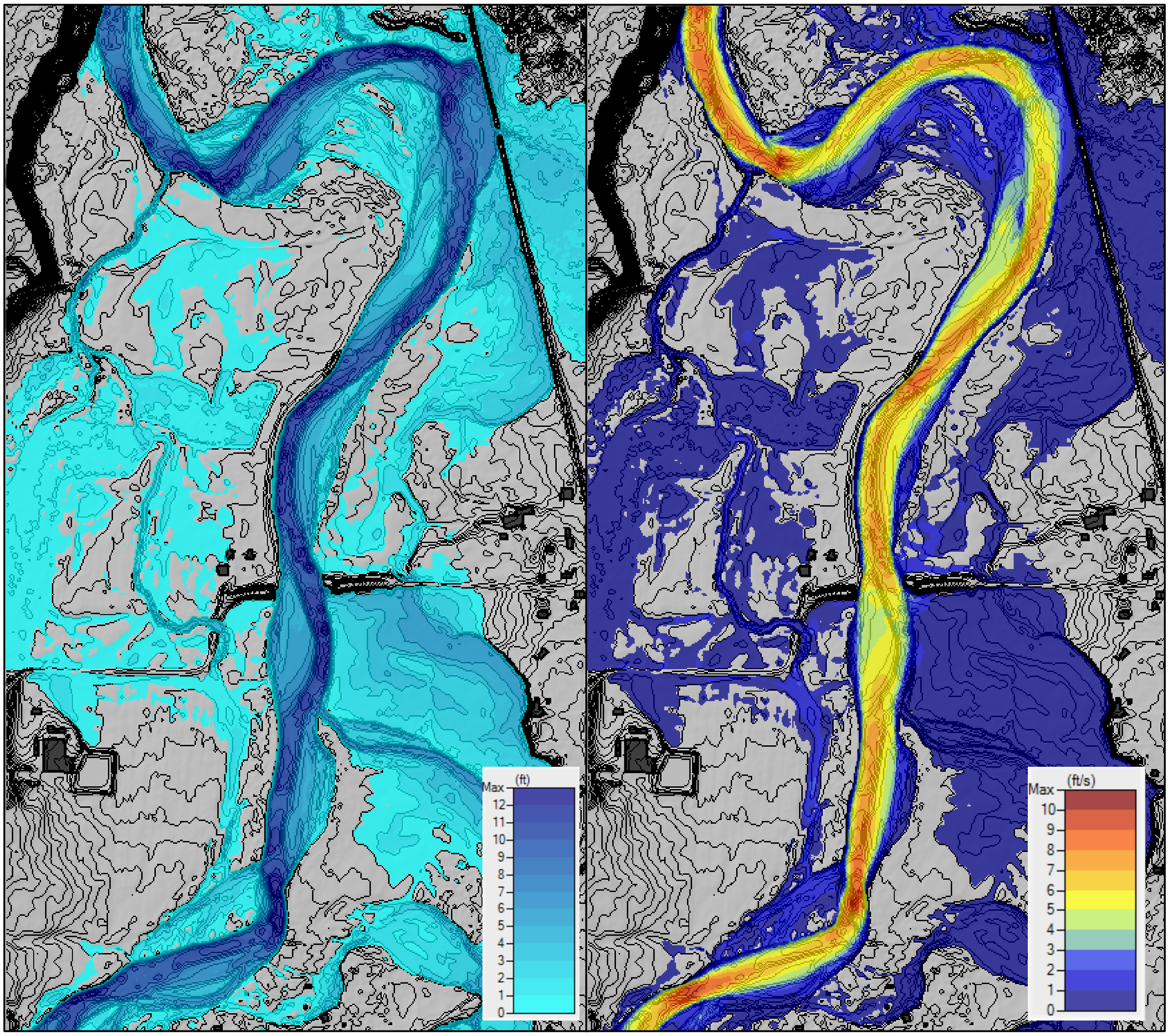

Figure 48. Simulated depths and velocities within the Black Slough reach at the 2-yr flow.

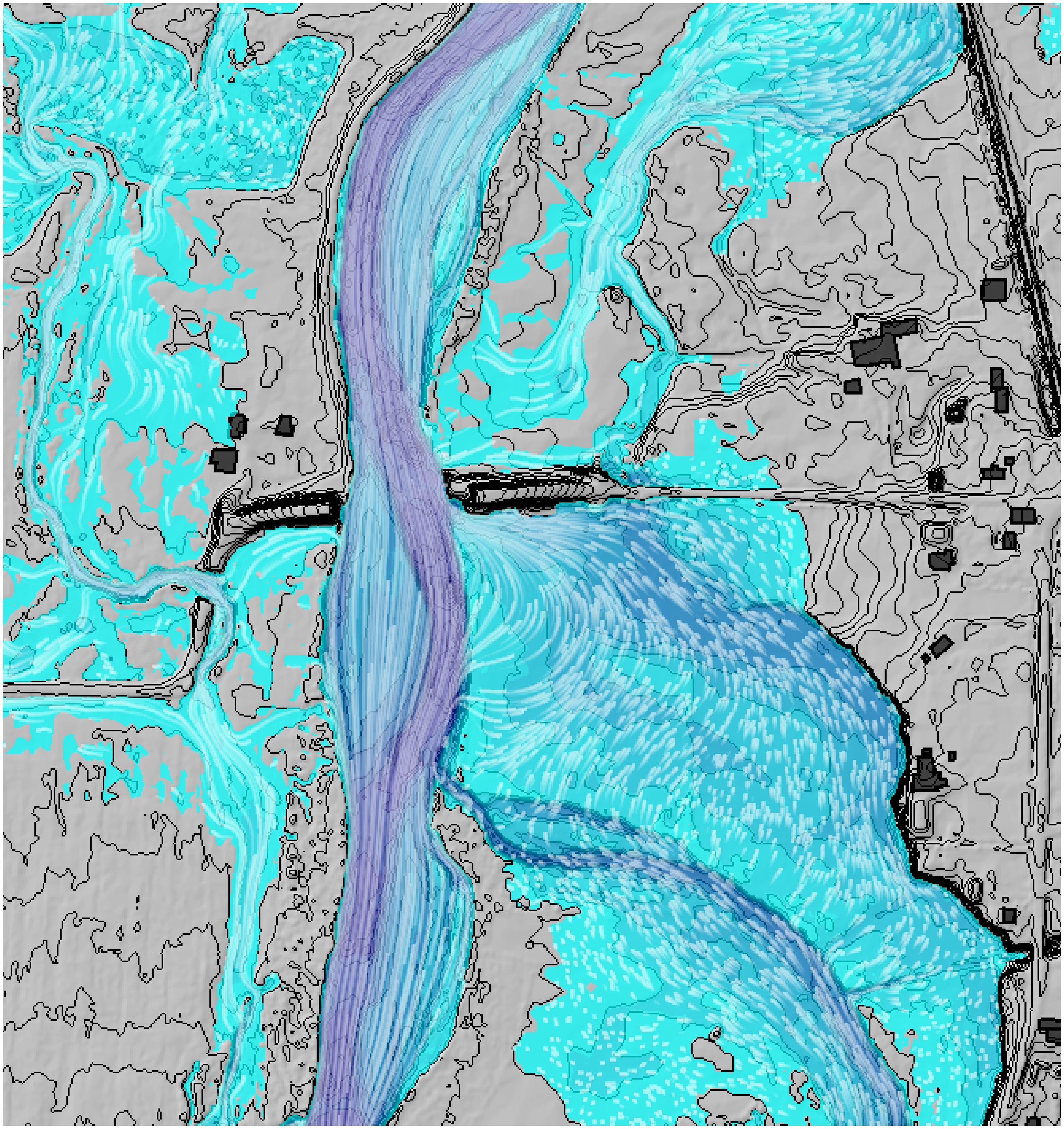

Figure 49. Flow trace of mainstem and floodplain flow near Potter Road bridge at the 2-yr event.

While portions of the project reach experience overbank flow consistent with a naturally connected floodplain other portions of the reach feature anthropogenic features which directly impact floodplain processes. The impact of manmade features on floodplain hydraulics is most notable at:

- The Potter Road bridge and associated approaches.
- Immediately downstream of the Potter Road bridge along the privately owned left bank floodplain.

- Near the downstream end of the project reach where the BNSF railway bisects the right bank floodplain.

A brief description of the impacts on floodplain hydraulics at each of these areas is provided below.

Potter Road Bridge

Upstream of the Potter Road bridge the floodplain hydraulics are fairly complex. The main channel draining Black Slough proper crosses Highway 9 and meanders to the west where it joins the mainstem approximately 750 ft upstream of the bridge. The channel draining Black Slough proper overtops its right bank onto the broader floodplain which shunts water south toward Potter Road. Approximately halfway between the confluence of the Black Slough channel confluence with the mainstem South Fork the right bank of the mainstem also overtops and contributes additional flow onto the right bank floodplain where it initially flows southeast toward Potter Road. The floodplain flow from both of these sources is ultimately largely forced back to the bridge opening when the flowpaths hit Potter Road. An existing culvert at the east end of the Potter Road bridge approach is not large enough to convey the full volume of floodplain flow and as a result flow is forced back to the mainstem channel along the upstream edge of the eastern bridge approach as flowpaths in Figure 49 illustrate. While natural floodplain topography is responsible for a portion of flow shunting back toward the mainstem, the presence of the bridge approach and lack of conveyance through the bridge approach are clearly the larger contributing factors to diminished floodplain activation on the right bank downstream of the Potter Road Bridge. Our model suggests that approximately 500 cfs flows onto the floodplain upstream of the bridge and the culvert east of the bridge approach conveys a negligible volume resulting in almost all right bank floodplain flow upstream of the bridge being shunted back toward the mainstem channel.

Downstream of Potter Road

Immediately downstream of the Potter Road bridge, a small portion of flow overtops the right bank floodplain and flows southeast across the right bank floodplain toward the BNSF railway. Floodplain activation on the left bank is clearly diminished due to the presence of a high berm along the left bank. This berm extends approximately 2.5 to 3 ft above the adjacent floodplain elevation and forces flow that would otherwise flow onto the left bank floodplain to remain in the mainstem channel (Figure 50). While our model indicates that a significant portion of the left bank floodplain downstream of the bridge is inundated at the 2-yr event, none of this inundation is directly from overbank flow in this portion of the reach. This concentration of flow in the mainstem at the 2-yr event results in increased depths, velocities, and shear stress in the main channel compared to an unaltered floodplain.

BNSF Railway

The BNSF Railway which bisects the right bank floodplain near the downstream end of the project reach also has a notable impact on floodplain hydraulics. Flow that makes its way onto the right bank floodplain downstream of the Potter Road bridge concentrates into a floodplain swale that flows southeast then east directly toward the railroad embankment where it is forced to turn north and flow along the embankment. On the east side of the railway several small tributaries including Tawes Creek and Van Zandt Creek drain to what is now a large wetland mosaic between Highway 9 and the railway. Our model includes an estimated flow input from these tributary drainages and suggests that the embankment impounds flow from these tributaries on the east side. The railroad embankment impedes natural floodplain flow along approximately 2,300 ft of floodplain on the right bank and features a single approximately 50 ft wide opening which allows for limited flow exchange between the mainstem and the impounded area.

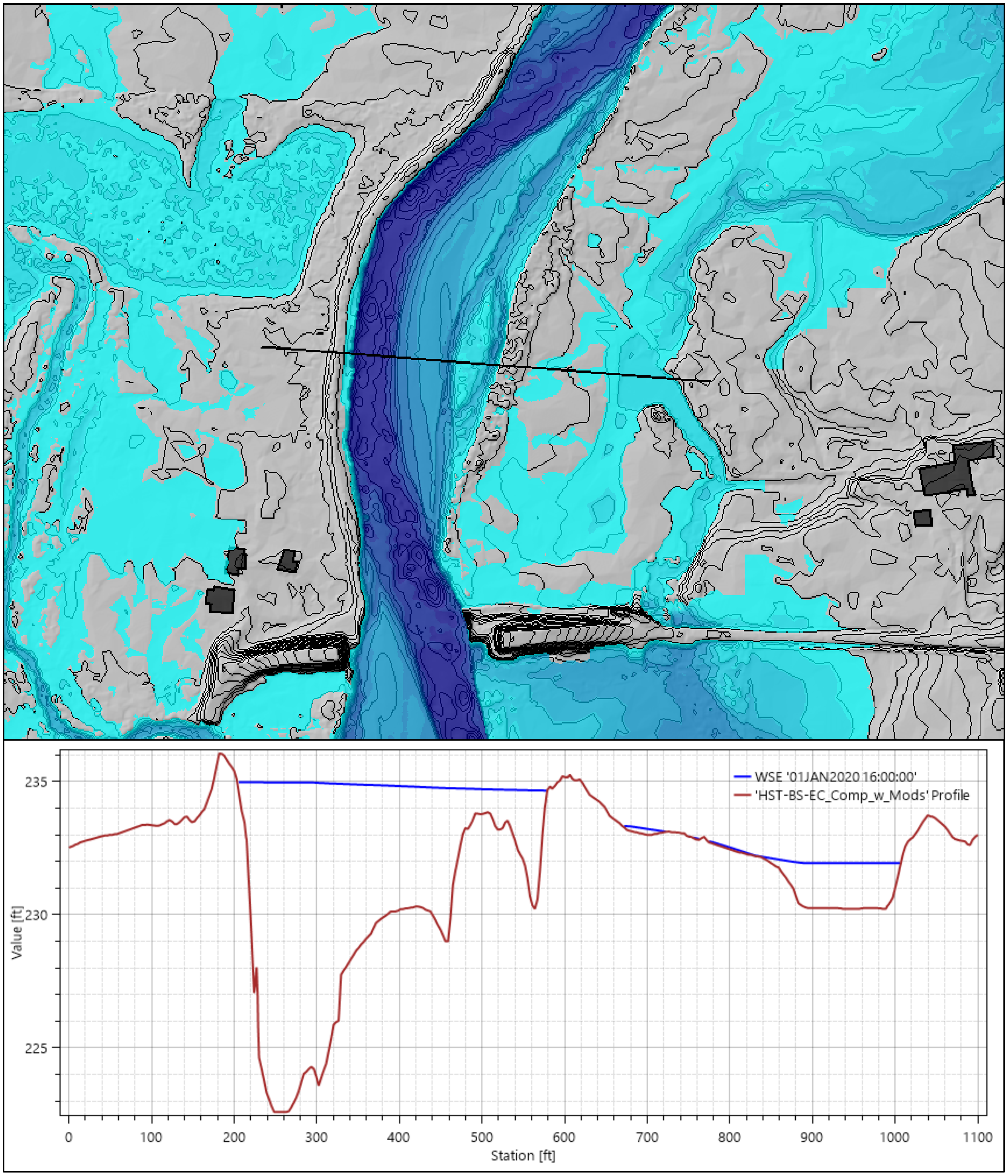

Figure 50. Cross-section location and profile view illustrating impacts of high berm along left bank downstream of Potter Road on floodplain connectivity at 2-yr flow.

6.2.3 Peak Flow (10-yr and 100-yr) Hydraulic Conditions

The 10-yr and 100-yr peak flows utilized for this analysis share remarkably similar inundation extents within the Black Slough reach (Figure 51); both events inundate the full valley with only a slight increase in inundation area for the 100-yr event compared to the 10-yr event. Given that both events inundate the full valley it is not surprising that depths, velocities, and water surface elevations of the 100-yr event are consistently higher than those for the 10-yr event (Figure 52). In particular, differences in velocity are most noticeable around the Potter Road bridge where velocities overtopping the western approach of the bridge are on the order of 5-6 ft/sec. at the 100-yr flow.

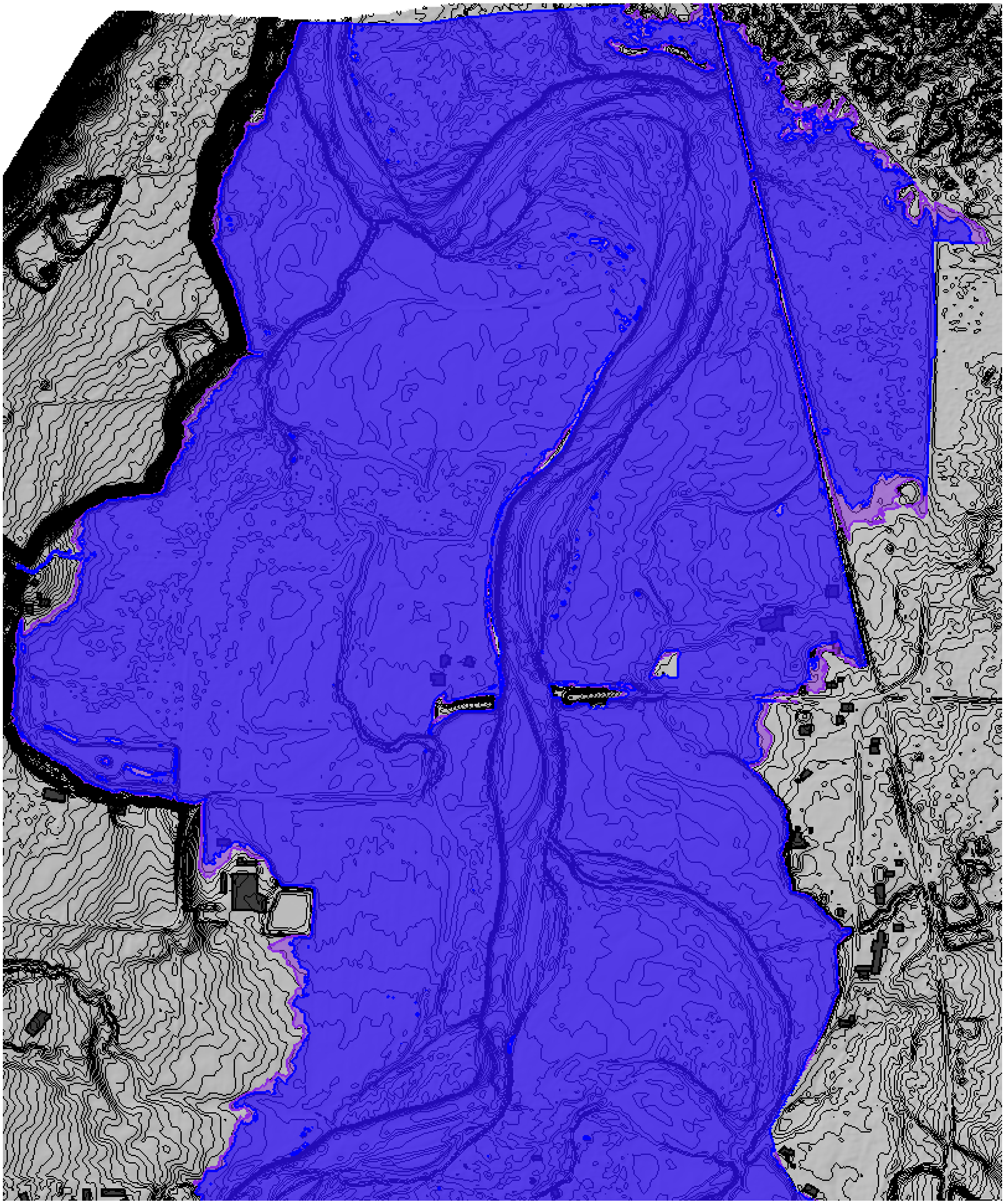

Figure 51. Simulated inundation limits for the 10-yr (blue) and 100-yr (purple) events in the project reach.

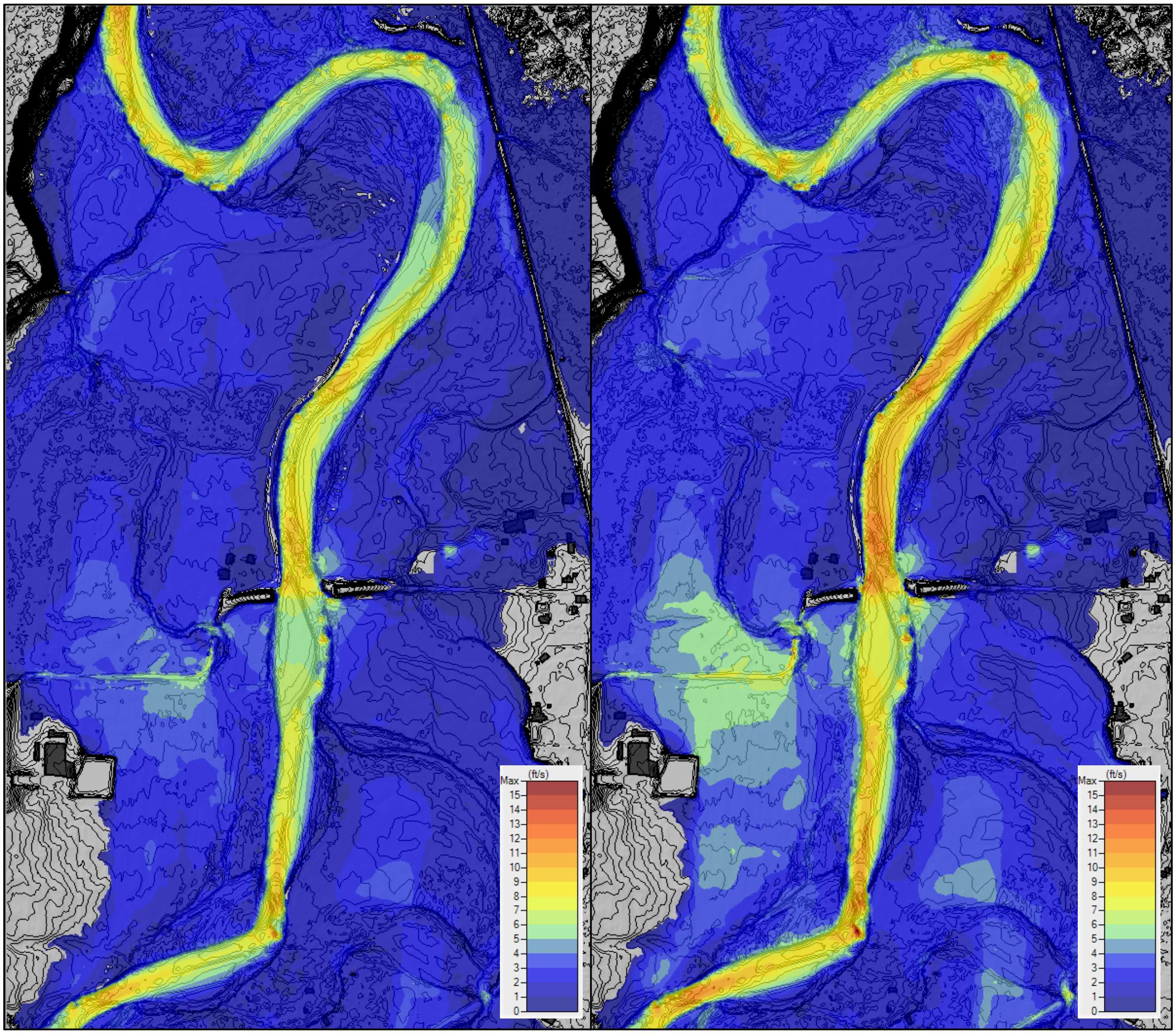

Figure 52. Simulated velocities at the 10-yr (left) and 100-yr (right) events in the project reach.

In general, the increase in velocities is related to the overall increase in discharge but is not directly proportional to this increase; the relative increase in velocity between the 10-yr and 100-yr flows is similar in magnitude to that as the increase from 2-yr to 10-yr despite flow magnitude increasing over 100% from 2-yr to 10-yr and approximately 33% from the 10-yr to 100-yr (Figure 53). This highlights the role that floodplain inundation plays in reducing stress on the mainstem channel. However, since the 10-yr and 100-yr events essentially share the same inundation extents the velocity increase between the 10-yr and 100-yr flows appears more pronounced.

At both flows, a number of privately owned structures are within the inundation footprint and a number of additional structures are immediately adjacent to the inundation footprint. Flow overtops Highway 9 upstream of the project reach at the 10-yr event and this overtopping extends a further distance at the 100-yr event extending from approximately Nelson Road (which itself is overtopped during both events) down to the location where the channel draining Black Slough proper crosses Highway 9.

Our model indicates that a significant backwater on the order of 3.5-4 ft develops upstream of the Potter Road bridge. Water that backs up above the bridge as flow contraction at the bridge opening forces nearly all flow on the right bank floodplain to flow nearly perpendicular to the mainstem before flowing through the bridge opening. The bridge also serves and approaches serve as another mechanism which redirects floodplain flow on the left bank across Potter Road before continuing downstream. Immediately downstream of the bridge opening, flow experiences a rapid expansion across the right bank floodplain which causes two eddies to form on the right bank floodplain both of which are associated with large local differences in water surface elevation. The railroad embankment which bisects the right bank floodplain in the lower half of the project reach is not overtopped during either event. Our inundated simulated inundation extents are similar to the effective SFHA areas delineated by FEMA with one notable exception east of Highway 9 where our model shows no inundation but FEMA included this area in the SFHA (Figure 54).

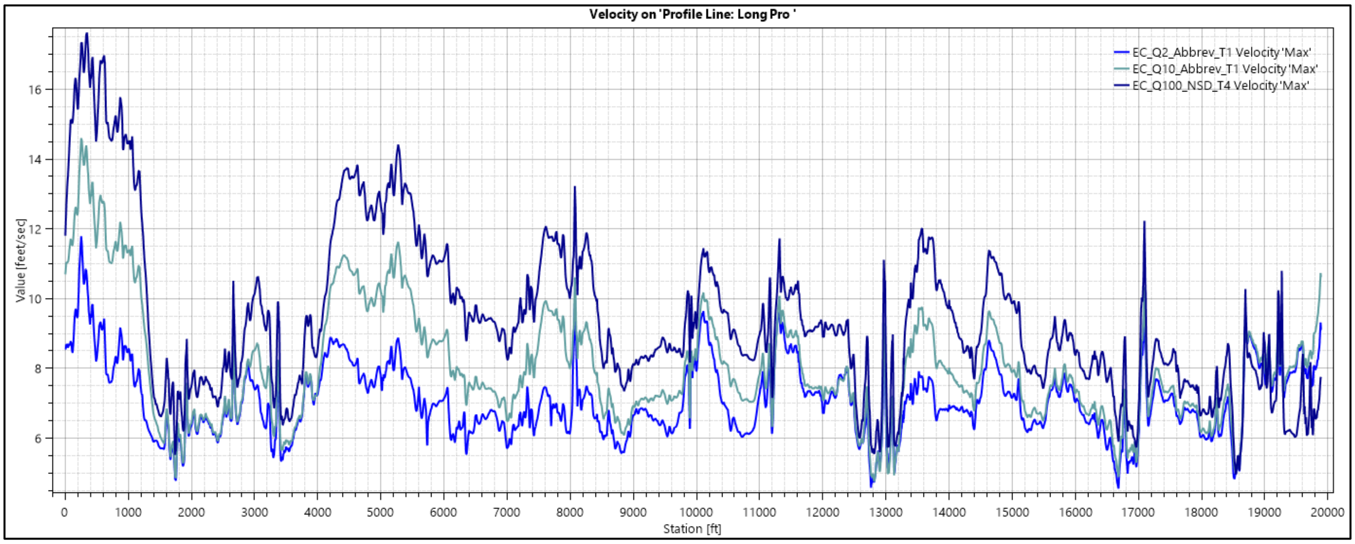

Figure 53. Longitudinal profile of simulated mainstem velocity within the model domain (upstream to downstream) at the 2-, 10-, and 100-yr runs.

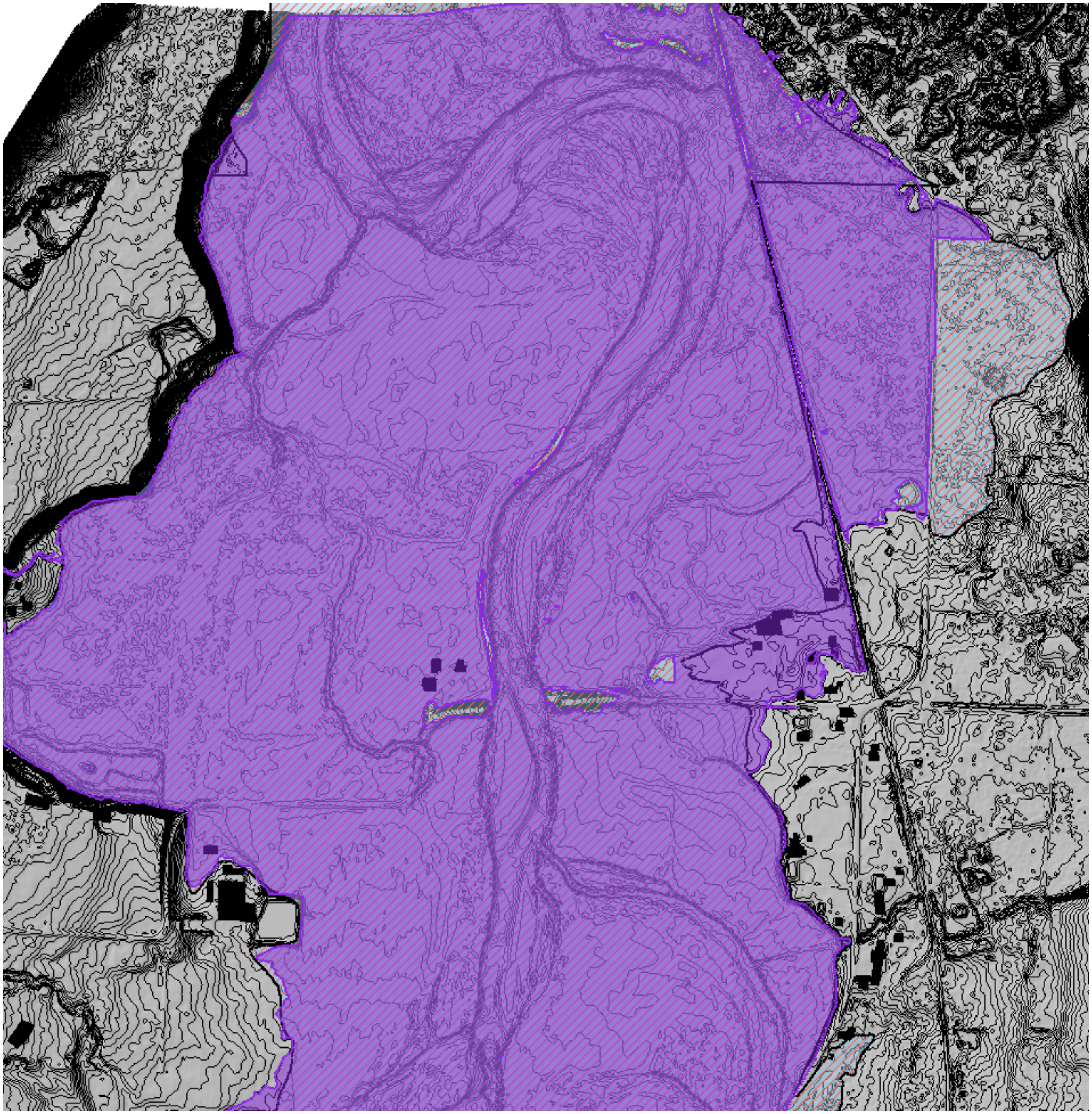

Figure 54. Comparison of simulated inundation extents at the 100-yr event (purple) and effective SFHA (hatched area).

6.2.4 Climate Change Peak Flow (100-yr) Conditions

To simulate peak flows when considering climate change, we took a simplified approach of increasing inflows to the model based on a lower end projection of 23% corresponding to a mid-century, high emissions scenario. Inflows from the 100-yr run were increased by this percentage uniformly at all inflow locations. Recognizing the the hydraulic model is limited in terms of changes to roughness and bed topography that may also occur with climate change, the simulated hydraulic conditions of this run represent a reasonably likely scenario. Even if channel changes were to occur, the inundation area and overall reach-scale hydraulic patterns would likely remain similar to those represented in our analysis of peak flows when considering climate change.

Similar to the 100-yr results, the increased peak flows used for this model scenario nearly entirely inundate the valley with only small, localized increases in inundation extent. Due to the fact that water cannot spread out further laterally on the floodplain, the increase in flow rate is manifested through increases in both depth and velocity throughout the reach. Depth increases are most pronounced downstream of the Potter Road bridge where the effective conveyance area shrinks some partly due to the presence of the BNSF railway; downstream of the bridge, our model suggests depth increases on the order of approximately 1 ft (or roughly 8%) for much of this area while increases in velocity are comparatively lower at approximately 0.3 ft/sec (or roughly 3%). Increases of depth and velocity on this order of magnitude could have significant impacts on floodplain infrastructure as the only portions of the floodplain not inundated during this event are anthropogenic (Figure 55).

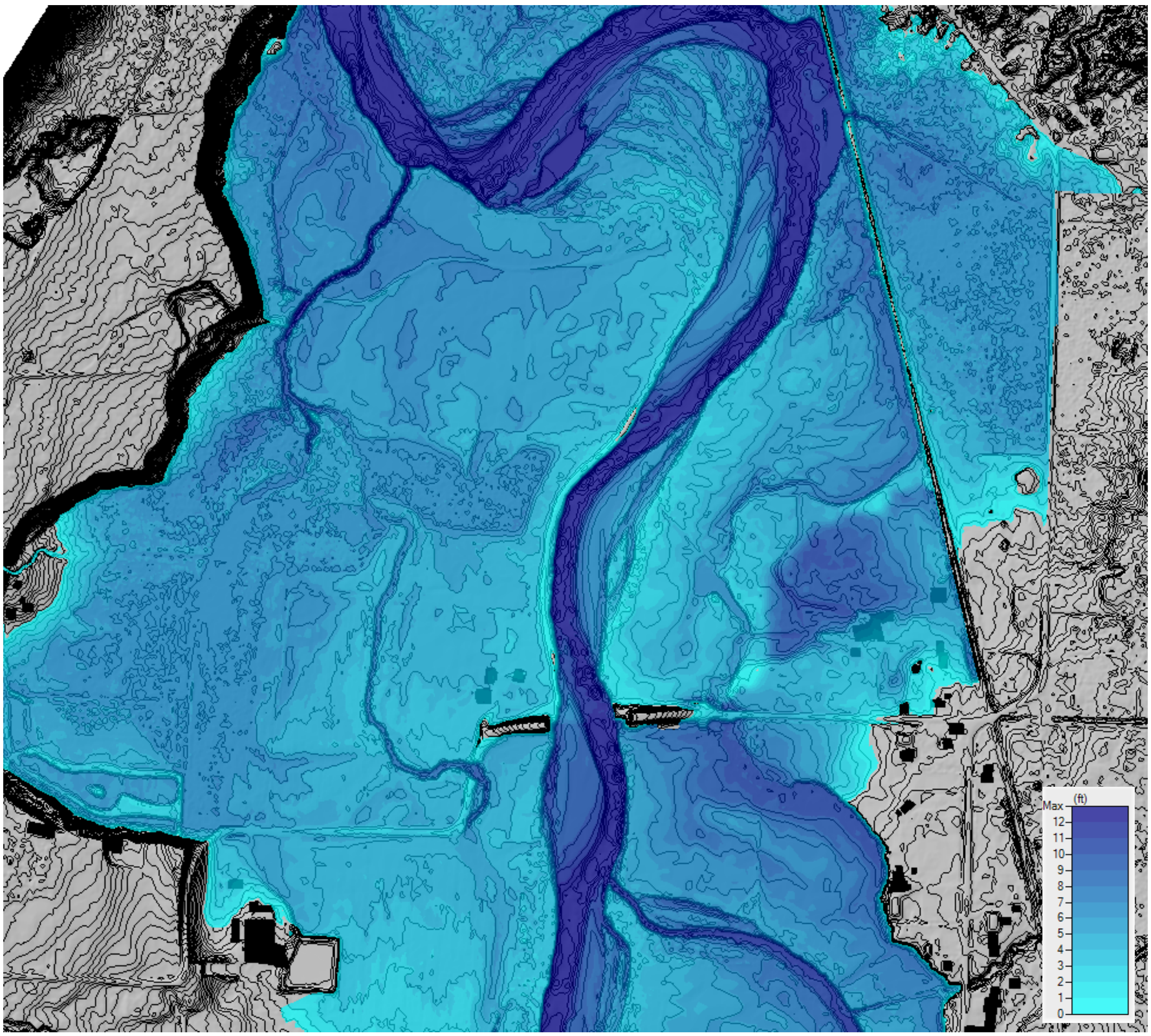

Figure 55. Simulated depths of climate change Q100 flow near Potter Road Bridge.

7 INSTREAM HABITATS AND LIMITING FACTORS

As discussed previously, the SFNR supports nine species of Pacific salmonids: Chinook salmon, coho salmon, sockeye salmon, chum salmon, pink salmon, steelhead/ rainbow trout, bull trout, and Dolly Varden. Conditions of instream habitats supporting these, and other aquatic species have been studied widely. This section summarizes instream habitat conditions specific to the Black Slough reach.

7.1 Limiting Factors and Habitat Metrics

Limiting factors for salmonid habitat within the Lower SFNR were established in the 2005 WRIA 1 Salmon Recovery Plan. High severity limiting factors are elevated water temperatures and decreased habitat diversity. Moderate severity limiting factors are key habitat quantity, elevated fine sediment, decreased stream flow, and harassment and poaching (WRIA 1 SRB 2005).

Habitat status and trends and goals for the Nooksack River including the Lower SFNR were updated in 2021 for the WRIA 1 Recovery Plan. The 2021 update provides comparisons with historical conditions, 2005 conditions, and conditions as of 2021, and outlines near-term 10 year and long-term 50 goals for habitat recovery (Maudlin 2021). To generate a list of habitat metrics for evaluating existing conditions within Black Slough, we integrated metrics from the 2021 Update to the WRIA Recovery Plan, along with the 2020 Nooksack River Instream Project Effectiveness (Maudlin et al 2020), (Maudlin 2021) and 2023 WRIA 1 SRFB Grant Cycle – Habitat Indicators, Method, and Guidance Matrix.

7.1.1 Habitat Mapping Methods

For full consideration of habitat within and immediately adjacent to the Black Slough reach, habitat conditions for were evaluated from RM 1 to 3.5. We utilized the most recently available data sources including drone imagery and an updated hydromodifications layer collected by NSD + CGS in March 2024 and a digital elevation model and hydraulic model results generated as part of this project as described in Section 5.3 and 6.1. Aquatic habitat units were mapped based on the wetted channel from the drone flight (approx. 500 cfs) using a combination of drone imagery, relative elevation model, hydraulic model results, and field observations. Log jams and key pieces were mapped from drone imagery and full description of large wood mapping methods is available in Section 5.

7.1.2 Habitat Conditions

Habitat conditions and targets are presented in Table 11 and mapped habitat is presented in Figure 56. Table 11 includes trends in conditions for available metrics reported in 2005, Maudlin et al 2020, and Maudlin 2021. Direct comparison to the current condition is not entirely feasible, as trend data has been reported at different spatial scales ranging from the entire Lower SFNR to sub-reach level. Instead, the trends presented for the Black Slough reach are qualitative to provide context on the general trajectory of habitat conditions beyond the snapshot of current conditions. Some metrics from the 2023 WRIA SRFB Grant Cycle matrix historical data are not available as indicated in Table 11.

Overall habitat conditions in the Black Slough reach are below management targets across all metrics. For metrics with data available since 2005, conditions are improving, but in most cases still need substantial improvement to meet habitat recovery goals. Aquatic habitat is simplified, with a lack of pools, habitat diversity, and large wood to support habitat formation processes. Most of the reach is devoid of log jams or woody cover and is comprised of long open runs with very little cover or habitat complexity. Pool habitat is poor with pools occurring less frequently than the target and the quality of pools is deficient as measured by the number of primary pools and high quality pools formed by large wood. Most of the large wood in the reach accumulated along the meander near RM 1.3. Where log jams are present, particularly along the wetted channel, they are forcing pool formation and providing cover (Figure 56). Pools not formed by large wood are created by riprap located along the outside of meander bends.

The channel is limited to a single mainstem thread with no forested islands and no perennial side channels or any side channels suitable for habitat up to the 2-year flood. Long sections of the banks are modified with riprap, which limits channel migration and formation. The combination of a lack of log jams and presence of riprap along the banks impair geomorphic processes that develop habitat complexity, side channel formation, and floodplain activation. A more detailed discussion of channel migration and hydromodifications including a map of current hydromodifications is available in Section 5.2.

Table 11. Habitat goals, conditions, and trends in Black Slough.

CATEGORY	METRIC	TARGET	BLACK SLOUGH EXISTING CONDITION	TREND SINCE 2005
Pools and habitat diversity	Pool frequency [a,b]	1.4 Channel Widths / Pool	8.4 widths / pool	Increasing
	Number of primary pools [b]	22 for Black Slough (167 for L SFN)	6	Increasing
	Pools formed by large wood (%) [b]	70%	44%	Increasing
	Number of High quality pools: > 1 m residual depth and formed by wood [b, c]	16 for Black Slough (117 for L SFN)	4	Increasing
	Habitat diversity: # of habitat units / km [a]	15 units / km (good) 20 units / km (very good)	6.2 / km	Increasing
Large wood	Key-sized wood: pieces > 9 m^3 per 100 m [b]	1.16 pieces / 100 m	0.13 pieces / 100 m	Increasing
	Area of wood engaged at low flow (m^2) [c]	Increase EC to PC	1,571 m^2	Not available
	Number of stable log jams [c]	Increase EC to PC	1	Not available
Channel and floodplain	Length of natural banks and bar edge types [a, b, c]	90% natural edge	72%	Increasing
	Perennial side channel length [c]	Increase EC to PC	0 ft	Not available
	Side channel length at 2-yr flood [c]	Increase EC to PC	0 ft	Not available
	2-yr flood area (acres) [c]	Increase EC to PC	118.1 acres	Not available
	100-yr flood area (acres) [c]	Increase EC to PC	778.2 acres	Not available

a. 2020 Nooksack River Instream Project Effectiveness
b. 2021 Summary of Habitat Status and Trends and Habitat Goals Update to WRIA 1 Salmon Recovery Plan
c. 2023 WRIA 1 SRFB Grant Cycle – Habitat Indicators, Methods, and Guidance Matrix

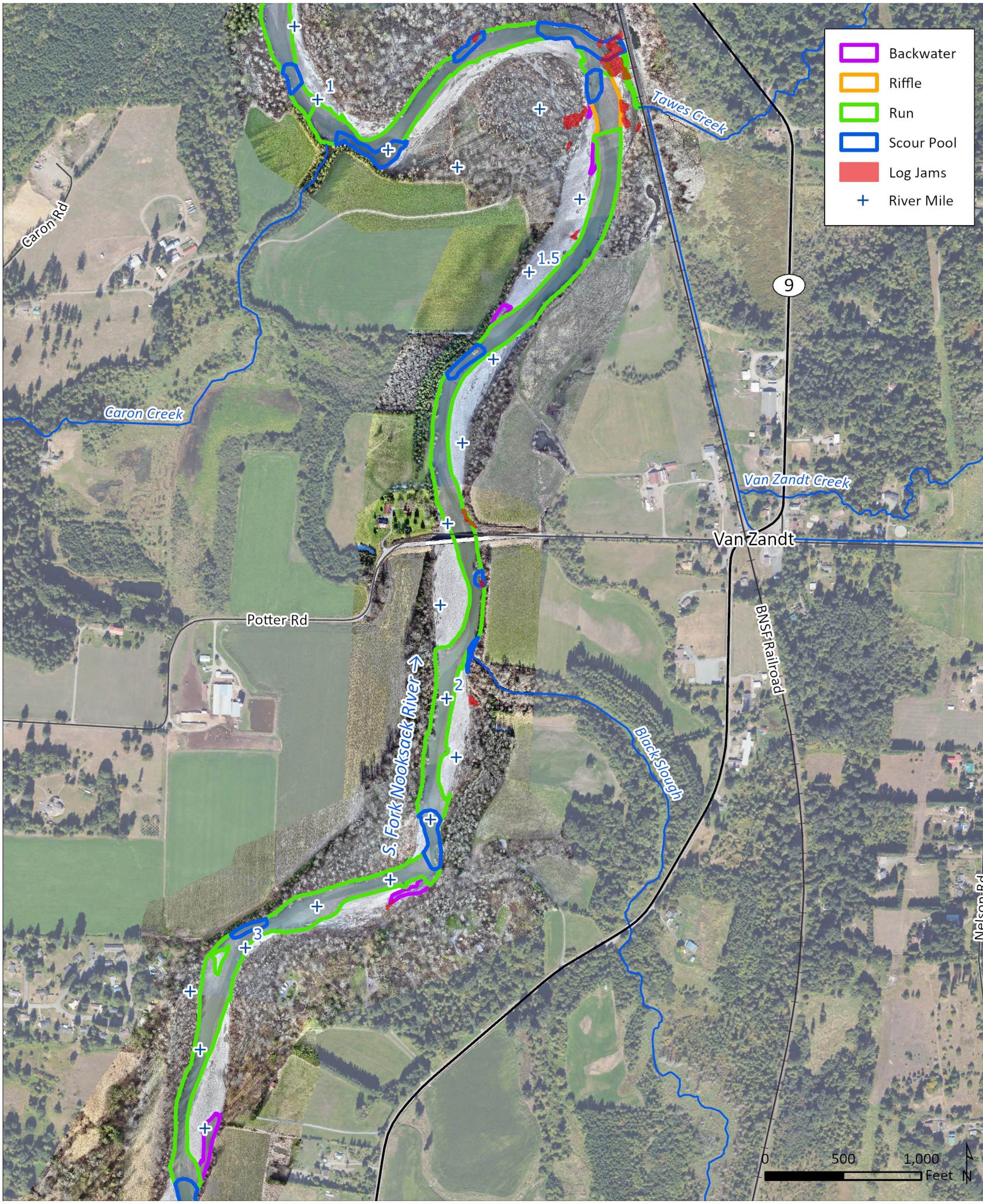

Figure 56. Map of aquatic habitat units within Black Slough.

7.2 Instream Temperatures and Water Quality Conditions

High water temperatures during summer impair habitat within the South Fork Nooksack. High temperatures can lead to prespawn mortality, incubation mortality, and limit the availability and quality of rearing habitat. Water temperatures are particularly a concern for Spring Chinook that enter the river and hold for an extended period before spawning, and spawn during the late summer and early fall.

The SFNR is listed on the Washington Department of Ecology's (Ecology) 303(d) list for water temperature and has a Total Maximum Daily Load (TMDL) Plan developed by Ecology (Ecology 2020). The TMDL study found water temperatures regularly exceeded limits for core salmonid habitat (16°C 7-day average of daily maximum temperatures (7-DADMax)) during July 2 to Aug 31 monitoring period and supplemental salmonid spawning and incubation (13°C 7-DADMax) during Sept 1 to July 1 monitoring period at several monitoring stations within the Black Slough reach. The TMDL recommendations to manage temperature impairment primarily focus on shading and management of riparian forests to reduce solar input and highlight implementation of instream restoration projects to increase thermal refugia. Riparian conditions for Black Slough reach are discussed in Section 8.2 of this report.

At least one thermal refuge currently exists within the Black Slough reach at the confluence of Black Slough (Figure 57, Ecology 2020). In addition, locations were log jams intercept hyporheic flow and form pools can form thermal refuges (Jantsch 2023). Additional refuges may exist in the Black Slough reach such as the log jams and ELJs near RM 1.3-1.4, however additional data is needed to confirm if refuges are present.

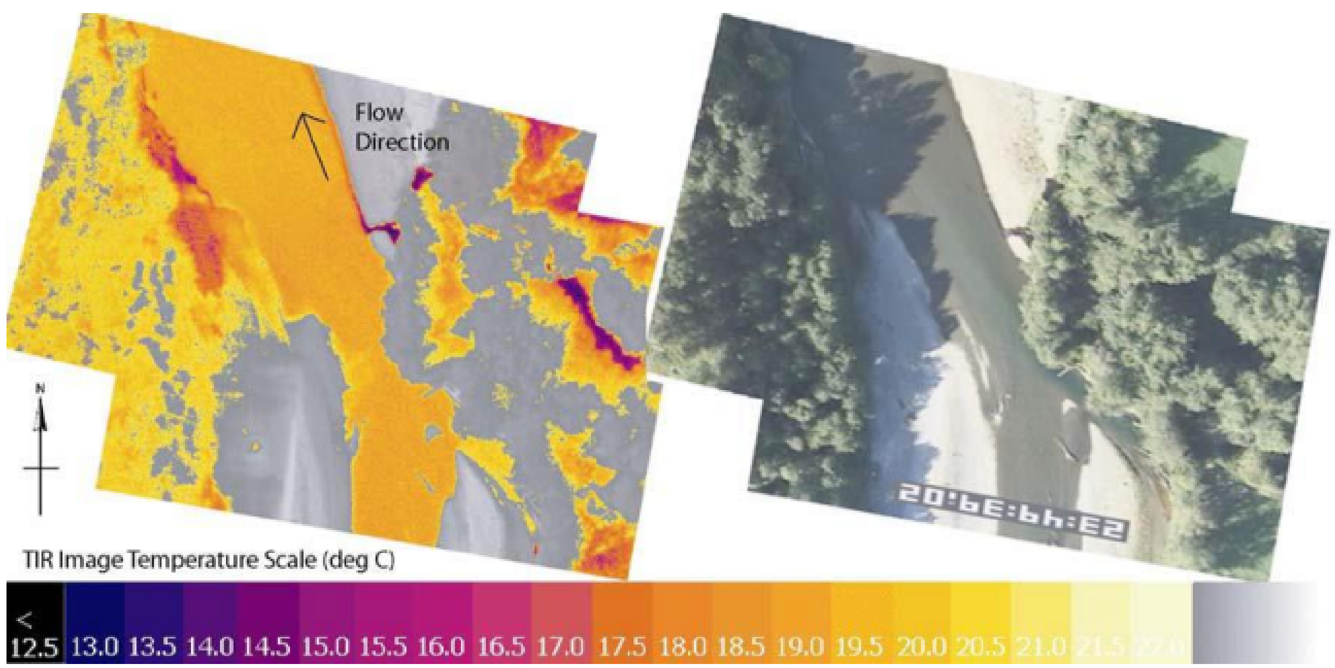

Frame: sfn0103-104: TIR/visible band images showing the SFNR (19.4 °C) at RM 2.0. The inflow of Black Slough (14.6 °C) is visible, except where obscured by vegetation, along the right bank near the center of the image.

Figure 57. Thermal Infrared (TIR) map of the Black Slough confluence with the SFN from 2002 FLIR Study by Watershed Sciences (Ecology 2020).

8 FLOODPLAIN AND RIPARIAN CONDITIONS

Floodplains are dynamic features which serve a variety of species and provide functional benefits including groundwater recharge, filtration of sediments and contaminants, and nutrient transport. In addition to these ecosystem functions and services, floodplains are valuable to society in that they reduce flood risk to private property and infrastructure by slowing runoff and absorbing flood waters. Floodplain geomorphic, hydrologic, and vegetative conditions are intertwined, each affecting stream channel morphology and the way in which water moves across the landscape. Soil characteristics, sediment transport regime, hydrologic and hydraulic conditions, and the size, persistence, and nature of floodplain vegetation combine to influence how and where sediment is deposited and if and to what extent large woody debris is recruited into the stream channel. Floodplain vegetation creates hydraulic roughness, slowing flood flows, and causing sediment deposition. These factors in turn affect the ability of floodplain forests to mature and enter the large wood cycle and ultimately affect the formation and persistence of diverse aquatic habitats supportive of spawning and rearing by salmonids.

As previously discussed, the fluvial landscape in the SFNR watershed prior to the arrival of the first Europeans would have been characteristic of the *Tsuga heterophylla* Zone (Franklin and Dryness 1988) and dominated by large old-growth conifers such as Douglas fir, western hemlock, Sitka spruce, and western red cedar, with large black cottonwood trees also occurring in the river's riparian zone. The river channel would have been connected to a diverse range of floodplain habitats including, but not limited to, perennial and ephemeral side channels, abandoned meander oxbow wetlands, large logjams, and beaver ponds. The river would have freely migrated across the valley bottom between glacial outwash terraces and valley hillslopes. Logjams and patches of mature forest would have provided stability to the river channel banks (logjams by deflecting flow, as well as roughening and strengthening banks, and mature trees through their extensive tree root systems).

Currently, because of channel incision and placement of bank hardening features such as riprap, floodplain conditions are hydrologically disconnected and constrained from overbank flows below Q2. Coupled with shifting climactic conditions, the conversion of vegetative cover from old-growth forest to agricultural fields, pastures, and residential areas reduces infiltration and speeds overland flow during rainfall events, leading to a "flashy" hydrology which is prone to more frequent and higher magnitude flood flows than was seen in historic conditions. The runoff from agricultural fields and roads also carries sediment, nutrients and other pollutants that reduce the water quality in the stream. The confinement of riverine processes and disconnection from floodplain habitats within the lower SFNR valley has contributed to the simplification of both instream and floodplain habitats.

To characterize floodplain and riparian conditions within the project reach, NSD + CGS focused on key ecosystem elements which, when functioning at optimal or high levels, can provide or improve instream habitats for salmonids. Table 12 presents key ecosystem elements and the functions they provide for instream habitats.

Table 12. Floodplain characteristics considered for improvement of instream habitats.

FLOODPLAIN ELEMENT	CHARACTERISTICS CONSIDERED	FUNCTION PROVIDED TO INSTREAM HABITATS
Soil / Substrate	• Hydraulic Conductivity • Ability to support wetland and riparian habitats	Drainage characteristics of substrate and their ability to capture and hold water for: • Water quality improvement • Cold water input to mainstem • Floodwater attenuation • Groundwater recharge

FLOODPLAIN ELEMENT	CHARACTERISTICS CONSIDERED	FUNCTION PROVIDED TO INSTREAM HABITATS
Wetland Presence	• Hydrologic Connectivity • Vegetation Composition • Soil Conditions	Characterization of hydrologic processes for the creation and preservation of off channel habitats, such as side channels and wetlands, which: • Provide off channel habitat • Provide allochthonous / nutrient input • Improve water quality • Recharge groundwater
Vegetation	• Species composition • Age class and longevity • LWM recruitment potential	Characterization vegetation communities and extents to determine availability of: • Shade for instream / side channel habitats • Allochthonous / nutrient input • LWM recruitment potential • Bank stabilization
Land Use	• Infrastructure • Land Use / Management	Evaluation of existing infrastructure and land use to determine: • Change in floodplain connectivity • Change in LWM potential • Change in availability of off channel habitats and associated water quality improvement potential

8.1 Groundwater Recharge and Storage Potential

8.1.1 Soils and Hydraulic Conductivity

The US Department of Agriculture's Natural Resources Conservation Service (NRCS) maintains a national database of mapped soil data known as the Web Soil Survey (NRCS 2024). Review of NRCS soil mapping is useful for understanding characteristics of soils relative to their location, parent material, hydraulic conductivity, and nutrient content, among others. Mapping, and the parameters included are primarily geared towards determining soil suitability for agricultural uses, however evaluation of these characteristics gives us insight into the hydraulic regime of each soil type, or soil series, for the purposes of floodplain reengagement and groundwater recharge to support instream flows and cold water inputs. Soil material, permeability, and nutrient content can also indicate the type(s) of off channel and riparian habitats that may potentially support or be supported by a specific soil series such as wetlands or groundwater recharge areas.

Review of NRCS-mapped soil types occurring within and immediately adjacent to the main channel indicates that the reach contains soils with moderate hydraulic conductivity and a moderately high water table (Figure 58, Table 13). The NRCS considers hydraulic conductivity to be "a quantitative measure of a saturated soil's ability to transmit water when subjected to a hydraulic gradient" (Ditzler 2017). Two of the mapped soil types within the reach (e.g., Pangborn muck, drained, 0-2% slopes [map unit 116] and Briscot silt loam, drained, 0-2% slopes [map unit 22]) are listed as "drained," meaning a noticeable reduction in the availability of groundwater is present. Limitations to available groundwater can impact the potential for relict floodplain features (e.g., abandoned side channels and swales) to function as viable off channel habitat, as well as limit the potential for riparian vegetation to establish and mature. Both of these soil types typically contain characteristics which may support wetlands or groundwater recharge, however, may be less conducive to provide these ecosystem function s in their drained state.

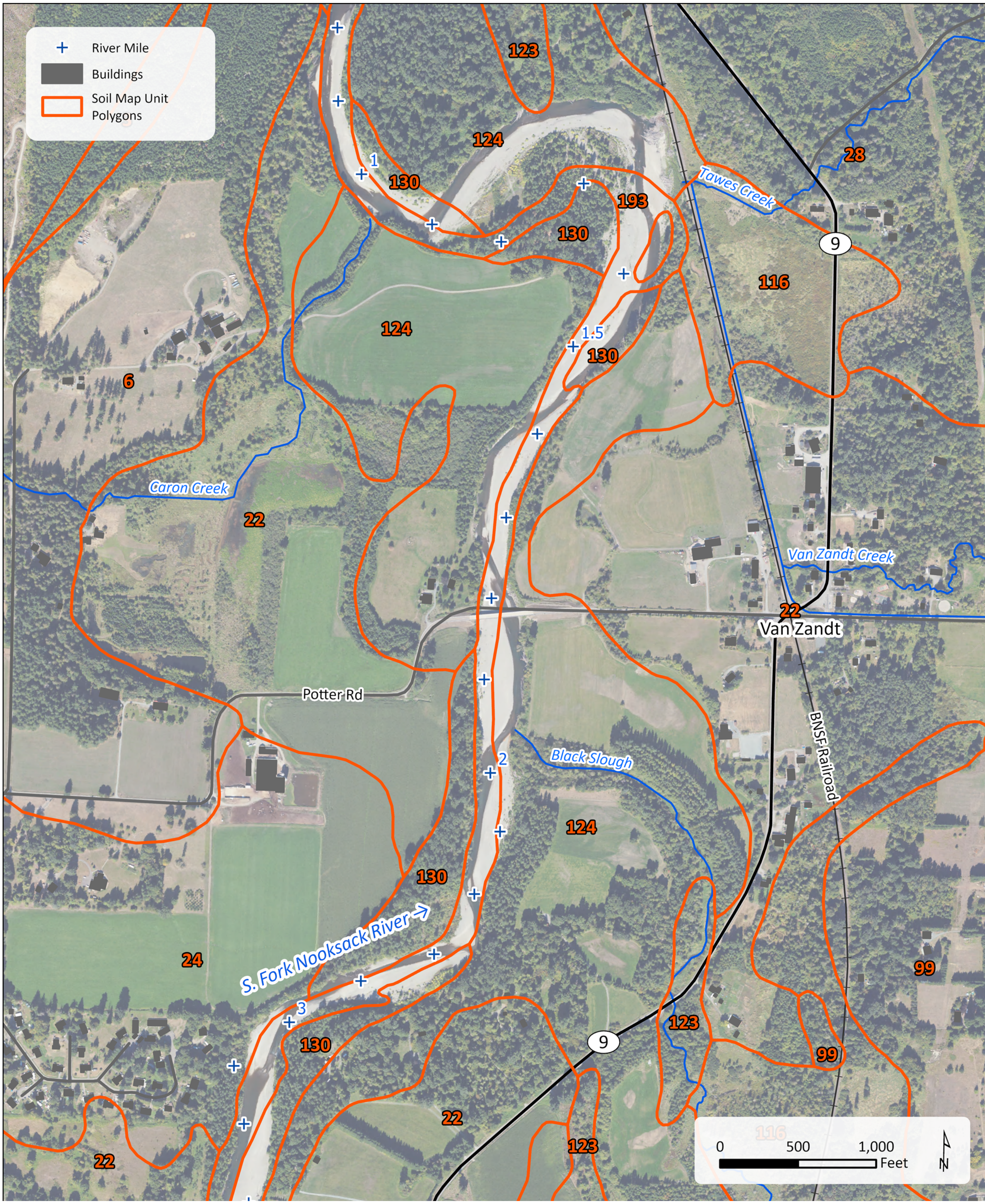

Figure 58. NRCS-mapped soils occurring within the Black Slough reach.

Table 13. Characteristics of dominant mapped soil series in Black Slough reach floodplain.

SOIL SERIES (MAP SYMBOL)	LOCATION	GENERAL CHARACTER	PERMEABILITY/ AVAILABLE WATER CAPACITY	NATIVE VEGETATION
Riverwash (130)	Instream and/or adjacent gravel bars	Alluvial areas, usually coarse-textured, exposed along streams at low water and subject to shifting during normal high water Hydric Rating: YES	Upper profile (alluvium): high Lower profile (underlying soils): low Depth to water table: 0-24"	N/A (NRCS-defined as "barren alluvial areas")
Puyallup fine sandy loam, 0-2% slopes (124)	Typically occurs on floodplains and low terraces	Coarse-loamy textured over sandy or sandy-skeletal alluvial deposits. Contains very fine sand, fine sandy loam, sandy loam, and silt loam Hydric Rating: NO	Well drained; high saturated hydraulic conductivity Depth to water table: more than 80"	Douglas-fir, western redcedar, bigleaf maple, black cottonwood, western hemlock, and red alder, with an understory of trailing blackberry, salmonberry, Oregon-grape, western swordfern, vine maple, and western brackenfern
Pangborn muck, drained, 0-2% slopes (116)	Depressional areas on outwash terraces, till plains, and stream terraces	Soils formed in herbaceous and woody organic deposits; moderate medium granular structure Hydric Rating: YES	Very poorly drained; very slow or ponded runoff; moderate permeability. Depth to water table: About 18 to 30"	Sitka spruce, western redcedar, western hemlock, lodgepole pine, and red alder, with an understory of sedge, rush, Douglas spirea, salmonberry, trailing blackberry, devils club, and skunk cabbage
Briscot silt loam, drained, 0-2% slopes (22)	Occur on floodplains in river valleys; formed in recent alluvium	Coarse-loamy, mixed containing 5 to 15 percent clay, and 0 to 2 percent coarse fragments Hydric Rating: YES	Poorly drained; very slow runoff; moderate permeability. Depth to water table: About 12 to 35"	Western redcedar, western hemlock, red alder, and Douglas-fir with an understory of western swordfern, salal, vine maple, western brackenfern, trailing blackberry, rose, northern bedstraw, and northern twinflower

SOIL SERIES (MAP SYMBOL)	LOCATION	GENERAL CHARACTER	PERMEABILITY/ AVAILABLE WATER CAPACITY	NATIVE VEGETATION
Puget silt loam, drained, 0-2% slopes (123)	Occurs on floodplains at elevations ranging from l0 to 650 feet	Silty clay loam soils formed in recent alluvium on floodplains and low river terraces Hydric Rating: YES	Poorly drained Slow to ponded runoff Moderate slow permeability Depth to water table: 12-35”	Red alder, black cottonwood, western redcedar, and willow with an understory of trailing blackberry, salmonberry, Oregon-grape, western swordfern, Indian plum, hardhack, willow, and rush.
Chuckanut loam, 3-8% slopes (24)	Occurs on hills and mountain slopes; formed in volcanic ash and colluvium from sandstone and glacial till	0 to 15% gravel and 0 to 5% cobbles Hydric Rating: NO	Well drained. Moderately high saturated hydraulic conductivity. Depth to water table: More than 80”	Douglas-fir, western hemlock, western redcedar, and red alder, with an undergrowth of salal, western brackenfern, western swordfern, Oregon-grape, red huckleberry, deer fern, princes pine, bedstraw, and Pacific trillium.

8.1.2 Wetland Presence

Excluding Riverwash – which is primarily comprised of instream gravels and cobbles – three of the five main soil series mapped within the Black Slough reach are categorized by the NRCS as hydric (Table 13, Figure 58); wetlands frequently occur in areas of mapped hydric soils. However, a non-hydric soil series can also contain hydric inclusions that have not previously been mapped – essentially, wetlands can occur on soils not mapped as hydric. Hydric soils are defined as soils that are saturated, flooded, or ponded for sufficient duration during the growing season to develop anaerobic (i.e., reducing) conditions in the upper horizons, which favor the growth and regeneration of vegetation adapted to live in moist or wet environments, otherwise known as hydrophytic (Environmental Laboratory 1987, 2010). Hydric soils may be further classified as drained or undrained, with drained hydric soils being those for which sufficient ground or surface water has been removed by an artificial means (e.g., ditching, subsurface drain tile) to such an extent that the area would no longer support hydrophytic vegetation (Environmental Laboratory 1987, 2010). All three of the soil series mapped within the Black Slough reach as hydric are categorized as “drained” (Table 13). As such, not all areas of hydric soil are wetlands.

The National Wetlands Inventory (NWI; USFWS 2024) online mapping program illustrates three types of features within the project reach: freshwater emergent wetland, freshwater forested/shrub wetland and riverine (Figure 59). The SFNR is mapped as riverine throughout the reach, as well as the Black Slough channel, along with portions of Caron Creek. Note the sizeable shift in river location at the downstream end of the project shown in Figure 59, since NWI mapping for the Black Slough reach was completed (USFWS 2024). Pockets of freshwater forested/shrub wetlands are mapped along the mainstem and at the downstream end of reach within the active meander bend at RM 1.3. A large mosaic of emergent wetland is present on the right overbank at approximately RM 1.4 (Figure 60) which conveys flow from Tawes Creek and Van Zant Creeks through a narrow bridge below the railroad prism to the mainstem (Figure 61). The low, saturated area is further confined by Highway 9 to the east and the BNSF railway to the west as shown in Figure 60, and further discussed in Section 6.2.2.

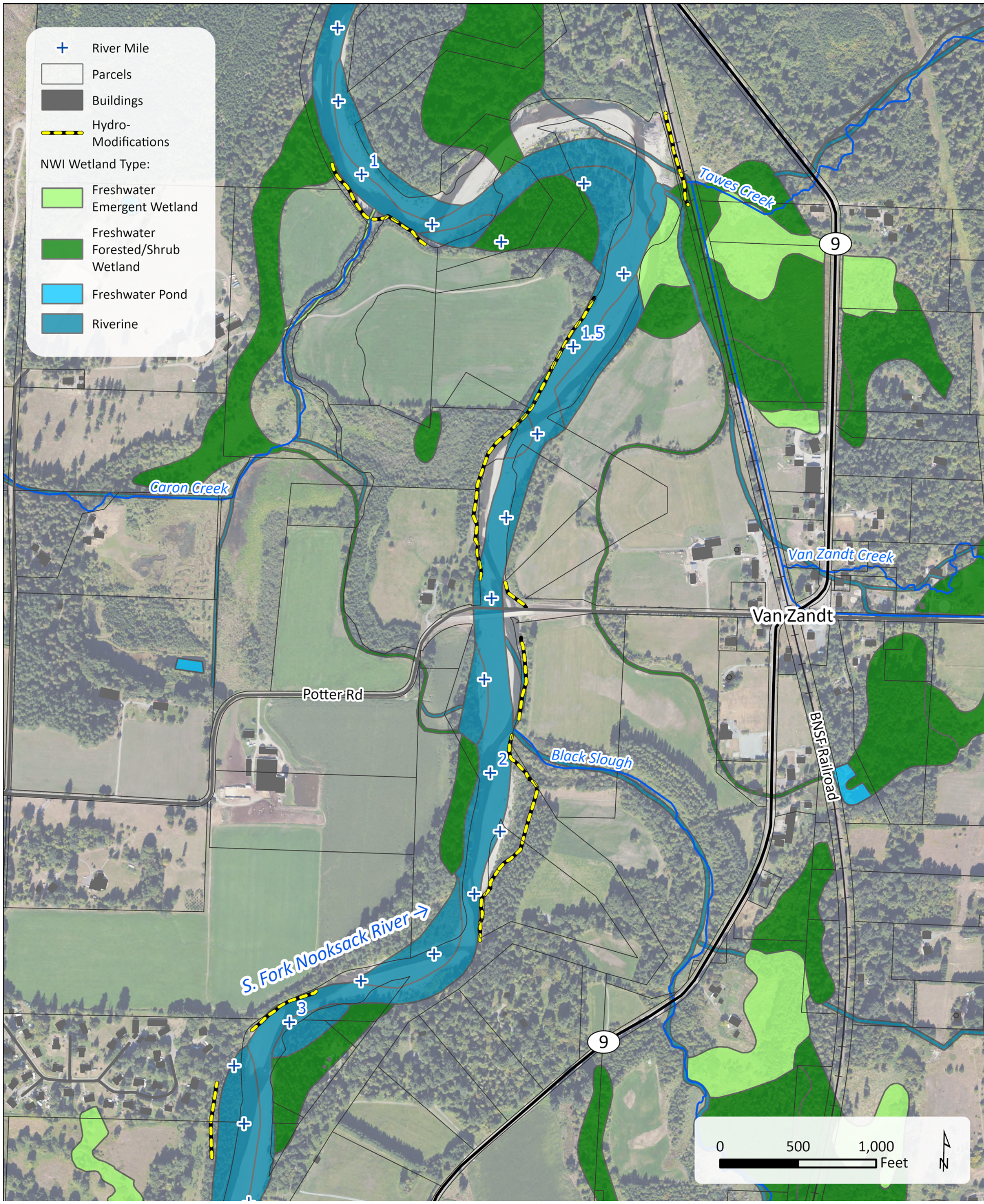

Figure 59. NWI-mapped wetlands occurring within the Black Slough reach.

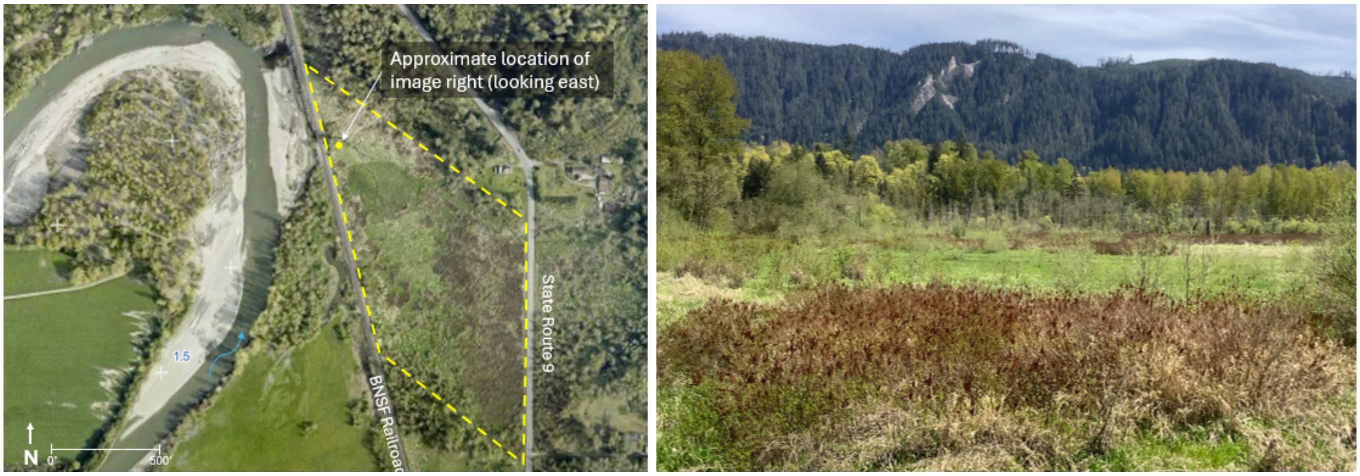

Figure 60. Approximate extents of observed wetland complex at RM 1.3.

Figure 61. Confined wetland complex and tributary connection to the SFNR at approximately RM 1.3, photo taken looking east.

Although NWI mapping provides a cursory indication of areas which may potentially meet wetland criteria, it is a cursory estimate based on aerial imagery from 1981 (USFWS 2024); site specific verification is required to determine actual wetland presence. Select field observations indicate hydric soils are present in some locations which receive overbank flows (Figure 48), or within topographic depressions and swales which are capable of capturing and holding water for extended periods of time.

Notably, no wetlands are mapped by the NWI within the floodplain along Black Slough, although field observations indicate that wetland features (e.g., indicators of hydric soils and hydrophytic vegetation) have developed within the narrow band of riparian vegetation on the northern side of the channel. Hydraulic modeling output (Figure 48) supports this development, indicating that the areas receive overbank flows at a frequency and duration capable of developing and sustaining wetland characteristics. Similarly, hydric soil indicators were observed along a narrow strip of inset floodplain on river right at RM 2.1, and again along river left at RM 2.3 (Figure 62).

Figure 62. Observed hydric soils along left overbank at approximately RM 2.4 in an NRCS-mapped area of Riverwash.

A second large wetland complex occurs on the river left overbank, approximately between RM 1.6 and 1.9, stretching across three parcels owned by the Washington Department of Transportation (WSDOT). The three parcels, and wetland complex, are a compensatory wetland mitigation site which was constructed to offset impacts incurred elsewhere in the basin by a WSDOT project. The site is currently in its tenth and final year of monitoring for permit compliance and will be managed in perpetuity by WSDOT. Public access is restricted. According to personal communication with WSDOT, since the original design and implementation of the project in ~2015, the site has developed a different vegetation community and hydrology regime due to beaver activity than what was originally designed and permitted. These parcels are currently hydrologically disconnected from the SFNR by a length of riprap bank hardening shown in Figure 59.

8.2 Land Use, Riparian Shade, and Large Wood Potential

Forests in the SRNR basin have been systematically removed, both cleared out to make way for agricultural use and harvested for timber since the arrival of settlers in the mid-late 1800s. Logging activities removed most of the old-growth forest from the valley bottom and riparian areas throughout the watershed. Large scale timber clearing and rural development in the valley bottom has contributed to bank instability and a disconnection between the stream and its floodplain. To develop agricultural fields, floodplain wetlands and low-lying marshy areas were ditched and drained, cutting those areas of former habitat off from the river, confining floodwaters to the channel, thereby increasing erosional force. Some areas of deciduous forest have regenerated in floodplains within the project reach – in many cases with early successional species such as red alder and black cottonwood (<60-year-old) and lacking significant stands of conifers. Existing riparian and floodplain forests generally lack potential key member size large woody debris (LWD) source trees. Without conifer infill plantings, these riparian forests will lack future key member size LWD.

Vegetative age class and community composition vary across the Black Slough reach and directly correlate with land use, as illustrated in Figure 63. Dominant communities include mixed coniferous-deciduous forest and agricultural fields. The type and composition of vegetative communities can be indicative of the duration of available soil moisture, frequency of inundation from overbank flows, and the depth and availability of groundwater. Both the forested and scrub-shrub communities are composed of predominately native and commonly occurring floodplain forest species that are tolerant of moist soils and frequent prolonged inundation. The mix of species present indicates high soil moisture holding capacity in the soils and presumably a high-water table that extends well into the late spring and early summer.

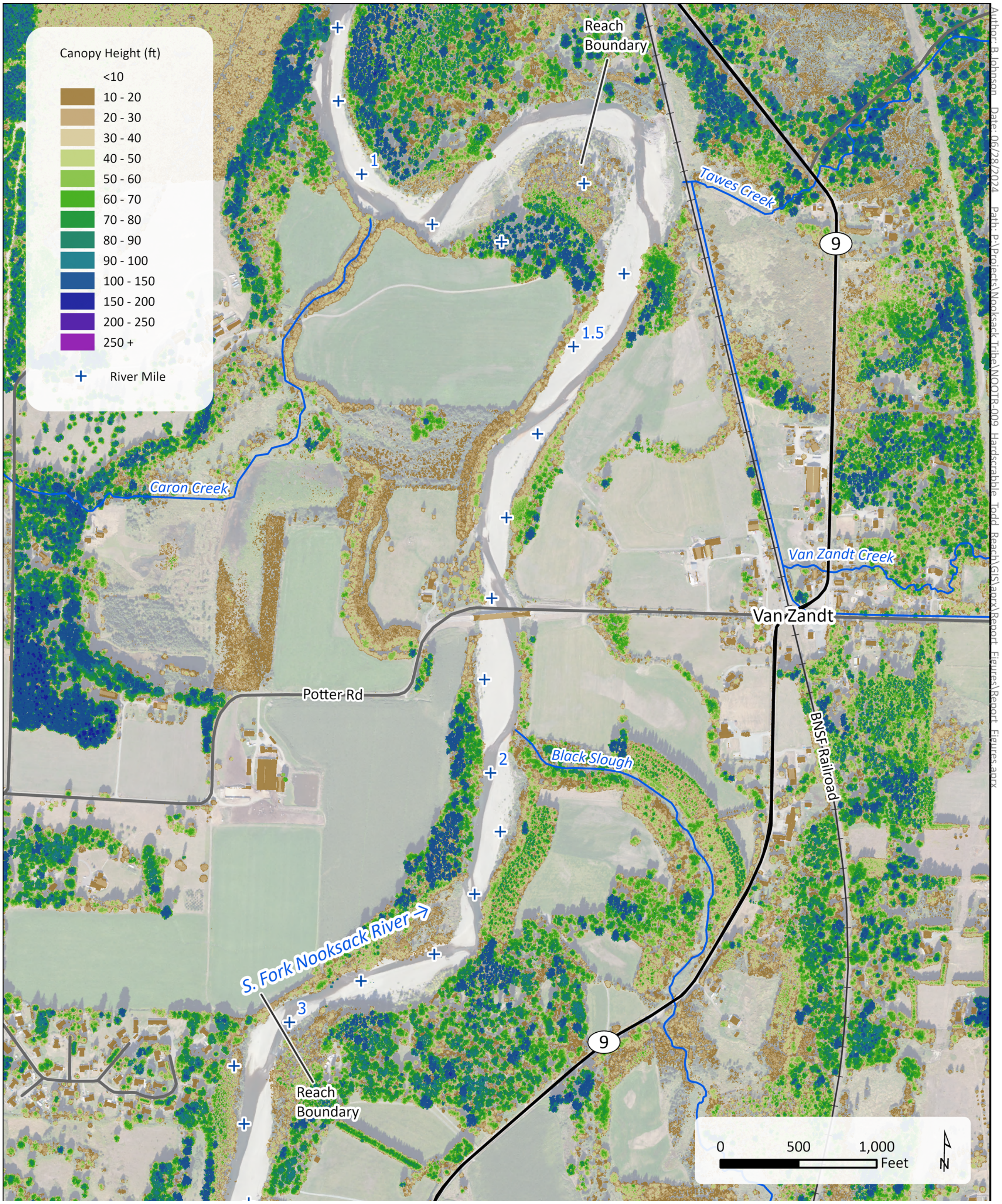

Figure 63. Canopy height map of project reach and lower SFNR valley.

As shown in Figure 63, the dominant vegetation type with the project reach is crop and pasture, some of which extends into the riparian buffer area that would typically contain woody trees and shrubs. Ecology estimates that crop and pasture land account for 6% of the riparian buffer area along the entire mainstem of the South Fork Nooksack (Ecology 2020). Further, the composition of available riparian areas gives us insight into potential for sustained shade to the mainstem as well as strong root cohesion for erosion protection, which is lacking in some areas (Figure 64). An estimated 2% of the lower SFNR watershed contains coniferous forest, whereas an estimated 46% of the upper SFNR watershed contains coniferous forest (Ecology 2020). Dominance of red alder (*Alnus rubra*) and cottonwood (*Populus trichocarpa*) indicates that currently forested riparian areas are fairly short-lived; red alder is an early successional tree that commonly does not live beyond 60 years (Franklin and Dryness 1988) (Figure 65).

Figure 64. Segment of actively eroding bank along river right at RM 1.4.

Figure 65. Riparian conditions dominated by alder, willow, and cottonwood at approximately RM 1.3; note lack of coniferous species.

8.2.1 Implication for Instream Habitats

A number of studies have found that logging and removal of riparian vegetation can cause stream temperatures to increase by 5°C or more (Moore et al. 2005) and can cause significant spikes in diel fluctuations compared to historic or old growth riparian conditions (Thomas et al., 1986). A 2018 study (Seixas et al.) found that that accounting for tree growth along channel margins in the Chehalis River basin reduced projected exceedance of lethal thresholds for juvenile salmonids in 2080 by 30% across streams compared to models that did not account for tree growth. Riparian growth, particularly in the form of deciduous riparian shrubs and trees, also provides an important food source /prey for juvenile salmonids (Grunblatt et al. 2019).

An analysis of canopy height within the project reach (Figure 63) concluded that the general height distribution of vegetation provides little shade relief for the mainstem. We used a used a generalized centerline of the SFNR and offset this centerline by 300 feet on either side (black polygon, Figure 66), to create a riparian area. A 300-ft offset was determined to be the greatest width where riparian vegetation could influence available shade within the mainstem, and/or provide large wood loading. This method indicates that 67% of the riparian area contains vegetation or landcover that is less than 10-ft in height. 20% of this polygon contains vegetation that is between 10-50-ft in height, and the remaining 15% contains vegetation greater than 50-ft in height. The highest signature within this buffer area is 171-ft. Notably, this cursory method did not distinguish between open water, gravel bar, or road features within the buffer. Because of this, the category representing land uses or vegetation less than 10-ft over represents the area potentially available for vegetation growth, however it is useful in describing the sever lack of shade within the Black Slough reach.

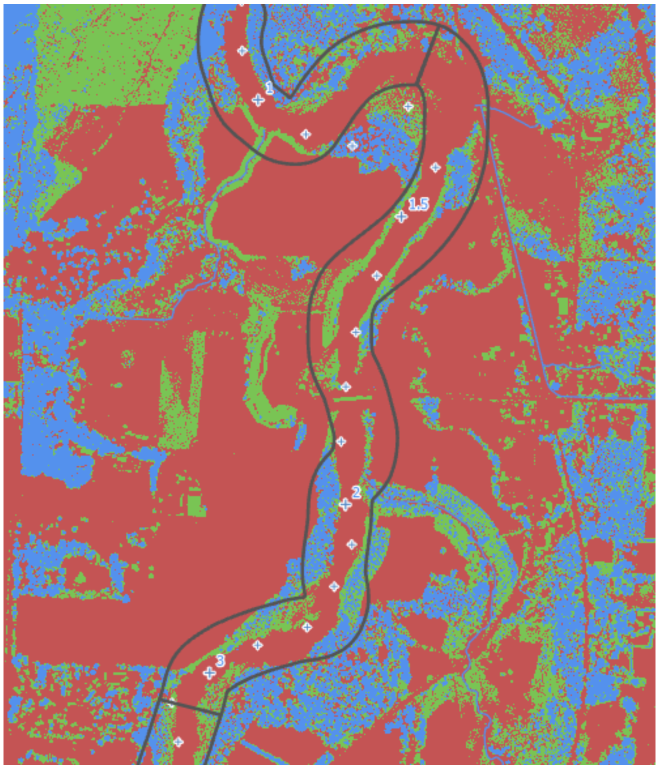

Figure 66. Generalized height distribution of land cover within the Black Slough reach

The Department of Ecology's South Fork Nooksack Temperature TMDL Water Quality Improvement Report (Ecology 2020) recommends management of instream temperature impairments by focusing on shading and management of riparian forests to reduce solar input. The study calculated effective shade available from current (2007 and 2010) riparian vegetation using a Shade model. Their study concluded that the amount of available shade to the mainstem SFNR is decreasing based on patterns in land use and geomorphic changes to banks through erosion and scour of unstable banks lacking woody vegetation (Figure 67).

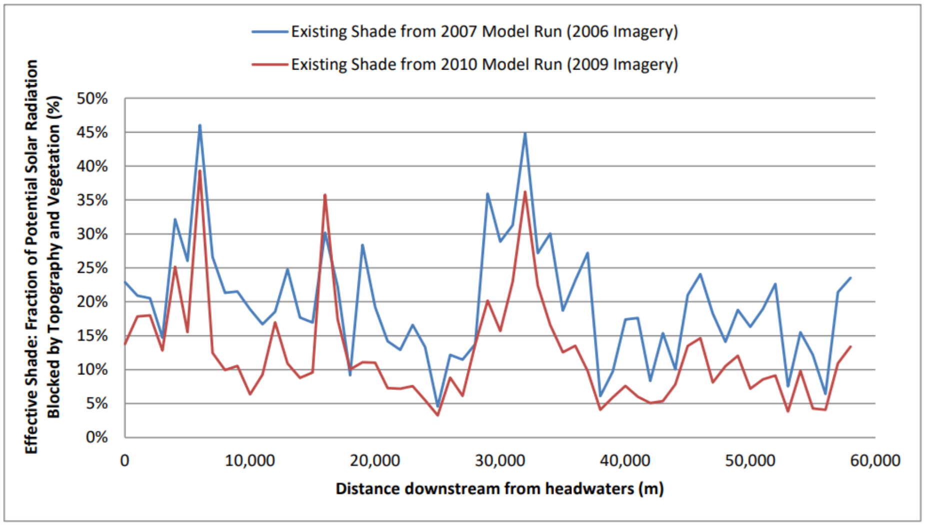

Figure 67. Effective riparian shade available to the mainstem SFNR under 2006 and 2009 vegetation conditions (Ecology 2020).

9 SUMMARY OF IMPAIRMENTS

The following section attempts to briefly summarize key findings and impairments identified within the project reach as a result of these analyses. Impairments are organized by discipline, or process, however most have intertwined and overarching implications on the functions and services provided by other processes within the reach. As is true with complex and dynamic systems, we recognize that a number of key findings may share a root cause, yet the affect of that cause may have manifested in a variety of ways across the project reach. The intent of this section is to focus the project team's attention on key concepts and observations which may offer opportunity for modification and thus the improvement of instream habitats and ultimately meeting the project goals.

Influence of Geomorphic Trends on Channel Stability and Floodplain Processes

Historical land use impacts and active removal of wood jams have altered channel migration patterns and sediment dynamics in the reach. A substantial change in channel pattern occurred between the 1919 mapping and 1933 aerial photos showing a bend cutoff that shortened and straightened the channel upstream of Potter Road and the disconnection of a split flow channel which had previously engaged the western floodplain and formed a large island downstream of Potter Road (Figure 25). A series of riprap revetments were constructed between the 1950s and 1980s which have temporarily limited bank erosion in the reach.

These anthropogenic changes have led to existing conditions; the channel is now constrained within a relatively narrow corridor with low sinuosity leaving relict channels in the floodplain that are largely disconnected from the main channel. Recruitment of large wood has been limited by forest clearing and riprap armoring such that only 1 stable log jam was observed in the 1.8-mile-long reach. Following a period of moderate channel incision in response to wood removal, evidence suggests the channel has maintained relative stability between sediment supply and transport capacity since the mid-1900s.

Influence of Hydraulic Trends on Channel Stability and Instream Habitats

The mainstem SFNR currently lacks diverse habitat conditions – the majority of the project reach is classified as a "run." Some pools are present within the project reach and are concentrated on the outside of meander bends and are associated with wood presence. Notably, floodplain connectivity is an issue, particularly in conjunction with anthropogenic features that impact and restrict floodplain processes such as the Potter Road bridge and associated infrastructure. Increased connectivity of overbank and/or inset floodplain area would lessen shear stress on channel bed material and decrease likelihood of redd scour and preservation of instream habitats.

Climate Change Impacts and Aquatic Habitat Resiliency

Modeling and observed trends indicate an increase in peak flows is expected in the SFNR. Studies show the increase in peak flows will be on the order of 23-34% of current conditions (Paul 2023). Increased peak flows typically contribute to an increase in instream velocities which increase potential for the mobilization and transport of sediments, causing scour and bank failure, ultimately incising or lowering the channel bed. Redistribution of channel and bank features due to high velocity floodwaters have shown to increase channel width and depth over time. This fact highlights the need for floodplain engagement, to capture, slow, and attenuate floodwaters, thus reducing risk to nearby infrastructure and instream habitats.

In conjunction with increased peak flows, decreased low flows are also predicted, on the order of -20% or greater. Some studies (Wenger 2010) show a decrease of up to -65% at low flow. These changes represent a drop in Q1 flows from 157 cfs (historical conditions) to 122 cfs (mid-century conditions) and 102 cfs (late-century conditions). Lower low flows will manifest as lower water depths and increased areas of dewatering, both within the mainstem and likely in contributing tributaries. Lower water depths present concern for increased instream temperatures highlighting the need for pools and high quality low flow habitat.

Influence of Floodplain and Riparian Conditions on Water Quality

As noted, access to floodplain area is lacking throughout the reach as overbank flows are confined to the mainstem channel. Because of this, there is currently little presence of shade in the form of vegetation for the mainstem, and no vegetated islands are present within the reach. Connection to the few available overbank habitats (e.g., wetlands, tributaries, inset floodplain) is limited by bank hardening, infrastructure (e.g., Potter Road bridge, BNSF railroad), and accessibility of these habitats is decreasing due to ongoing channel incision. The lack of riparian cover contributes to bank instability and erosion throughout the project reach and is unable to provide adequate shade to alleviate increasing instream temperatures for the deepening and widening channel. Existing vegetation structure is comprised of short-lived species and offers little potential for large wood recruitment.

The Black Slough tributary connection offers opportunity for the reconnection of off channel habitats, development of complex wetland conditions, and greater availability of riparian shade and allochthonous input for the mainstem. Floodplain soils indicate potential for water storage in currently poorly drained soils. A number of planting initiatives have been undertaken in recent years which are contributing the improvement of riparian conditions within the reach.

10 NEXT STEPS

The results of this analysis are intended to inform the collaborative development of conceptual designs for the Black Slough reach which will aim to address identified limiting factors and reset habitat-forming and sustaining processes within the reach. LNR is committed to working with local landowners and stakeholders to identify opportunities to create solutions which benefit instream habitats and the lower South Fork Nooksack valley community as a whole. To that end, a community meeting is planned on September 10, 2024, to meet with stakeholders, describe the project intent, discuss identified impaired processes, and gain input from landowners. Following the community meeting, NSD + CGS and LNR will collaboratively develop design alternatives, from which a preferred alternative will be carried forward into conceptual design.

11 LITERATURE CITED

Abatzoglou J.T. and Brown T.J. A comparison of statistical downscaling methods suited for wildfire applications, International Journal of Climatology (2012), 32, 772-780. https://rmets.onlinelibrary.wiley.com/doi/full/10.1002/joc.2312

Anchor Environmental, LLC. 2003. Fish Periodicity in WRIA 1. January 2003 draft. Prepared for City of Bellingham Public Works Department.

Butcher, J.B., M. Faizullabhoy, H. Nicholas, P. Cada, and J.T. Kennedy. 2016. Quantitative Assessment of Temperature Sensitivity of the South Fork Nooksack River Nooksack River under Future Climates using QUAL2Kw. EPA/600/R-14/233. Western Ecology Division, National Health and Environmental Effects Research Laboratory, Corvallis, OR.

Cooke, S. 1997. A Field Guide to Common Wetland Plants of Western Washington and Northwestern Oregon. Seattle Audubon Society. Seattle, Washington.

Ditzler, C. 2017. A Glossary of Terms Used in Soil Survey and Soil Classification Including Definitions and Brief Commentary. January 2017. Available: https://www.nrcs.usda.gov/sites/default/files/2022-08/A_Glossary_of_Terms_Used_in_Soil_Survey_and_Classification.pdf.

Environmental Laboratory. 1987. U.S. Army Corps of Engineers Wetland Delineation Manual. Technical Report Y-87-1. U.S. Army Waterways Experiment Station. Vicksburg, MS.

Environmental Laboratory. 2010. U.S. Army Corps of Engineers Regional Supplement to the Corps of Engineers Wetland Delineation Manual: Western Mountains, Valleys, and Coast Region (Version 2.0). Technical Report TR-10-3. U.S. Army Engineer Research and Development Center. Vicksburg, MS.

Environmental Protection Agency (EPA). 2016. Qualitative Assessment: Evaluating the Impacts of Climate Change on Endangered Species Act Recovery Actions for the South Fork Nooksack River, WA. EPA/600/R-16/153. Western Ecology Division, National Health and Environmental Effects Research Laboratory, Corvallis, OR.

Gendaszek, A., 2014. Hydrogeologic Framework and Groundwater/Surface-Water Interactions of the South Fork Nooksack River Basin, Northwestern Washington (No. 2014–5221). U.S. Geological Survey, Reston, Virginia.

Grah, O., O'Neil, H., Coe, T., 2018. South Fork Nooksack River Watershed Conservation Plan. Nooksack Indian Tribe Natural Resources Department.

Jantsch, S. 2023. A Characterization of Hyporheic Temperatures with Applications for Salmon Habitat Restoration in a Thermally Impaired River. WWU Graduate School Collection. 1251. https://cedar.wwu.edu/wwuet/1251

Malick, G., 2018. Geologic Development and Ongoing Activity of the Van Zandt Landslide Complex, Northwest WA, USA (Masters Thesis). Western Washington University.

Maudlin, M., A. Levell, and N. Rice. 2020. Nooksack River Instream Project Effectiveness. April 2020. Prepared by Nooksack Tribe and Lummi Nation.

Maudlin, M. 2021. Summary of Habitat Status and Trends Indicators and Habitat Goals. WRIA 1 Nooksack Salmon Chapter Update. Nooksack Indian Tribe Natural and Cultural Resources Department.

Natural Systems Design (NSD). 2021. Upper South Fork Nooksack River Effectiveness Monitoring - Assessment and Recommendations. Produced for Lummi Nation Natural Resources Department.

Neiman, P. J., Schick, L. J., Ralph, F. M., Hughes, M., & Wick, G. A. (2011). Flooding in Western Washington: The

Connection to Atmospheric Rivers. Journal of Hydrometeorology, 12(6), 1337–1358. https://doi.org/10.1175/2011JHM1358.1

Nooksack Indian Tribe (NIT). 2018. South Fork Nooksack River Watershed Conservation Plan. Published May 2017 and Final Update January 2018. Prepared by the Nooksack Indian Tribe Natural Resources Department.

Soicher, A., Coa, T., Currence, N., 2006. South Fork Nooksack River Acme-Confluence Reach Restoration Planning: Analysis of Existing Information and Preliminary Restoration Strategies. Nooksack Indian Tribe Natural Resources Department.

USGS StreamStats, n.d.

Ralph, F. M., & Dettinger, M. D. (2011). Storms, floods, and the science of atmospheric rivers. Eos, Transactions American Geophysical Union, 92(32), 265–266. https://doi.org/10.1029/2011EO320001

Salathé, E.P., Hamlet, A.F., Mass, C.F., Lee, S.-Y., Stumbaugh, M., and Steed, R., 2014, Estimates of Twenty-First-Century Flood Risk in the Pacific Northwest Based on Regional Climate Model Simulations: Journal of Hydrometeorology, v. 15, p. 1881–1899, doi:10.1175/JHM-D-13-0137.1.

Warner, M. D., & Mass, C. F. (2017). Changes in the Climatology, Structure, and Seasonality of Northeast Pacific Atmospheric Rivers in CMIP5 Climate Simulations. Journal of Hydrometeorology, 18(8), 2131–2141. https://doi.org/10.1175/JHM-D-16-0200.1

Nooksack Indian Tribe. 2018. South Fork Nooksack River Watershed Conservation Plan. Nooksack Indian Tribe Natural Resources Department. May 2017, updated January 2018.

Washington Department of Ecology (Ecology). 2020. South Fork Nooksack River Temperature Total Maximum Daily Load Water Quality Improvement Report and Implementation Plan. Publication No. 20-10-007. https://apps.ecology.wa.gov/publications/documents/2010007.pdf

Wenger, S. J., Luce, C. H., Hamlet, A. F., Isaak, D. J., & Neville, H. M. (2010). Macroscale hydrologic modeling of ecologically relevant flow metrics. Water Resources Research, 46(9). https://doi.org/10.1029/2009WR008839

Whatcom County (2020), Whatcom County Climate Action Plan: Summary of Observed Trends and Projected Climate Change Impacts. https://www.whatcomcounty.us/DocumentCenter/View/53837/Whatcom-County-Climate-Science-Summary-2020

Whatcom County (2021), Climate Action Plan, https://www.whatcomcounty.us/DocumentCenter/View/69472/WC-2021-Climate-Action-Plan---pages

WRIA 1 Salmon Recovery Board (SRB). 2005. WRIA 1 Salmonid Recovery Plan. https://wria1project.whatcomcounty.org/resources/guiding-documents-plans/wria-1-watershed-management-plan-associated-documents

Appendix A

Mapbook of Historical Imagery

South Fork Nooksack River, Black Slough Reach
Historical Maps and Imagery (1855-2024)

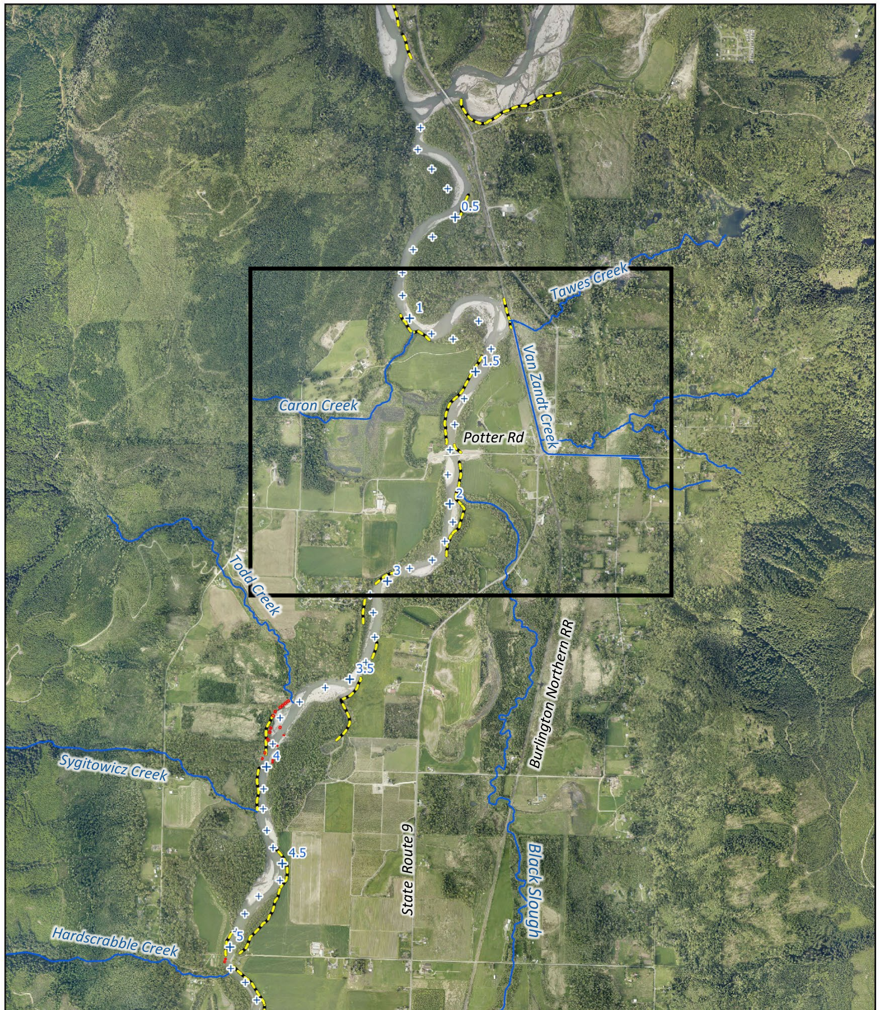

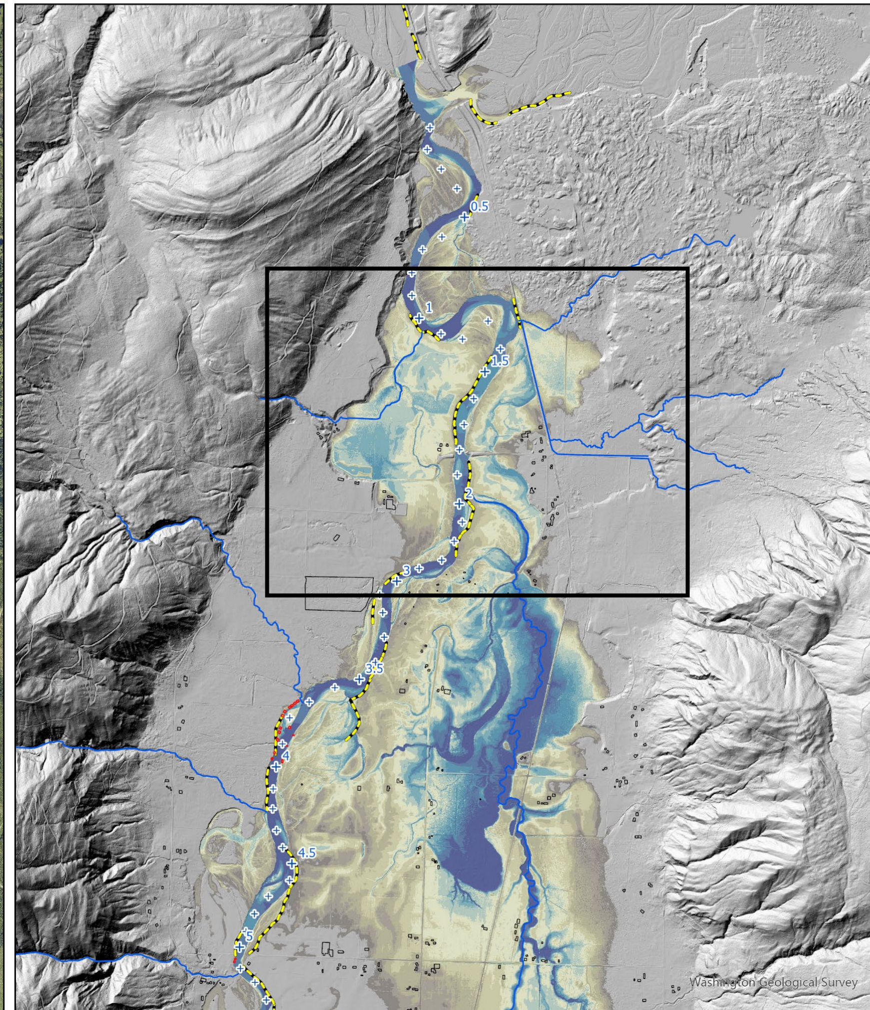

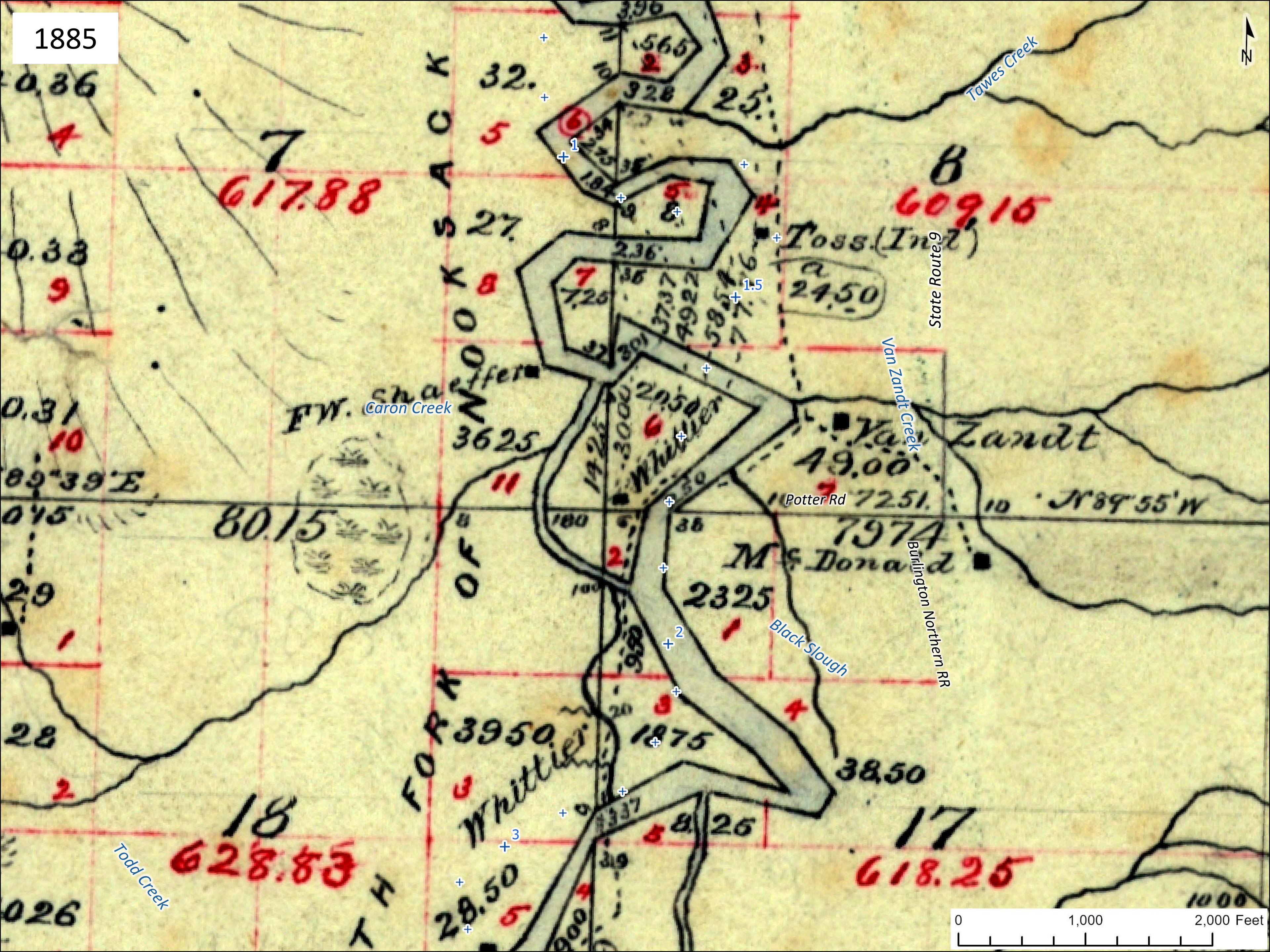
1885
Tawes Creek
State Route 9
Van Zandt Creek
Caron Creek
Potter Rd
Burlington Northern RR
Black Slough
Todd Creek
N
Toss.(Int.)
Van Zandt
F.W. Shaeffer
Whittier
M^c Donald
N. FORK OF NOOKSACK
617.88
609.16
628.83
618.25
N 89°55'W
0
1,000
2,000 Feet

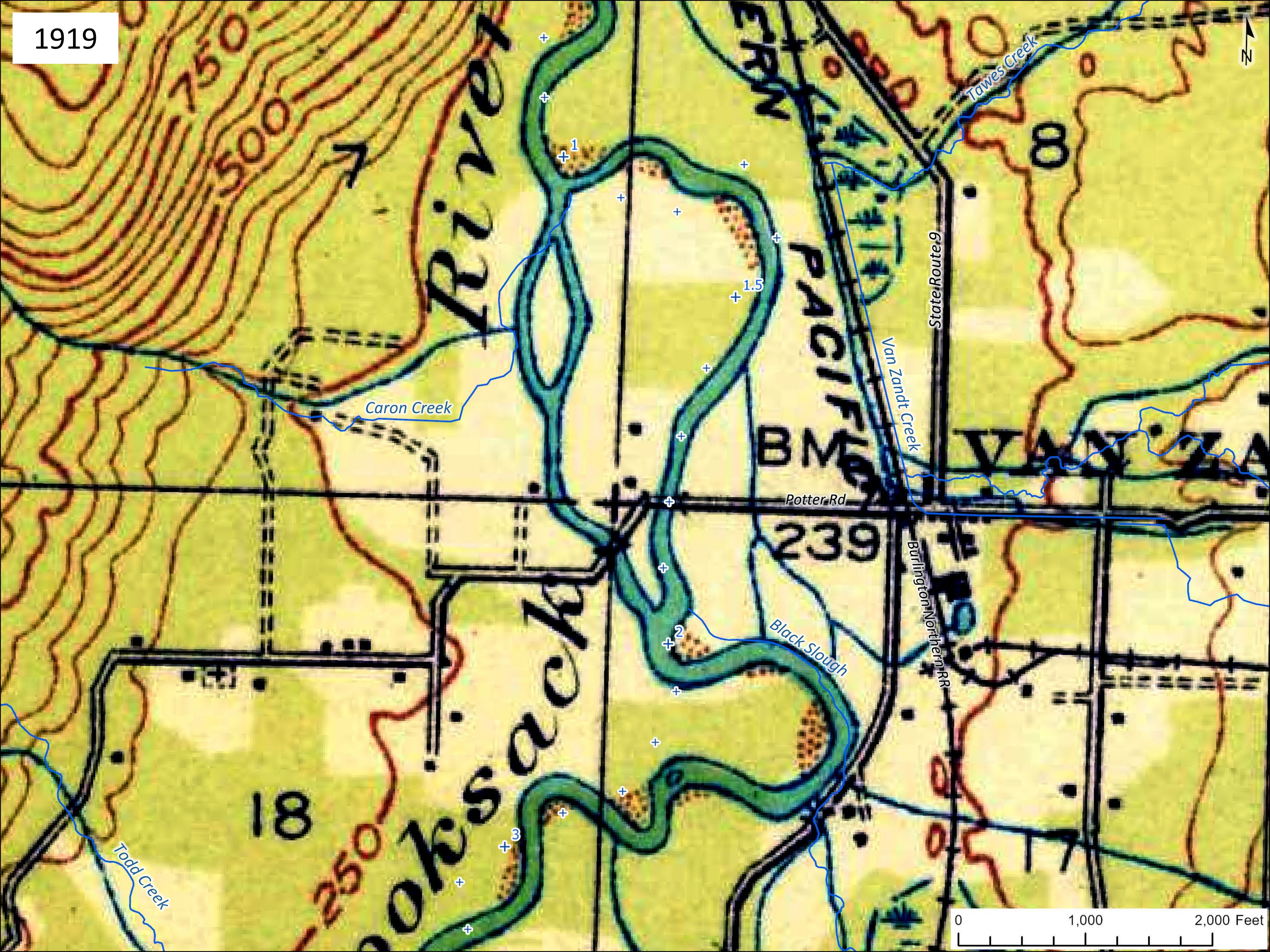
1919
N
750
500
250
River
Nooksack
Caron Creek
Tawes Creek
Van Zandt Creek
State Route 9
Potter Rd
BM
239
VAN ZA
Black Slough
Burlington Northern RR
Todd Creek
8
18
17
1
1.5
2
3
0
1,000
2,000 Feet

1933
N
Tawes Creek
State Route 9
Van Zandt Creek
Caron Creek
Potter Rd
Burlington Northern RR
Black Slough
Todd Creek
1
1.5
2
3
0
1,000
2,000 Feet

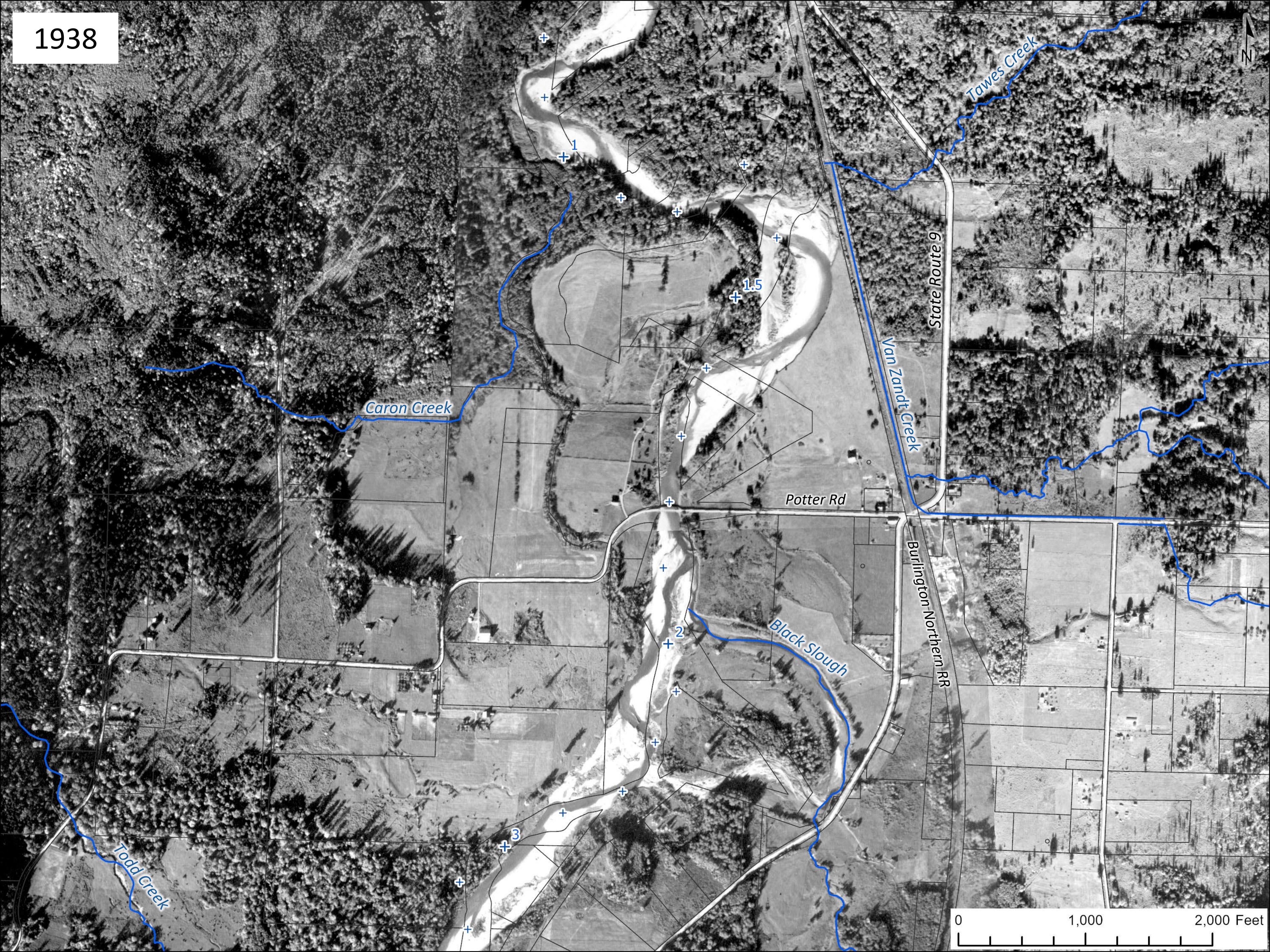
1938
Tawes Creek
State Route 9
Van Zandt Creek
Caron Creek
Potter Rd
Burlington Northern RR
Black Slough
Todd Creek
1
1.5
2
3
0
1,000
2,000 Feet
N

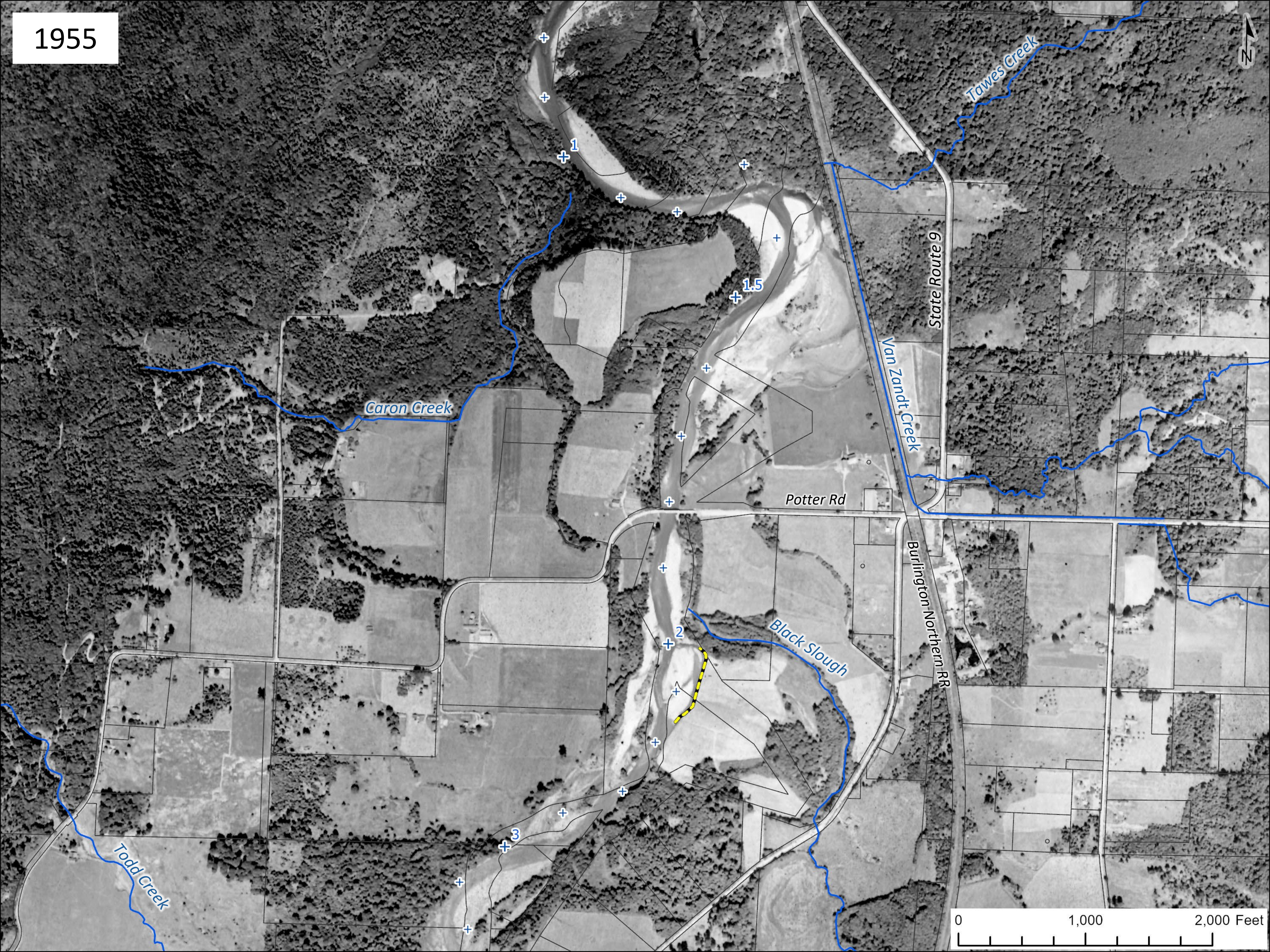
1955
N
Tawes Creek
State Route 9
Van Zandt Creek
Caron Creek
Potter Rd
Burlington Northern RR
Black Slough
Todd Creek
1
1.5
2
3
0
1,000
2,000 Feet


1967
N
1
1.5
2
3
Tawes Creek
State Route 9
Van Zandt Creek
Caron Creek
Potter Rd
Burlington Northern RR
Black Slough
Todd Creek
0
1,000
2,000 Feet


1976
Tawes Creek
State Route 9
Van Zandt Creek
Caron Creek
Potter Rd
Burlington Northern RR
Black Slough
Todd Creek
1
1.5
2
3
0
1,000
2,000 Feet
N

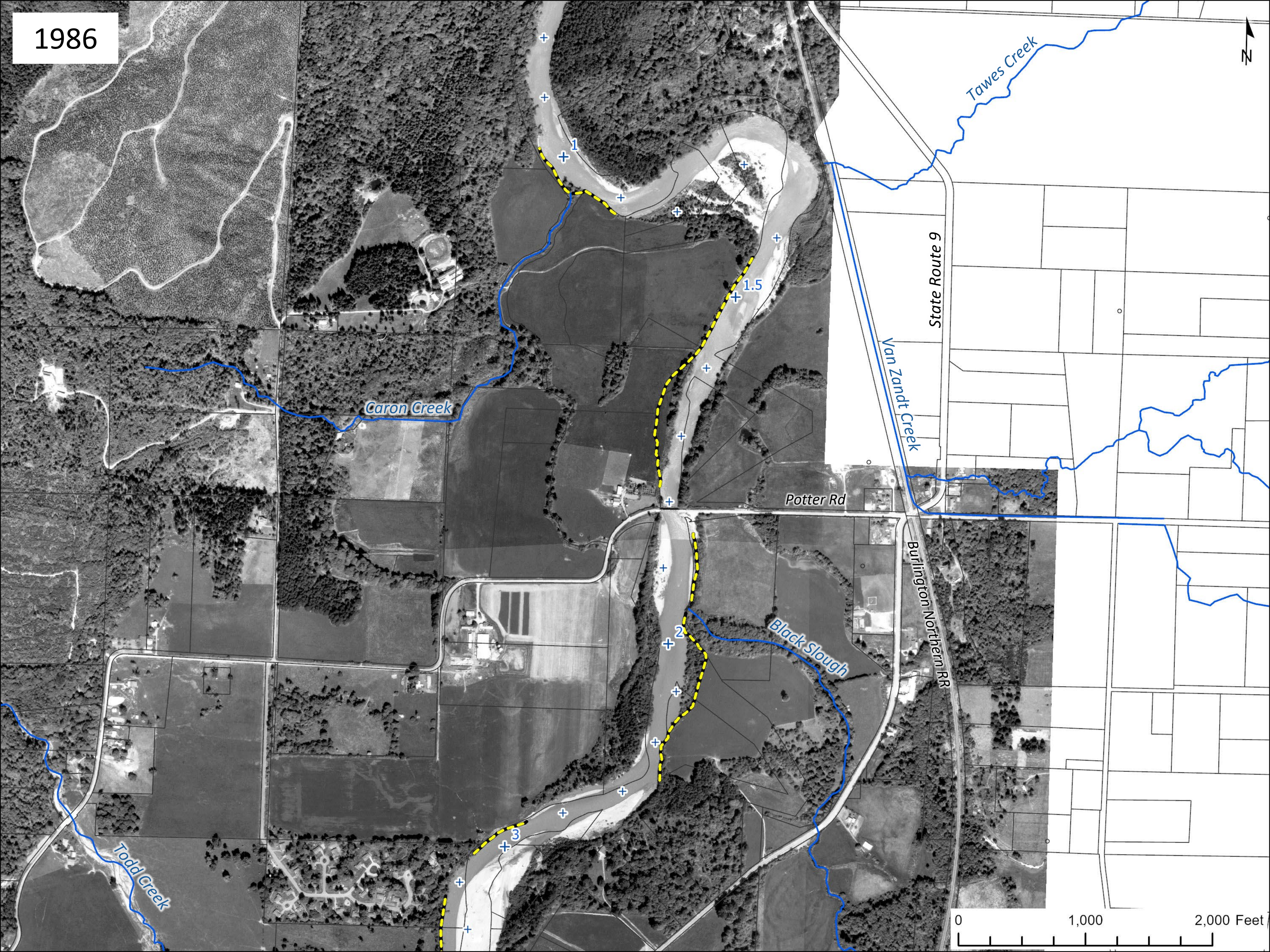
1986
N
Tawes Creek
State Route 9
Van Zandt Creek
Caron Creek
Potter Rd
Burlington Northern RR
Black Slough
Todd Creek
1
1.5
2
3
0
1,000
2,000 Feet


1998
N
Tawes Creek
State Route 9
Van Zandt Creek
Caron Creek
Potter Rd
Burlington Northern RR
Black Slough
Todd Creek
1
1.5
2
3
0
1,000
2,000 Feet


2006
N
Tawes Creek
State Route 9
Van Zandt Creek
Caron Creek
Potter Rd
Burlington Northern RR
Black Slough
Todd Creek
1
1.5
2
3
0
1,000
2,000 Feet

2016
N
Tawes Creek
1
1.5
State Route 9
Van Zandt Creek
Caron Creek
Potter Rd
2
Black Slough
Burlington Northern RR
3
Todd Creek
0
1,000
2,000 Feet

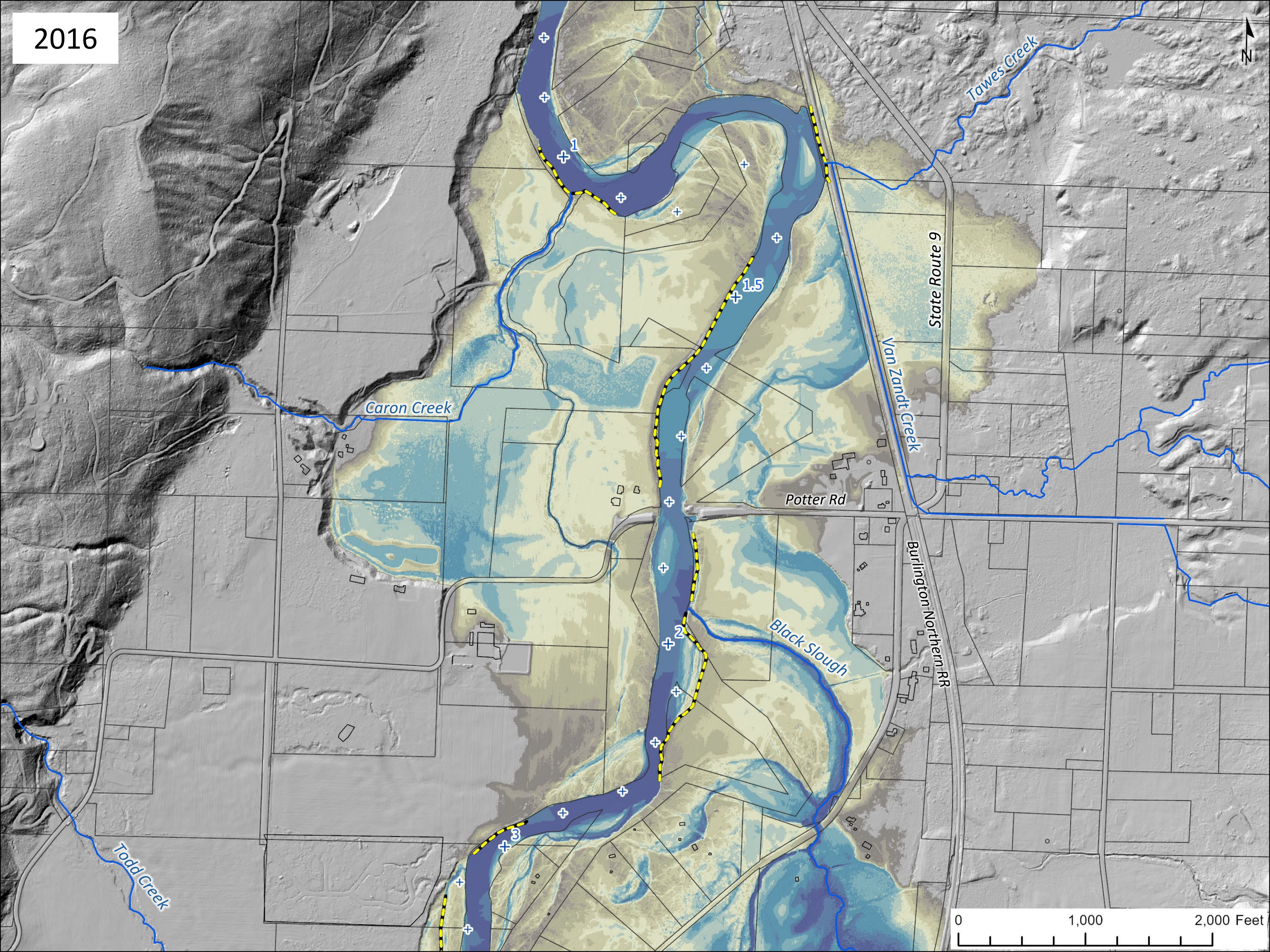
2016
N
Tawes Creek
State Route 9
Van Zandt Creek
Caron Creek
Potter Rd
Burlington Northern RR
Black Slough
Todd Creek
1
1.5
2
3
0
1,000
2,000 Feet

2023
Tawes Creek
State Route 9
Van Zandt Creek
Caron Creek
Potter Rd
Burlington Northern RR
Black Slough
Todd Creek
1
1.5
2
3
0
1,000
2,000 Feet
N

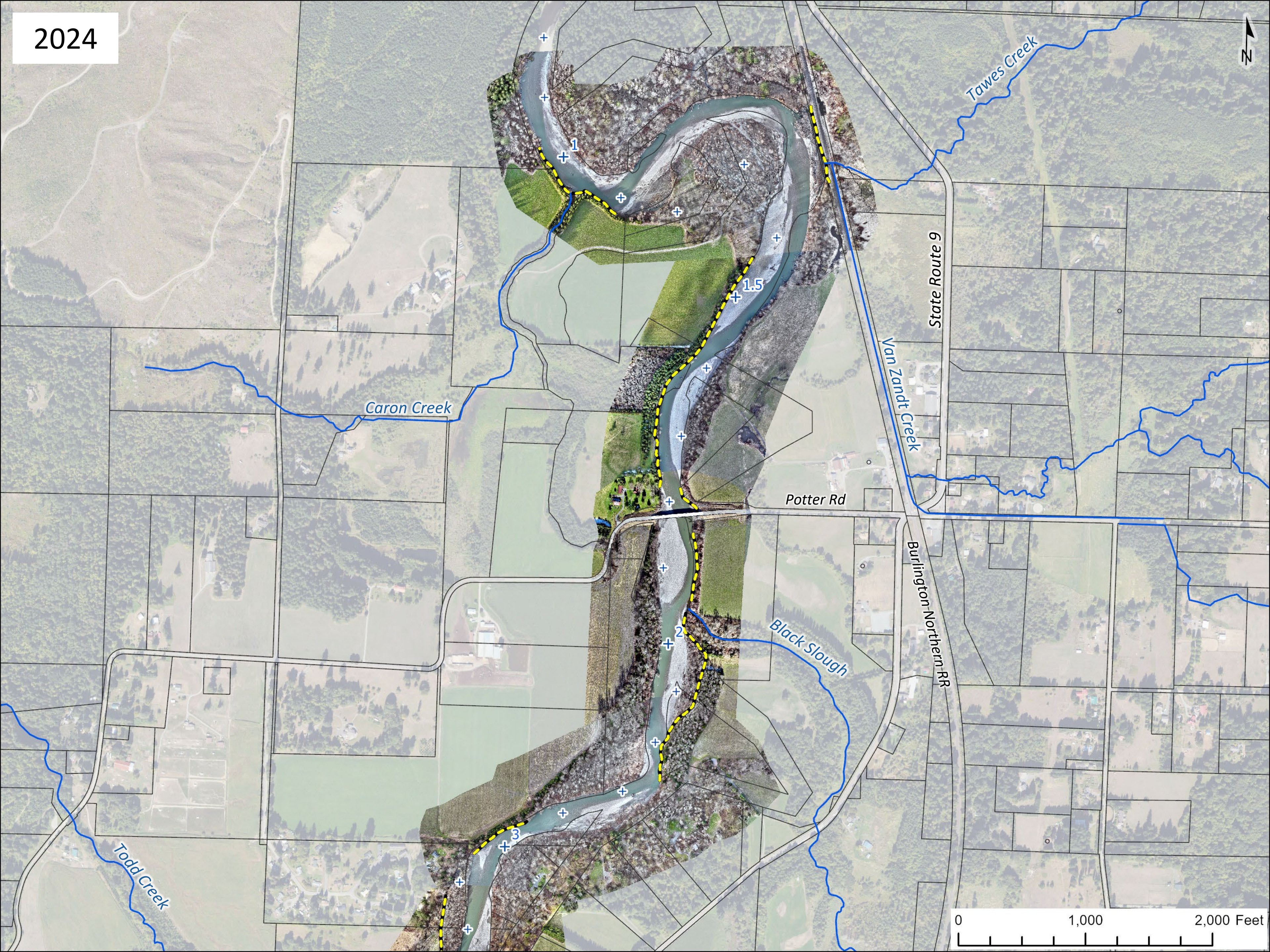

2024
N
1
1.5
2
3
Tawes Creek
Caron Creek
State Route 9
Van Zandt Creek
Potter Rd
Burlington Northern RR
Black Slough
Todd Creek
0
1,000
2,000 Feet